NISEE/COMPUTER APPLICATIONS
DAVIS HALL
UNIVERSITY OF CALIFORNIA
BERKELEY, CALIFORNIA 94720
(415) 642-5113

REPORT NO.
UC SESM 75-10

STRUCTURES AND MATERIALS RESEARCH
DEPARTMENT OF CIVIL ENGINEERING

THREE-DIMENSIONAL STOCHASTIC RESPONSE OF OFFSHORE TOWERS TO WAVE ACTION

BY

B. BERGE

J. PENZIEN

OCTOBER 1975

COLLEGE OF ENGINEERING
UNIVERSITY OF CALIFORNIA
BERKELEY CALIFORNIA

Structures and Materials Research
Department of Civil Engineering
Division of Structural Engineering
and Structural Mechanics

THREE-DIMENSIONAL STOCHASTIC RESPONSE OF OFFSHORE TOWERS TO WAVE ACTION

by

Bent Berge

and

Joseph Penzien

SESM REPORT 75-10

Structural Engineering Laboratory
University of California
Berkeley, California

October 1975

ABSTRACT

A theory is developed to calculate the dynamic response of offshore towers to random wave forces. Vibrations are considered simultaneously for translations in the orthogonal horizontal directions and for rotations about a vertical axis. The idealized structure for the dynamic analysis has its masses lumped at discrete horizontal levels.

The ocean waves are considered to be a zero mean stationary ergodic Gaussian random process described by the directional wave spectrum, which specifies the distribution of wave energy with respect to frequency and direction. This is an approximation to reality since such a wave spectrum is based upon the superposition of "linear" waves. Using linear wave theory and the Morison wave force equation, modified to take structure motion into account, spectral densities for the wave forces are obtained. The wave forces are applied to the structure at the submerged levels where the tower legs are located, thus the method takes into account the fact that wave forces are not in phase over the horizontal extension of the structure. Drag forces on the structure are linearized. The equations of motions are solved in the frequency domain using the normal mode superposition. Modal damping coefficients are uncoupled through an optimizing procedure. Spectral densities are obtained for the response in the various modes in normal coordinates, and mean products of the responses are obtained by integrating the spectral densities numerically over the frequency range. These response quantities are then transformed into statistics of displacements, rotations, shear forces and bending and twisting moments. Tower leg displacements are determined by combining trans-

lations and rotations of the structure.

Two computer programs, one for towers symmetric about two vertical planes and one for towers symmetric about one vertical plane, have been written to determine the above mentioned quantities. The computer solution for a tower that is symmetric about a vertical plane which has its masses lumped at 7 horizontal levels (21 degrees of freedom), requires approximately 1 minute central processor time on the CDC 6400 computer when 11 frequencies are used for the numerical integration of the spectral density functions.

Numerical results for seven deep water towers having heights of 475, 675, 875 and 1075ft, are presented. These results include standard deviations and mean peak values for displacements, rotations, shear forces and twisting and bending moments. They show that the directional spread of the waves normally has little effect on the rotational response, and that the effect of the rotational response on the overall structural response is small.

TABLE OF CONTENTS

ACKNOWLEDGEMENTS

I would like to express my sincere gratitude to Professor J. Penzien for his helpful guidance, criticism and support during this course of study. I am also extremely grateful to Professor R. L. Wiegel for his advice in the hydrodynamic part of this investigation and to Professor G. W. Brown for his review of the dissertation and valuable suggestions.

This research was initiated due to a research grant from the Standard Oil Company of California. Their support and interest in this topic is very much appreciated. Computer facilities were generously provided by the University of California Computer Center.

I am very thankful for the fellowships I received for part of my study from Johan Helmich Janson and Marcia Jansons Foundation and from Royal Norwegian Council for Scientific and Industrial Research.

The friendly cooperation of Ms. Renee E. Dayce when typing the dissertation is gratefully acknowledged.

Finally, I am extremely in debt to my wife Anne for her patience, support and encouragement throughout my studies. She also drew the figures, for which I am very thankful.

CHAPTER 1

INTRODUCTION

The increased world demand for petroleum products has made it necessary to carry out drilling operations in the ocean where hostile sea conditions are common. The cost of building structures in such an environment is enormous, and the structural design and analysis are extremely important. It has been common to use static design loads based upon a 50 or 100 year maximum wave. Today, platform structures are built in water deeper than 400ft and even structures in more than 1000ft of water are expected to be built in the future.

It is extremely important to determine the dynamic behavior of such structures in severe storms. This problem is complicated, however, since ocean waves are not deterministic in nature. Thus, a nondeterministic analysis should be carried out, if possible, to find the structural response to wave forces. Normally the waves are specified by a "power" spectrum (wave energy density spectrum), that describes the distribution of wave energy with respect to frequency. This investigation, however, uses the directional spectrum (distribution of wave energy density with respect to frequency and direction) to specify the ocean waves. At the present time, except for a few instances, the only spectra available are based upon an analysis that assumes the waves to be a superposition of "linear" waves. The waves are not linear, however, so that this method is an approximation to reality.

It is common to use linear wave theory [1-2][1] to determine water

---

[1] Numbers in brackets are reference numbers.

particle velocities and accelerations, and then describe the wave forces on the structure by the Morrison equation [3]. This equation has been used in theoretical [4-12] and in laboratory studies [13-14] to predict the dynamic response of fixed offshore platforms. The basic equation for wave forces on an oscillating pile requires numerical values to be assigned to the coefficients of inertia C_M and drag C_D. Even though a wide range of values has been proposed for these coefficients, it is quite common to set $C_M = 2.0$ and C_D equal to a value in the range 1.0 to 1.4 [15]. These coefficients may be somewhat frequency dependent for oscillating structures [16] and are coupled. The effect of having a body accelerating in water, is included by the so-called "added mass" (or virtual mass), whose coefficient in this investigation is assumed to be C_M-1. Laboratory studies have been carried out presently to determine hydrodynamic damping and added mass for offshore platforms [17].

In this dissertation a theory is developed to determine statistics of the dynamic response of offshore structures to random waves as described by the directional spectrum. Translations in the orthogonal horizontal directions and rotations about a vertical axis are considered for the structure and the method accepts an arbitrary directional spectrum, and the ocean waves may come from any direction. Of special interest in this investigation are the statistics of the rotational response of the tower. An equivalent theory to determine the statistics of structural response in one horizontal direction using the one-dimensional wave height spectrum has been developed by Foster [4-5] and Malhotra and Penzien [6-8]. A summary of this theory

and numerical results are given in [9].

Chapter II gives a review of random vibration and extreme value statistics. In Chapter III a theory to find response statistics is developed based upon known spectral densities for water particle accelerations and velocities. Expressions for these quantities are developed in Chapter IV. The method takes into account the fact that wave forces are not in phase over the structure. Chapter V gives a summary of the computer solution of the problem and numerical results are presented in Chapter VI for seven deep water towers (see Appendix A for structural data). Finally, a summary and conclusions are given in Chapter VII.

CHAPTER II

RANDOM VIBRATION

The dynamic response of structures exitated by forces that are nondeterministic can only be described in a probabilistic way. To simplify the analysis of such dynamic systems, the theory of random vibration has been developed. Wave, wind and earthquake forces are typical examples of nondeterministic forces.

For detailed treatment of the theory of stochastic processes and random vibration, the reader is referred to the literature, [18-27]. A summary of random vibration, however, is given in the following paragraphs.

A. STOCHASTIC PROCESSES

A stochastic process may be defined as a process that develops in time or space according to a probabilistic law. An ensemble of random variables, $x^{(k)}(t)$, $k = 1,2,\ldots,n$, $n \to \infty$, is called a stochastic or random process. For this case t is a time parameter. Each random variable, $x^{(k)}(t)$, is called a member of the process, $x(t)$.

The following functions are of special interest in this investigation:

(1) the mean value function

$$m(t) = E[x(t)] \tag{2.1}$$

where $E[\ \ ]$ denotes the average over the ensemble;

(2) the covariance function

$$R_{xx}(t_1, t_2) = \text{Cov}\,[x(t_1), x(t_2)] = E[\{x(t_1) - m(t_1)\}\,\{x(t_2) - m(t_2)\}] \tag{2.2}$$

(3) the variance function

$$\sigma_x^2(t) = \text{Var}\,[x(t)] = \text{Cov}\,[x(t), x(t)] \tag{2.3}$$

In general, both the mean value function and the covariance function for a stochastic process are time dependent. These stochastic processes are called nonstationary or evolutionary processes. In certain cases, however, the ensemble averages are independent of time. This special type of stochastic process is the stationary process. For stationary processes the mean value functions and the variance functions are constants, i.e.

$$m_x(t) = m_x \tag{2.4}$$

and

$$\sigma_x^2(t) = \sigma_x^2 \tag{2.5}$$

and the covariance functions are functions only of "lag" i.e. $\tau = t_2 - t_1$; thus,

$$R_{xx}(t_1,t_2) = R_{xx}(\tau) = \text{Cov}\,[x(t), x(t+\tau)] \tag{2.6}$$

Normally it is desirable to work with processes with zero mean value. If a stationary process does not have zero mean value, it is easy to define a new process with zero mean by subtracting the mean value, i.e.

$$x^*(t) = x(t) - m_x \tag{2.7}$$

The covariance function for a zero mean stationary process

$x(t)$ can then be defined as

$$R_{xx}(\tau) = E[x(t)x(t+\tau)] \qquad (2.8)^{1}$$

and the variance function becomes the mean square value, i.e.

$$\sigma_x^2 = R_{xx}(0) = E[\{x(t)\}^2] \qquad (2.9)$$

A subclass of stationary processes is the ergodic process. A necessary condition that a stationary process shall be ergodic is that the time averages for a single member of the process are equal to the ensemble averages for the process. Thus the ergodic process is fully described by a single member.

The covariance function for a zero mean ergodic process can be calculated as:

$$R_{xx}(\tau) = \langle x(t)x(t+\tau)\rangle = \lim_{T \to \infty} \frac{1}{T} \int_{-\frac{T}{2}}^{\frac{T}{2}} x(t)x(t+\tau)\, dt \qquad (2.10)$$

where $\langle \quad \rangle$ denotes time average.

A stationary stochastic process can also be described by its spectral density function, which is a frequency decomposition of the mean square value. This function and the covariance function are Fourier transform pairs, i.e.

$$S_{xx}(\omega) = \frac{1}{2\pi} \int_{-\infty}^{\infty} R_{xx}(\tau) \exp(-i\omega\tau)\, d\tau \qquad (2.11)$$

---

[1] $R_{xx}(\tau)$ is also called the auto-correlation function, and Eq. (2.8) defines this function for a stationary process without requiring zero mean.

and

$$R_{xx}(\tau) = \int_{-\infty}^{\infty} S_{xx}(\omega) \exp(i\omega\tau)\, d\omega \qquad (2.12)$$

and the variance of the process is

$$\sigma_x^2 = R_{xx}(0) = \int_{-\infty}^{\infty} S_{xx}(\omega)\, d\omega \qquad (2.13)$$

The most common type of stochastic processes is the Gaussian or normal process. These processes are especially simple to deal with mathematically because they are completely defined by the covariance function or the spectral density function.

Sometimes it is necessary to superimpose random processes. For this purpose, consider the random process

$$z(t) = x(t) + y(t) \qquad (2.14)$$

where $x(t)$ and $y(t)$ are zero mean stationary processes. According to the definition, Eq. (2.8), the covariance function is:

$$R_{zz}(\tau) = E[z(t)\, z(t+\tau)] = E[x(t)\, x(t+\tau)] + E[x(t)\, y(t+\tau)]$$

$$+ E[y(t)\, x(t+\tau)] + E[y(t)\, y(t+\tau)] = R_{xx}(\tau) + R_{xy}(\tau) + R_{yx}(\tau) + R_{yy}(\tau) \qquad (2.15)$$

where $R_{xy}(\tau)$ and $R_{yx}(\tau)$ are the cross covariance functions for $x(t)$ and $y(t)$, defined by:

$$R_{xy}(\tau) = E[x(t)\, y(t+\tau)] \qquad (2.16)$$

$$R_{yx}(\tau) = E[y(t)\, x(t+\tau)] \qquad (2.17)$$

Taking the Fourier transform of Eq. (2.15) one obtains the spectral density function

$$S_{zz}(\omega) = S_{xx}(\omega) + S_{xy}(\omega) + S_{yx}(\omega) + S_{yy}(\omega) \qquad (2.18)$$

where $S_{xy}(\omega)$ and $S_{yx}(\omega)$ are the cross spectral density functions for $x(t)$ and $y(t)$, and are Fourier transforms of $R_{xy}(\tau)$ and $R_{yx}(\tau)$, respectively.

The following relationships exist for the cross covariance functions and for the complex cross spectral density functions, namely

$$R_{xy}(\tau) = R_{yx}(-\tau) \qquad (2.19)$$

$$S_{xy}(\omega) = \bar{S}_{yx}(\omega) \qquad (2.20)$$

where the bar denotes complex conjugate. The real part of the cross spectral density function is an even function while the imaginary part is an odd function.

B. RESPONSE STATISTICS OF LINEAR SYSTEMS

The response of a linear system to a forcing function $X(t)$ is given by the following convolution integral (Duhamel Integral)

$$Y(t) = \int_{-\infty}^{t} X(\tau)\, h(t-\tau)\, d\tau \qquad (2.21)$$

where $h(t-\tau)$ is the systems response caused by a unit impulse at time $t=\tau$.

If the forcing function $X(t)$ is a zero mean, ergodic, Gaussian process, the response $Y(t)$ will also be a zero mean, ergodic, Gaussian

process and it will be fully characterized by its covariance function

$$R_{YY}(\tau) = E[Y(t)\ Y(t+\tau)] = \langle Y(t)\ Y(t+\tau)\rangle \qquad (2.22)$$

Often one is interested in some response quantity, $z(t)$, that is linearly related to the responses $Y_r(t)$ caused by the forcing functions $X_r(t)$, $r = 1,2,--,N$, i.e.

$$z(t) = \sum_{r=1}^{N} B_r\ Y_r(t) \qquad (2.23)$$

where B_r, $r = 1,2,--,N$, are known coefficients. Thus the covariance function for the response $z(t)$ is

$$R_{zz}(\tau) = \langle z(t)\ z(t+\tau)\rangle = \sum_{r=1}^{N}\sum_{s=1}^{N} B_r\ B_s\ \langle Y_r(t)\ Y_s(t+\tau)\rangle \qquad (2.24)$$

Substituting Eq. (2.21) into Eq. (2.24) gives

$$R_{zz}(\tau) = \sum_{r=1}^{N}\sum_{s=1}^{N} B_r\ B_s \left\langle \int_{-\infty}^{t} X_r(\gamma_1)\ h_r(t-\gamma_1)\ d\gamma_1 \int_{-\infty}^{t+\tau} X_s(\gamma_2)\ h_s(t-\gamma_2)\ d\gamma_2 \right\rangle \qquad (2.25)$$

where γ_1 and γ_2 are dummy time variables. Introducing new time variables $\gamma_3 = t-\gamma_1$ and $\gamma_4 = t+\tau - \gamma_2$ and inverting the limits of integration in Eq. (2.25), one obtains

$$R_{zz}(\tau) = \sum_{r=1}^{N}\sum_{s=1}^{N} B_r\ B_s \int_0^{\infty}\int_0^{\infty} h_r(\gamma_3)\ h_s(\gamma_4)\ R_{X_rX_s}(\tau+\gamma_3-\gamma_4)\ d\gamma_3\ d\gamma_4 \qquad (2.26)$$

where

$$R_{X_rX_s}(\tau+\gamma_3-\gamma_4) = \langle X_r(t-\gamma_3)\ X_s(t+\tau-\gamma_4)\rangle$$

Since the unit impulse response function is zero for negative arguments, the lower limits of integration in Eq. (2.26) may be replaced by $-\infty$. This equation represents the time domain solution for the response process. For computational purposes, however, it is desirable to work in the frequency domain. The spectral density function for the response $z(t)$ can be obtained by taking the Fourier transform of Eq. (2.26), i.e.

$$S_{zz}(\omega) = \frac{1}{2\pi} \int_{-\infty}^{\infty} \sum_{r=1}^{N} \sum_{s=1}^{N} B_r B_s \int_{-\infty}^{\infty} \int_{-\infty}^{\infty} h_r(\gamma_3)\, h_s(\gamma_4)\, R_{X_r X_s}(\tau+\gamma_3-\gamma_4)\, d\gamma_3\, d\gamma_4 \exp(-i\omega\tau)\, d\tau \quad (2.27)$$

Introducing a new variable $\gamma_5 = \tau+\gamma_3-\gamma_4$, Eq. (2.27) can be expressed in the form

$$S_{zz}(\omega) = \sum_{r=1}^{N} \sum_{s=1}^{N} B_r B_s \int_{-\infty}^{\infty} h_r(\gamma_3) \exp(i\omega\gamma_3)\, d\gamma_3 \int_{-\infty}^{\infty} h_s(\gamma_4) \exp(-i\omega\gamma_4)\, d\gamma_4 \frac{1}{2\pi} \int_{-\infty}^{\infty} R_{X_r X_s}(\gamma_5) \exp(-i\omega\gamma_5)\, d\gamma_5 \quad (2.28)$$

Hence the spectral density function for the response $z(t)$ is:

$$S_{zz}(\omega) = \sum_{r=1}^{N} \sum_{s=1}^{N} B_r B_s \bar{H}_r(i\omega) H_s(i\omega) S_{X_r X_s}(\omega) \quad (2.29)$$

where $S_{X_r X_s}(\omega)$ is the cross spectral density function for the forcing functions $X_r(t)$ and $X_s(t)$, $H(i\omega)$ is the complex frequency response function and $\bar{H}(i\omega)$ is the complex conjugate of $H(i\omega)$. Functions $H(i\omega)$ and $h(t)$ are Fourier transform pairs as given by

$$H(i\omega) = \int_{-\infty}^{\infty} h(t) \exp(-i\omega t)\, dt \quad (2.30)$$

and

$$h(t) = \frac{1}{2\pi}\int_{-\infty}^{\infty} H(i\omega)\, \exp\,(i\omega t)\, d\omega \qquad (2.31)$$

Having obtained the spectral density function for the response z(t), the variance of z(t) can be determined by using Eq. (2.13), i.e.

$$\sigma_z^2 = R_{zz}(0) = \int_{-\infty}^{\infty} S_{zz}(\omega)\, d\omega \qquad (2.32)$$

C. EXTREMES OF GAUSSIAN PROCESSES

Although the probability distribution for a zero mean Gaussian process is completely determined by its variance, the maximum value of the process is of special interest. In structural design this is a very important quantity. For detailed discussion of extreme value statistics, the reader is referred to Gumbel [28]. In this investigation, the following results [29-31] have special interest: Consider a zero mean ergodic Gaussian process x(t) with spectral density function $S_{xx}(\omega)$ and variance

$$\sigma_x^2 = \int_{-\infty}^{\infty} S_{xx}(\omega)\, d\omega \qquad (2.33)$$

For this process, the probability density function for the maxima z is given by

$$p(z) = \frac{1}{\sqrt{2\pi}\,\sigma_x}\Big[\,\varepsilon \exp\Big(-\frac{x^2}{2\sigma_x^2\,\varepsilon^2}\Big) + \sqrt{1-\varepsilon^2}\;\frac{x}{\sigma_x}\exp\,\Big(-\frac{x^2}{2\sigma_x^2}\Big) \int_{-\infty}^{\frac{x}{\sigma_x}\sqrt{1-\varepsilon^2}/\varepsilon} \exp\,\Big(-\frac{y^2}{2}\Big)\, dy\Big] \qquad (2.34)$$

where

$$\varepsilon = \frac{m_0 m_4 - m_2^2}{m_0 m_4} \tag{2.35}$$

where

$$m_r = \int_{-\infty}^{\infty} \omega^r S_{XX}(\omega)\, d\omega \tag{2.36}$$

Even though Eq. (2.34) gives the distribution of the maxima, one is especially interested in the distribution of the largest of these maxima Z, based upon the duration T of the process. The probability density function for Z is given by

$$p(Z) = \frac{Z}{\sigma_X^2} \nu T \exp\left[- \frac{Z^2}{2\sigma_X^2} - \nu T \exp\left(- \frac{Z^2}{2\sigma_X^2} \right)\right] \quad Z \geq \sigma \tag{2.37}$$

where

$$\nu = \frac{1}{2\pi} \frac{m_2}{m_0} \tag{2.38}$$

is the frequency where most of the energy in the spectrum $S_{XX}(\omega)$ is concentrated.

The expected value of the largest maxima Z is

$$E[Z] = \sigma_X \left\{ \sqrt{2 \ln \nu T} + \frac{.5772}{\sqrt{2 \ln \nu T}} \right\} \tag{2.39}$$

and the standard deviation is

$$\sigma_Z = \sigma_X \frac{\pi}{\sqrt{6}} \frac{1}{2 \ln \nu T} \tag{2.40}$$

Figure 2.1 shows the probability distribution for the largest maxima Z, Eq. (2.37) for νT = 100, 1000, 10000, and 100000. The

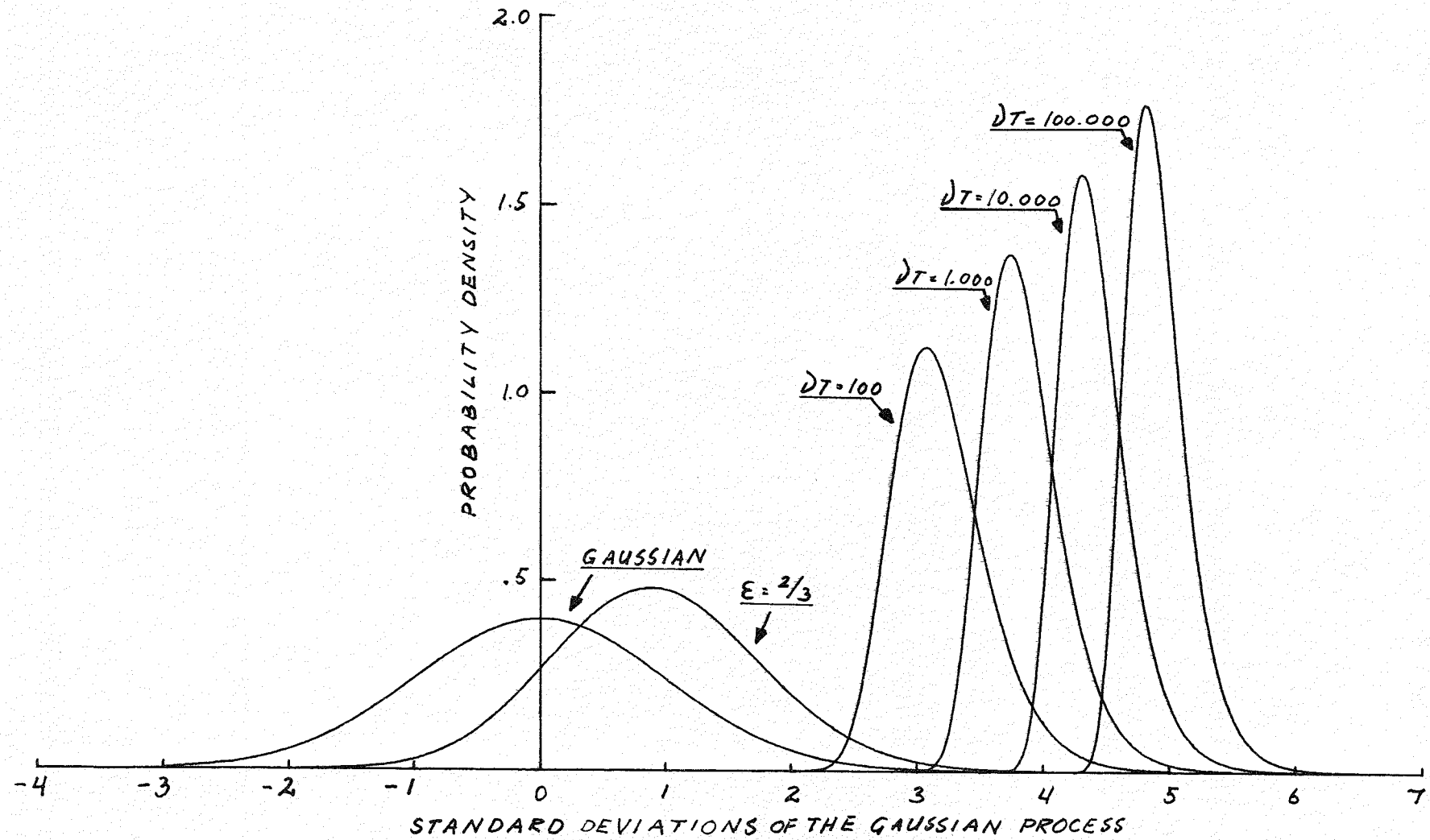

FIG. 2.1 DISTRIBUTION FOR A GAUSSIAN PROCESS, ITS MAXIMA FOR $\varepsilon = 2/3$ AND THE LARGEST MAXIMA FOR DIFFERENT VALUES OF ∂T

Gaussian distribution and the distribution for the maxima z, Eq. (2.34) (for $\varepsilon = 2/3$) are also included. Examining this figure, it is seen that the distribution of the peak value is very narrow, especially for large values of νT. This characteristic is also shown on Fig. 2.2 where $E[Z]$ and $E[Z] + \sigma_Z$ are plotted as functions of process duration T for $\nu = 0.1$ cps and for $\nu = 5$ cps. Thus, the mean peak value gives a good estimate of the magnitude of the largest value of the process, but the distribution of the peak values should be considered when making design decisions.

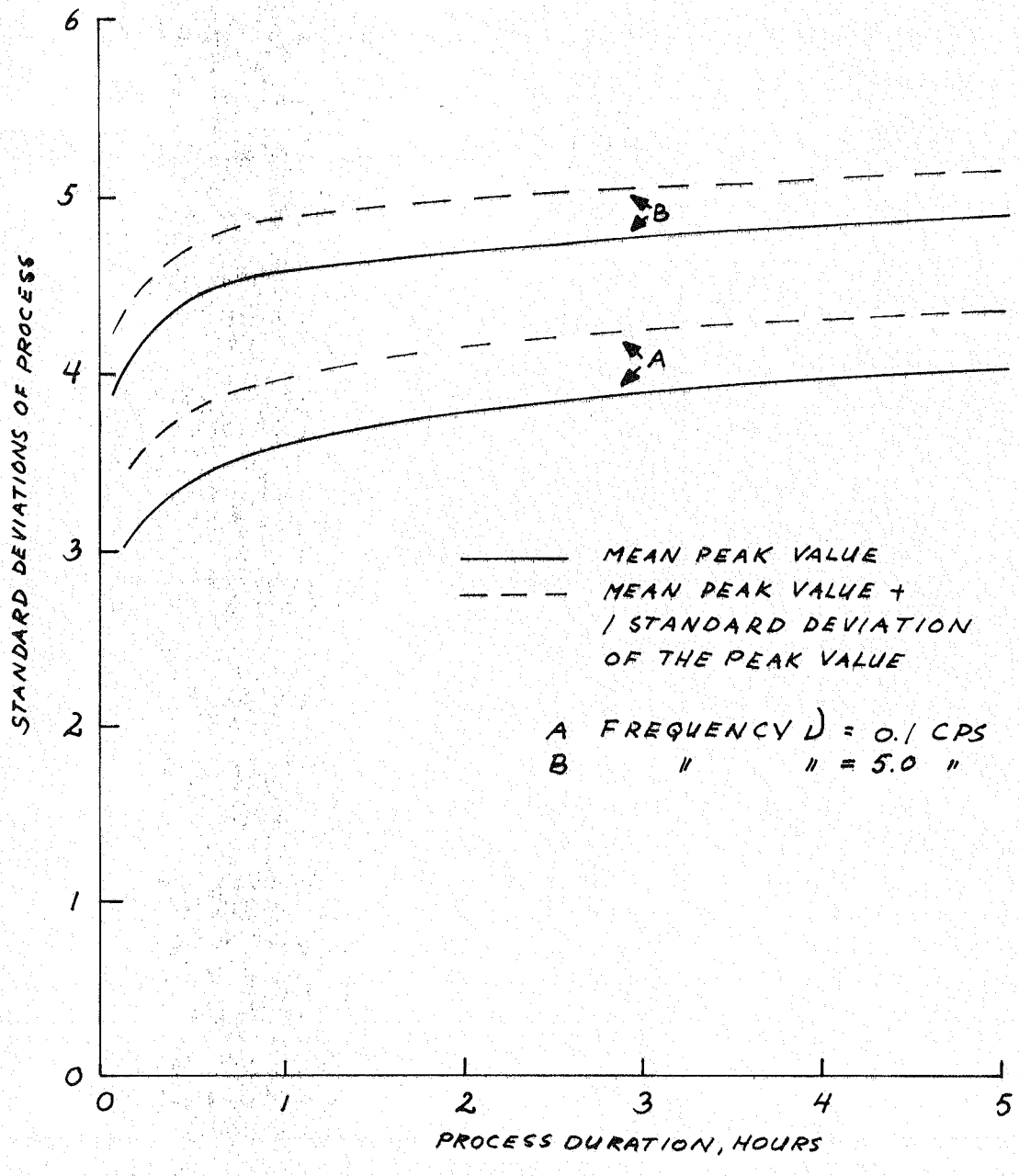

FIG. 2.2 EXTREME VALUES VS. DURATION FOR A GAUSSIAN PROCESS

CHAPTER III

STRUCTURAL DYNAMIC RESPONSE TO RANDOM WAVE FORCES

A. STRUCTURAL IDEALIZATION

Figure 3.1 shows an idealized model of an offshore tower with 4 legs, symmetric about the vertical xz-plane. Since offshore towers in general have at least one vertical plane of symmetry, the following theoretical development is based upon symmetry about a vertical plane.

The idealized dynamic model has the structural masses lumped at horizontal levels (shaded areas on Fig. 3.1), and inertia effects in the vertical direction are neglected. Thus the dynamic model has no rotational inertia about horizontal axes. The structure at each horizontal level is assumed to act as a rigid diaphragm. The number of degrees of freedom at each level to be included in the dynamic analysis is therefore reduced to 3, namely translations in the horizontal x and y directions and rotation about the vertical z-axis. Figures 3.1 and 3.2 show these degrees of freedom.

Although the wave forces act on the whole submerged part of the structure (their effects decay rapidly with increasing water depth in deep water), they are only applied in the orthogonal horizontal directions at 4 locations at each level on this model, namely where the tower legs are located. See Fig. 3.2 for the locations of the wave forces at the i th level. The wave forces are applied at different horizontal locations because they are not in phase over the structure. The reasons for selecting the location of the tower legs only are that the legs are significantly larger than the interconnect-

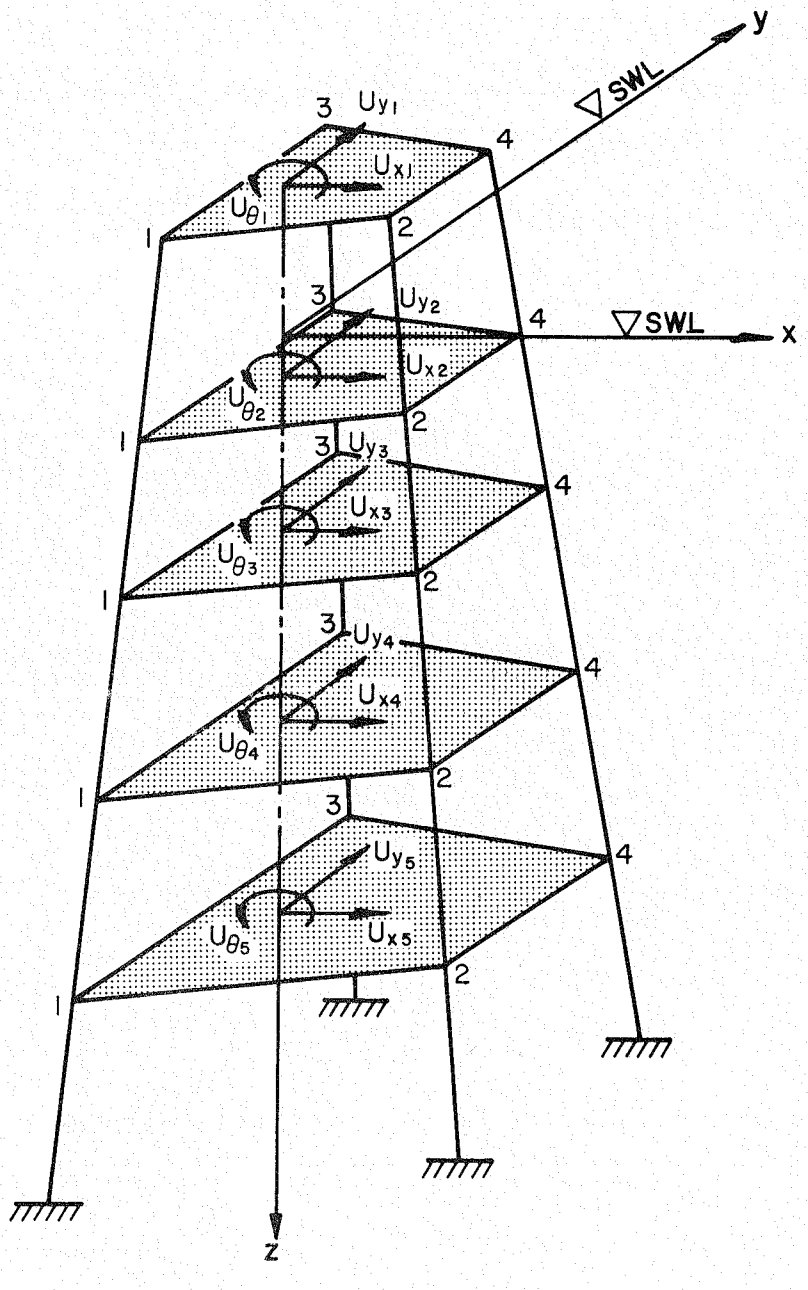

IDEALIZED TOWER

FIG. 3.1

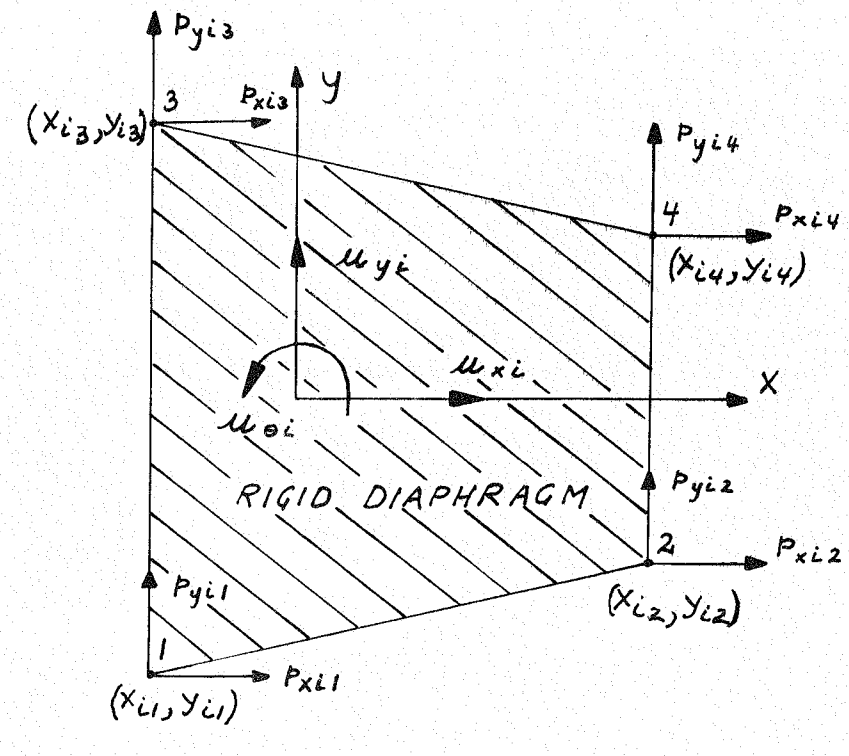

FIG. 3.2 DEGREES OF FREEDOM AND WAVE FORCES AT LEVEL i OF TOWER

ing members and that the computational effort for the statistical analysis procedure developed in this investigation varies quadratically with the number of points where the wave forces are applied.

Examining Fig. 3.2, the displacements of node k are:

(1) x-direction

$$u_{xik} = u_{xi} - y_{ik}\, u_{\theta i} \tag{3.1}$$

(2) y-direction

$$u_{yik} = u_{yi} + x_{ik}\, u_{\theta i} \tag{3.2}$$

B. EQUATIONS OF MOTION

The dynamic equations of motion for the dynamic model can be written in matrix form as

$$\underset{3N\times 3N}{[M_s]}\ \underset{3N}{\{\ddot{U}(t)\}} + \underset{3N\times 3N}{[C_s]}\ \underset{3N}{\{\dot{U}(t)\}} + \underset{3N\times 3N}{[K]}\ \underset{3N}{\{U(t)\}} = \underset{3N}{\{P_t(t)\}} \tag{3.3}$$

where symbols [ ] and { } indicate matrix and vector, respectively; $[M_s]$ represent lumped structural masses and rotational inertia about the vertical z-axis; $[C_s]$ and $[K]$ represent structural damping and stiffness coefficients, respectively (including foundation effects, if desired); $\{\ddot{U}(t)\}$, $\{\dot{U}(t)\}$ and $\{U(t)\}$ represent structural accelerations, velocities and displacements, respectively; $\{P_t(t)\}$ represents wave forces; and N is the number of discrete levels.

Arranging the displacement vector as follows:

$$\{U(t)\} = \begin{Bmatrix} \{U_x(t)\} \\ \hline \{U_y(t)\} \\ \hline \{U_\theta(t)\} \end{Bmatrix} \tag{3.4}$$

where $\{U_x(t)\}$ and $\{U_y(t)\}$ are the displacement vectors in x and y directions, respectively; and $\{U_\theta(t)\}$ is the rotational vector; the matrices in Eq. (3.3) can be written in the following partitioned forms

(1) the mass matrix

$$[M_s] = \left[\begin{array}{c|c|c} [M_{sxx}] & 0 & 0 \\ \hline 0 & [M_{syy}] & [M_{sy\theta}] \\ \hline 0 & [M_{s\theta y}] & [M_{s\theta\theta}] \end{array}\right] \tag{3.5}$$

where the submatrices are diagonal matrices,

(2) the damping matrix

$$[C_s] = \left[\begin{array}{c|c|c} [C_{sxx}] & 0 & 0 \\ \hline 0 & [C_{syy}] & [C_{sy\theta}] \\ \hline 0 & [C_{s\theta y}] & [C_{s\theta\theta}] \end{array}\right] \tag{3.6}$$

(3) the stiffness matrix

$$[K] = \left[\begin{array}{c|c|c} [K_{xx}] & 0 & 0 \\ \hline 0 & [K_{yy}] & [K_{y\theta}] \\ \hline 0 & [K_{\theta y}] & [K_{\theta\theta}] \end{array}\right] \tag{3.7}$$

In Eqs. (3.5) through (3.7) the subscripts xx and yy indicate translations in the x and y directions, respectively; $\theta\theta$ indicate rotation; $y\theta$ and θy indicate the coupling effects between translation in the y-direction and rotation.

The forcing vector can be written in partitioned form similar to Eq. (3.4), i.e.

$$\{P_t(t)\} = \left\{\begin{array}{c} \{P_{tx}(t)\} \\ \hline \{P_{ty}(t)\} \\ \hline \{P_{t\theta}(t)\} \end{array}\right\} \tag{3.8}$$

Examining Fig. 3.2, the wave forces at the i th level are:

(1) x-direction

$$p_{txi}(t) = \sum_{k=1}^{NNP} p_{xik}(t) \tag{3.9}$$

(2) y-direction

$$p_{tyi}(t) = \sum_{k=1}^{NNP} p_{yik}(t) \tag{3.10}$$

(3) rotation

$$p_{t\theta i}(t) = \sum_{k=1}^{NNP} [-y_{ik}\, p_{xik}(t) + x_{ik}\, p_{yik}(t)] \tag{3.11}$$

where $p_{xik}(t)$ and $p_{yik}(t)$ are the wave forces at node ik in x and y directions, respectively; and NNP is the number of nodes where forces at the i th level are applied.

The wave forces are described by the Morrison equation [3]. Because this equation was originally developed for fixed piles, it is modified to the following form for oscillating piles:

$$p(t) = C_M \rho b\, \ddot{v}(t) - (C_M - 1)\rho\, b\, \ddot{u}(t) + \tfrac{1}{2} C_D \rho a |\dot{v}(t) - \dot{u}(t)| (\dot{v}(t) - \dot{u}(t)) \tag{3.12}$$

where C_M and C_D are coefficients of inertia and drag, respectively; ρ is density of fluid; b is volume of member; a is projected area of member perpendicular to motion of fluid; $\ddot{v}(t)$ and $\dot{v}(t)$ are fluid acceleration and velocity, respectively; and $\ddot{u}(t)$ and $\dot{u}(t)$ are structural acceleration and velocity, respectively.

The water particle velocity and acceleration in Eq. (3.12)

relate to the instantaneous deflected position of the structure, but since wave lengths are significantly larger than structural deflections, no noticeable error is introduced by considering these quantities at the undeflected position of the structure.

Calling the relative velocity between water particles and structure $\dot{v}_r(t)$, given by

$$\dot{v}_r(t) = \dot{v}(t) - \dot{u}(t) \tag{3.13}$$

the drag force in Eq. (3.12) can be written as

$$p_D(t) = \tfrac{1}{2} C_D \rho a |\dot{v}_r(t)| \dot{v}_r(t) \tag{3.14}$$

Thus the drag force is proportional to $|\dot{v}_r(t)|\dot{v}_r(t)$, i.e. the relative velocity squared with the exception of the absolute sign, which preserves the direction of the force. Practical solution of this particular statistical dynamic problem, however, requires a linear system of differential equations. It is therefore necessary to linearize the drag force. This is done by the method of equivalent linearization, originally developed by Kryloff and Bogoliuboff [32]. Replacing the nonlinear term $|\dot{v}_r(t)|\dot{v}_r(t)$ with $d_\ell \dot{v}_r(t)$, introduces an error, e_ℓ, given by

$$e_\ell = |\dot{v}_r(t)|\dot{v}_r(t) - d_\ell \dot{v}_r(t) \tag{3.15}$$

For a stochastic process it is desirable to make this error as small as possible by minimizing the mean absolute error, $E[|e_\ell|]$ or the mean square error, $E[e_\ell^2]$. Normally the mean square error is minimized, [25, pg. 284], which requires that

$$\frac{\partial E[e_\ell^2]}{\partial d_\ell} = 0 = 2E[(|\dot{v}_r|\dot{v}_r - d_\ell\ \dot{v}_r)(-\dot{v}_r)] \qquad (3.16)$$

and that

$$\frac{\partial^2 E[e_\ell^2]}{\partial d_\ell^2} = 2E[\dot{v}_r^2] > 0 \qquad (3.17)$$

Eq. (3.17) indicates that the second derivative is always positive. Thus the mean square is minimized when Eq. (3.16) is solved for d_ℓ, which gives

$$d_\ell = \frac{E[|\dot{v}_r|\dot{v}_r^2]}{E[\dot{v}_r^2]} \qquad (3.18)$$

Since the input process (water particle motion) is assumed to be a zero mean ergodic Gaussian process (see Chapter IV, Section A), the linearized output process is also a zero mean ergodic Gaussian process. Thus, the probability density function for the relative velocity is

$$p(\dot{v}_r) = \frac{1}{\sqrt{2\pi}\ \sigma_{\dot{v}_r}} \quad \exp\left[\frac{-\dot{v}_r^2}{2\sigma_{\dot{v}_r}^2}\right] \qquad (3.19)$$

this permits one to write

$$E[|\dot{v}_r|\dot{v}_r^2] = \int_{-\infty}^{\infty} |\dot{v}_r|\dot{v}_r^2\ p(\dot{v}_r)\ d\dot{v}_r = \sqrt{\frac{8}{\pi}}\ \sigma_{\dot{v}_r}^3 \qquad (3.20)$$

and

$$E[\dot{v}_r^2] = \sigma_{\dot{v}_r}^2 \qquad (3.21)$$

The linearized drag factor d_ℓ is now determined when Eqs. (3.20) and (3.21) are substituted into Eq. (3.18) to give

$$d_\ell = \sqrt{\frac{8}{\pi}}\,\sigma_{\dot{v}_r} \qquad (3.22)^1$$

Equation (3.22) shows that it is only necessary to determine the standard deviations of the relative velocity between water particles and structure in order to linearize the drag force. For the calculation of the relative velocity deviations, see Section E. The linearization of the drag force is an iterative procedure because the calculated relative velocity deviations in one step are based upon the linearized drag force calculated in the previous step. Initial linearized drag forces are based upon water particle velocities, i.e. the structural velocities are temporarily assumed to be zero. Fortunately, acceptable convergence for the linearized drag forces is obtained after very few iteration steps.

The forcing function, Eq. (3.12), can now be written in linearized form as

$$p(t) = C_M \rho b\, \ddot{v}(t) - (C_M-1)\,\rho\, b\, \ddot{u}(t) + \tfrac{1}{2}\, C_D \rho a\, d_\ell [\dot{v}(t) - \dot{u}(t)] \qquad (3.23)$$

Since the wave forces are applied at the submerged nodal points of the structure, the forces at node k at level i of the structure are obtained by substituting Eqs. (3.1) and (3.2) into Eq. (3.23). Thus the force in the x-direction is

$$p_{xik}(t) = \alpha_{ik}\, \ddot{v}_{xik}(t) - (C_M-1)\,\rho\, b_{ik} [\ddot{u}_{xi}(t) - y_{ik}\, \ddot{u}_{\theta i}(t)] + \beta_{xik}\, [\dot{v}_{xik}(t) - \dot{u}_{xi}(t) + y_{ik}\, \dot{u}_{\theta i}(t)] \qquad (3.24)$$

---

[1] Equation (3.22) is similar to the first order term in statistical linearization of wave forces on a fixed pile [33].

where

$$\alpha_{ik} = C_M \rho \, b_{ik} \tag{3.25}$$

$$\beta_{xik} = \tfrac{1}{2} C_D \rho \, a_{xik} \, d_{\ell xik} \tag{3.26}$$

where a_{xik} is projected area perpendicular to x-direction and $d_{\ell xik}$ is linearized drag factor in x-direction; and the force in the y-direction is

$$p_{yik}(t) = \alpha_{ik} \, \ddot{v}_{yik}(t) - (C_M - 1) \, \rho \, b_{ik} [\ddot{u}_{yi}(t) + x_{ik} \, \ddot{u}_{\theta i}(t)] + \beta_{yik} \, [\dot{v}_{yik}(t) - \dot{u}_{yi}(t) - x_{ik} \, \dot{u}_{\theta i}(t)] \tag{3.27}$$

where

$$\beta_{yik} = \tfrac{1}{2} C_D \rho \, a_{yik} \, d_{\ell yik} \tag{3.28}$$

where a_{yik} is projected area perpendicular to y-direction and $d_{\ell yik}$ is linearized drag factor in y-direction

Substituting Eqs. (3.24) and (3.27) into Eqs. (3.9) through (3.11), the forces at the i th level of the structure are obtained:

(1) x-direction

$$p_{txi}(t) = \sum_{k=1}^{NNP} \{\alpha_{ik} \, \ddot{v}_{xik}(t) - (C_M - 1) \, \rho \, b_{ik} \, \ddot{u}_{xi}(t) + \beta_{xik} \, [\dot{v}_{xik}(t) - \dot{u}_{xi}(t) + y_{ik} \, \dot{u}_{\theta i}(t)]\} \tag{3.29}$$

(2) y-direction

$$p_{tyi}(t) = \sum_{k=1}^{NNP} \{\alpha_{ik} \, \ddot{v}_{yik}(t) - (C_M - 1) \, \rho \, b_{ik} [\ddot{u}_{yi}(t) + x_{ik} \, \ddot{u}_{\theta i}(t)] + \beta_{yik} \, [\dot{v}_{yik}(t) - \dot{u}_{yi}(t) - x_{ik} \, \dot{u}_{\theta i}]\} \tag{3.30}$$

(3) rotation

$$p_{t\theta i}(t) = \sum_{k=1}^{NNP} \{-y_{ik}\,\alpha_{ik}\,\ddot{v}_{xik}(t) - (C_M-1)\,\rho\,b_{ik}\,y_{ik}^2\,\ddot{u}_{\theta i}(t)$$
$$- \beta_{xik}\,[y_{ik}\,\dot{v}_{xik}(t) - y_{ik}\,\dot{u}_{xi}(t) + y_{ik}^2\,\dot{u}_{\theta i}(t)]$$
$$+ x_{ik}\,\alpha_{ik}\,\ddot{v}_{yik}(t) - (C_M-1)\,\rho\,b_{ik}[x_{ik}\,\ddot{u}_{yi}(t) + x_{ik}^2\,\ddot{u}_{\theta i}(t)]$$
$$+ \beta_{yik}\,[x_{ik}\,\dot{v}_{yik}(t) - x_{ik}\,\dot{u}_{yi}(t) - x_{ik}^2\,\dot{u}_{\theta i}(t)]\} \qquad (3.31)$$

C. SOLUTION OF THE LINEARIZED EQUATIONS OF MOTION

Equations (3.29) through (3.31) show that the linearized forcing functions depend not only on the water particle motions, but also on the motion of the structure. Including the latter effects in the mass and damping matrices, Eq. (3.3) can be rewritten as

$$[M]\,\{\ddot{U}(t)\} + [C]\,\{\dot{U}(t)\} + [K]\,\{U(t)\} = \{P(t)\} \qquad (3.32)$$

where $[M]$ represents the sums of structural masses and hydrodynamic masses (added masses); $[C]$ represents the sums of the structural damping coefficients and hydrodynamic damping coefficients; and $\{P(t)\}$ is the forcing vector for the new dynamic system which depends only on water particle motions.

Calling the added mass matrix $[M_a]$, the mass matrix in Eq. (3.32) is

$$[M] = [M_s] + [M_a] \qquad (3.33)$$

where $[M_s]$ is the mass matrix in Eq. (3.3). Partitioning the added

mass matrix as follows:

$$[M_a] = \begin{bmatrix} [M_{axx}] & 0 & 0 \\ 0 & [M_{ayy}] & [M_{ay\theta}] \\ 0 & [M_{a\theta y}] & [M_{a\theta\theta}] \end{bmatrix} \tag{3.34}$$

where the submatrices are diagonal matrices. The elements of the submatrices are:

(1) x and y directions

$$m_{axxii} = m_{ayyii} = \sum_{k=1}^{NNP} (C_M - 1)\ \rho\ b_{ik} \tag{3.35}$$

(2) rotation

$$m_{a\theta\theta ii} = \sum_{k=1}^{NNP} [(C_M - 1)\ \rho\ b_{ik}\ (y_{ik}^2 + x_{ik}^2)] \tag{3.36}$$

(3) coupled translation in y-direction and rotation

$$m_{ay\theta ii} = m_{a\theta yii} = \sum_{k=1}^{NNP} (C_M - 1)\ \rho\ b_{ik}\ x_{ik} \tag{3.37}$$

Consistent with the mass matrix, the hydrodynamic damping matrix can be called $[C_h]$; thus the damping matrix in Eq. (3.32) becomes

$$[C] = [C_s] + [C_h] \tag{3.38}$$

where $[C_s]$ is the damping matrix in Eq. (3.3). Rewriting the hydrodynamic damping matrix in partitioned form

$$[C_h] = \begin{bmatrix} [C_{hxx}] & 0 & [C_{hx\theta}] \\ 0 & [C_{hyy}] & [C_{hy\theta}] \\ [C_{h\theta x}] & [C_{h\theta y}] & [C_{h\theta\theta}] \end{bmatrix} \tag{3.39}$$

where the submatrices are diagonal matrices. The elements of the submatrices are:

(1) x-direction

$$C_{hxxii} = \sum_{k=1}^{NNP} \frac{1}{2} \rho C_D a_{xik} d_{\ell xik} \tag{3.40}$$

(2) y-direction

$$C_{hyyii} = \sum_{k=1}^{NNP} \frac{1}{2} \rho C_D a_{yik} d_{\ell yik} \tag{3.41}$$

(3) rotation

$$C_{h\theta\theta ii} = \sum_{k=1}^{NNP} \frac{1}{2} \rho C_D [a_{xik} d_{\ell xik} y_{ik}^2 + a_{yik} d_{\ell yik} x_{ik}^2] \tag{3.42}$$

(4) coupled translation in x-direction and rotation

$$C_{hx\theta ii} = C_{h\theta xii} = - \sum_{k=1}^{NNP} \frac{1}{2} \rho C_D a_{xik} d_{\ell xik} y_{ik} \tag{3.43}$$

(5) coupled translation in y-direction and rotation

$$C_{hy\theta ii} = C_{h\theta yii} = \sum_{k=1}^{NNP} \frac{1}{2} \rho C_D a_{yik} d_{\ell yik} x_{ik} \tag{3.44}$$

For structures symmetric about the vertical xz-plane (for which the theory is developed), the coupled hydrodynamic damping coefficients for translation in x-direction and rotation are zero in the initial calculation of structural response, and will be very small even when satisfactory convergence is obtained for the linearized drag forces. These damping coefficients depend only on the correlation between the translational velocities in x-direction and the angular velocities

of the structure. Thus, the error introduced by setting these damping coefficients equal to zero is negligible and because the vibration in x-direction will be uncoupled from vibration in y-direction and rotation, the solution process is simplified. The partitioned hydrodynamic damping matrix, Eq. (3.39) will then be reduced to the form

$$[C_h] = \begin{bmatrix} [C_{hxx}] & 0 & 0 \\ 0 & [C_{hyy}] & [C_{hy\theta}] \\ 0 & [C_{h\theta y}] & [C_{h\theta\theta}] \end{bmatrix} \tag{3.45}$$

The forcing vector in Eq. (3.32) written in partitioned form is

$$\{P(t)\} = \begin{Bmatrix} \{P_x(t)\} \\ \{P_y(t)\} \\ \{P_\theta(t)\} \end{Bmatrix} \tag{3.46}$$

where the subvectors include the terms in Eqs. (3.29) through (3.31) which depend on water particle motions only. Thus the forcing functions at the i th level are:

(1) x-direction

$$p_{xi}(t) = \sum_{k=1}^{NNP} [\alpha_{ik}\ \ddot{v}_{xik}(t) + \beta_{xik}\ \dot{v}_{xik}(t)] \tag{3.47}$$

(2) y-direction

$$p_{yi}(t) = \sum_{k=1}^{NNP} [\alpha_{ik}\ \ddot{v}_{yik}(t) + \beta_{yik}\ \dot{v}_{yik}(t)] \tag{3.48}$$

(3) rotation

$$p_{\theta i}(t) = \sum_{k=1}^{NNP} \{-y_{ik}[\alpha_{ik}\ \ddot{v}_{xik}(t) + \beta_{xik}\ \dot{v}_{xik}(t)] + x_{ik}[\alpha_{ik}\ \ddot{v}_{yik}(t) + \beta_{yik}\ \dot{v}_{yik}(t)]\} \tag{3.49}$$

Using the normal mode superposition, the response of the structure can be expressed as

$$\{U(t)\} = [\phi]\ \{Y(t)\} \tag{3.50}$$

where $\{Y(t)\}$ is the normal coordinate vector and $[\phi]$ is the modal matrix (eigenvectors) obtained by solving the eigenvalue problem for the undamped case, given by

$$[K]\ [\phi] = [M]\ [\phi]\ [\Omega]^2 \tag{3.51}$$

where

$$[\Omega]^2 = \text{diag}\ (\omega_r^2) \tag{3.52}$$

where ω_r is the r th natural frequency (square root of the eigenvalue).

For this particular dynamic system the modal matrix can be partitioned to the form

$$[\phi]_{3Nx3N} = \begin{bmatrix} [\phi_{xx}]_{NxN} & 0 \\ 0 & [\phi_{y\theta}]_{2Nx2N} \end{bmatrix} \tag{3.53}$$

where $[\phi_{xx}]$ is the modal matrix for vibration in x-direction and $[\phi_{y\theta}]$ is the modal matrix for coupled vibration for translation in y-direction and rotation.

Consistently, the frequency matrix in partitioned form is

$$[\Omega] = \begin{bmatrix} [\Omega_x]_{NxN} & 0 \\ 0 & [\Omega_{y\theta}]_{2Nx2N} \end{bmatrix} \tag{3.54}$$

where $[\Omega_x] = \text{diag}\,(\omega_{xr})$ and $[\Omega_{y\theta}] = \text{diag}\,(\omega_{y\theta r})$, i.e. the frequency matrices for vibration in x-direction and for coupled vibration for translation in y-direction and rotation, respectively. The normal coordinate vector in partitioned form is

$$\underset{3N}{\{Y\}} = \begin{Bmatrix} \{Y_x\} \\ \hline \{Y_{y\theta}\} \\ 2N \end{Bmatrix} \qquad (3.55)$$

where $\{Y_x\}$ and $\{Y_{y\theta}\}$ represent the normal coordinates for modes in the coordinate directions indicated. Using the coordinate transformation given by Eq. (3.50) and premultiplying Eq. (3.32) with $[\phi]^T$, the normal equations of motion are obtained

$$[M^*]\,\{\ddot{Y}(t)\} + [C_o^*]\,\{\dot{Y}(t)\} + [K^*]\{Y(t)\} = \{P^*(t)\} \qquad (3.56)$$

where

$$[M^*] = [\phi^T]\,[M]\,[\phi] = \text{generalized mass matrix} \qquad (3.57)$$

$$[C_o^*] = [\phi^T]\,[C]\,[\phi] = \text{generalized damping matrix} \qquad (3.58)$$

$$[K^*] = [\phi^T]\,[K]\,[\phi] = \text{generalized stiffness matrix} \qquad (3.59)$$

$$\{P^*(t)\} = [\phi^T]\,\{P\,(t)\} = \text{generalized force vector} \qquad (3.60)$$

Both the generalized mass and stiffness matrices are diagonal matrices, while the generalized damping matrix normally is a full matrix. Even if the structural damping is selected such that the orthogonality condition $\{\phi_r\}^T\,[C]\,\{\phi_s\} = 0$, $r \neq s$, is satisfied, the hydrodynamic damping due to drag forces will cause the generalized damping matrix to be a full matrix.

Partitioning the generalized force vector similar to Eq. (3.55)

i.e.

$$\underset{3N}{\{P^*(t)\}} = \begin{Bmatrix} \{P^*_x(t)\} \\ \hline \{P^*_{y\theta}(t)\} \\ 2N \end{Bmatrix} \qquad (3.61)$$

and noting the partitioned form of the modal matrix, Eq. (3.53), the elements of the generalized force vector are obtained by substituting Eqs. (3.47) through (3.49) and (3.53) into Eq. (3.60):

(1) mode r in x-direction

$$P^*_{xr}(t) = \sum_{i=1}^{N} \phi_{xxir} \sum_{k=1}^{NNP} [\alpha_{ik}\, \ddot{v}_{xik}(t) + \beta_{xik}\, \dot{v}_{xik}(t)] \qquad (3.62)$$

(2) mode r in coupled translation in y-direction and rotation

$$\begin{aligned} P^*_{y\theta r}(t) = \sum_{i=1}^{N} \{ & \phi_{y\theta ir} \sum_{k=1}^{NNP} [\alpha_{ik}\, \ddot{v}_{yik}(t) + \beta_{yik}\, \dot{v}_{yik}(t)] \\ & + \phi_{y\theta(i+N)r} \sum_{k=1}^{NNP} [-y_{ik}(\alpha_{ik}\, \ddot{v}_{xik}(t) + \beta_{xik}\, \dot{v}_{xik}(t) \\ & + x_{ik}(\alpha_{ik}\, \ddot{v}_{yik}(t) + \beta_{yik}\, \dot{v}_{yik}(t)]\} \end{aligned} \qquad (3.63)$$

For a practical solution of this dynamic problem, it is necessary to uncouple the set of dynamic equations given by Eq. (3.45). Thus the couplings between damping in the various modes must be removed. The procedure used to evaluate the optimal modal damping coefficients is similar to that used for the linearization of the drag force, namely minimizing the mean square error introduced. Calling the optimal diagonal damping matrix [C*], the error vector introduced by this procedure is

$$\{E(t)\} = [C_o^*]\ \{\dot{Y}(t)\} - [C^*]\ \{\dot{Y}(t)\} \qquad (3.64)$$

Minimizing the mean square value of the r th element in the error vector $\{E(t)\}$ requires that

$$\frac{\partial E[e_r^2]}{\partial C_{rr}^*} = 0 = 2E\left[\left(\sum_{s=1}^{N} C_{ors}^*\ \dot{Y}_s - C_{rr}^*\ \dot{Y}_r\right)(-\dot{Y}_r)\right] \qquad (3.65)$$

which solved gives

$$C_{rr}^* = \sum_{s=1}^{N} C_{ors}^*\ \frac{E[\dot{Y}_r\ \dot{Y}_s]}{E[\dot{Y}_r^2]} \qquad (3.66)$$

The mean square error is minimized, since

$$\frac{\partial^2 E[e_r]}{\partial C_{rr}^*} = 2E[\dot{Y}_r^2] > 0 \qquad (3.67)$$

Examining Eq. (3.66) it is easily seen that the optimization of the damping coefficients is an iterative procedure, since the mean products of the structural velocities in the generalized coordinate system, $E[\dot{Y}_r\ \dot{Y}_s]$, must be determined, see Section D, Eq. (3.88). These products depend on the damping of the system. The diagonal terms of $[C_o^*]$ are selected as initial modal damping coefficients. As for the linearization of drag forces, this optimization process converges rapidly. It should be noted, however, that it is necessary to optimize the damping coefficients for each iteration step in the linearization of the drag forces.

Neglecting the error vector $\{E\}$, the normal equations of motion can be expressed in the familiar uncoupled form

$$[M^*]\ \{\ddot{Y}(t)\} + [C^*]\ \{\dot{Y}(t)\} + [K^*]\ \{Y(t)\} = \{P^*(t)\} \qquad (3.68)$$

Premultiplying Eq. (3.68) by $[M^*]^{-1}$, the set of dynamic equations becomes

$$\{\ddot{Y}(t)\} + 2[\Omega]\ [\Xi]\ \{\dot{Y}(t)\} + [\Omega]^2\ \{Y(t)\} = [M^*]^{-1}\{P^*(t)\} \tag{3.69}$$

where

$$[\Xi] = \text{diag}\ (\xi_r) = \tfrac{1}{2}\ [M^*]^{-1}[\Omega]^{-1}[C^*] \tag{3.70}$$

where ξ_r is the damping ratio for the r th mode.

The response of the structure can be obtained by solving Eq. (3.69) through the time domain, which results in the convolution integral solution. Thus the response in the r th mode is

$$Y_r(t) = \int_{-\infty}^{t} P_r^*(\gamma)\ h_r(t-\gamma)\ d\gamma \tag{3.71}$$

where

$$h_r(t) = \frac{1}{\omega_{dr}\ m_r^*} \exp\ (-\xi_r\ \omega_r\ t)\ \sin\ (\omega_{dr}\ t) \tag{3.72}$$

is the unit impulse response function in the r th mode and where

$$\omega_{dr} = \omega_r\ \sqrt{1-\xi_r^2} \tag{3.73}$$

is the damped natural frequency of the r th mode.

D. RESPONSE STATISTICS

Since the input process (water particle motions) is assumed to be a zero mean ergodic Gaussian process, the response process for the structure is fully described by its covariance matrix, which for response in the normal coordinate system is

$$[R_{YY}(\tau)] = E[\{Y(t)\}^T \{Y(t+\tau)\}] = \langle \{Y(t)\}^T \{Y(t+\tau)\} \rangle \quad (3.74)$$

Substituting Eq. (3.71) into Eq. (2.26), the cross covariance function for the responses in the r th and s th modes is obtained, i.e.

$$R_{Y_r Y_s}(\tau) = \int_{-\infty}^{\infty} \int_{-\infty}^{\infty} R_{P_r^* P_s^*}(\tau - \gamma_2 + \gamma_1)\, h_r(\gamma_1)\, h_s(\gamma_2)\, d\gamma_1\, d\gamma_2 \quad (3.75)$$

where γ_1 and γ_2 are dummy time variables, and $R_{P_r^* P_s^*}(\tau)$ is the covariance function for the generalized forces in the r th and s th modes, i.e.

$$R_{P_r^* P_s^*}(\tau) = E[P_r^*(t)\, P_s^*(t+\tau)] = \langle P_r^*(t)\, P_s^*(t+\tau) \rangle \quad (3.76)$$

Taking the Fourier transform of Eq. (3.75) as derived in Chapter II, Section B, Eq. (2.29), the cross spectral density function for the responses in the r th and s th modes is obtained, i.e.

$$S_{Y_r Y_s}(\omega) = \bar{H}_r(i\omega)\, H_s(i\omega)\, S_{P_r^* P_s^*}(\omega) \quad (3.77)$$

where $S_{P_r^* P_s^*}(\omega)$ is the cross spectral density function for the generalized forces in the r th and s th mode; $H(i\omega)$ is the complex frequency response function and $\bar{H}(i\omega)$ is the complex conjugate of $H(i\omega)$. The complex frequency response function for the r th mode is given by

$$H_r(i\omega) = \frac{1}{m_r^*} \frac{1}{\omega_r^2 - \omega^2 + 2i\, \xi_r\, \omega_r\, \omega} \quad (3.78)$$

and it is the Fourier transform of the unit impulse response function, i.e.

$$H_r(i\omega) = \int_{-\infty}^{\infty} h_r(t) \exp(-i\omega t)\, dt \quad (3.79)$$

The covariance function for the generalized forces in the r th and s th modes is obtained by substituting Eqs. (3.62) and (3.63) into Eq. (3.76):

(1) modes r and s in x-direction

$$R_{P^*_{xr} P^*_{xs}}(\tau) = \langle P^*_{xr}(t)\, P^*_{xs}(t+\tau)\rangle \tag{3.80}$$

(2) mode r in x-direction and mode s in coupled translation in y-direction and rotation

$$R_{P^*_{xr} P^*_{y\theta s}}(\tau) = \langle P^*_{xr}(t)\, P^*_{y\theta s}(t+\tau)\rangle \tag{3.81}$$

(3) modes r and s in coupled translation in y-direction and rotation

$$R_{P^*_{y\theta r} P^*_{y\theta s}}(\tau) = \langle P^*_{y\theta r}(t)\, P^*_{y\theta s}(t+\tau)\rangle \tag{3.82}$$

Calculating the covariance functions, Eqs. (3.80) through (3.82) and taking the Fourier transform of each term, one obtains the cross-spectral density functions of the generalized forces:

(1) modes r and s in x-direction

$$S_{P^*_{xr} P^*_{xs}}(\omega) = \sum_{i=1}^{N}\sum_{j=1}^{N} \phi_{xxir}\,\phi_{xxjs} \sum_{k=1}^{NNP}\sum_{\ell=1}^{NNP} \{\alpha_{ik}\alpha_{j\ell}\, S_{\ddot{v}_{xik}\,\ddot{v}_{xj\ell}}(\omega)$$

$$+ \alpha_{ik}\beta_{xj\ell}\, S_{\ddot{v}_{xik}\dot{v}_{xj\ell}}(\omega) + \beta_{xik}\alpha_{j\ell}\, S_{\dot{v}_{xik}\ddot{v}_{xj\ell}}(\omega) + \beta_{xik}\beta_{xj\ell} S_{\dot{v}_{xik}\dot{v}_{xj\ell}}(\omega) \tag{3.83}$$

(2) mode r in x-direction and mode s in coupled translation in y-direction and rotation

$$S_{P^*_{xr}P^*_{y\theta s}}(\omega) = \sum_{i=1}^{N}\sum_{j=1}^{N} \phi_{xxir}\phi_{y\theta js} \sum_{k=1}^{NNP}\sum_{\ell=1}^{NNP} \{\alpha_{ik}\alpha_{j\ell} S_{\ddot{v}_{xik}\ddot{v}_{yj\ell}}(\omega)$$

$$+ \alpha_{ik}\beta_{yj\ell} S_{\ddot{v}_{xik}\dot{v}_{yj\ell}}(\omega) + \beta_{xik}\alpha_{j\ell} S_{\dot{v}_{xik}\ddot{v}_{yj\ell}}(\omega) + \beta_{xik}\beta_{yj\ell} S_{\dot{v}_{xik}\dot{v}_{yj\ell}}(\omega)\}$$

$$+ \sum_{i=1}^{N}\sum_{j=1}^{N} \phi_{xxir}\phi_{y\theta(j+N)s} \sum_{k=1}^{NNP}\sum_{\ell=1}^{NNP} \{-y_{j\ell}[\alpha_{ik}\alpha_{j\ell} S_{\ddot{v}_{xik}\ddot{v}_{xj\ell}}(\omega)+\alpha_{ik}\beta_{xj\ell}S_{\ddot{v}_{xik}\dot{v}_{xj\ell}}(\omega$$

$$+ \beta_{xik}\alpha_{j\ell} S_{\dot{v}_{xik}\ddot{v}_{xj\ell}}(\omega) + \beta_{xik}\beta_{xj\ell} S_{\dot{v}_{xik}\dot{v}_{xj\ell}}(\omega)]+ x_{j\ell}[\alpha_{ik}\alpha_{j\ell} S_{\ddot{v}_{xik}\ddot{v}_{yj\ell}}(\omega)$$

$$+ \alpha_{ik}\beta_{yj\ell} S_{\ddot{v}_{xik}\dot{v}_{yj\ell}}(\omega) + \beta_{xik}\alpha_{j\ell} S_{\dot{v}_{xik}\ddot{v}_{yj\ell}}(\omega) + \beta_{xik}\beta_{yj\ell} S_{\dot{v}_{xik}\dot{v}_{yj\ell}}(\omega)]\}$$

(3.84)

(3) modes r and s in coupled translation in y-direction and rotation

$$S_{P^*_{y\theta r}P^*_{y\theta s}}(\omega) = \sum_{i=1}^{N}\sum_{j=1}^{N} \phi_{y\theta ir}\phi_{y\theta js} \sum_{k=1}^{NNP}\sum_{\ell=1}^{NNP} \{\alpha_{ik}\alpha_{j\ell} S_{\ddot{v}_{yik}\ddot{v}_{yj\ell}}(\omega)$$

$$+ \alpha_{ik}\beta_{yj\ell} S_{\ddot{v}_{yik}\dot{v}_{yj\ell}}(\omega)+\beta_{yik}\alpha_{j\ell} S_{\dot{v}_{yik}\ddot{v}_{yj\ell}}(\omega)+\beta_{yik}\beta_{yj\ell} S_{\dot{v}_{yik}\dot{v}_{yj\ell}}(\omega)\}$$

$$+ \sum_{i=1}^{N}\sum_{j=1}^{N} \phi_{y\theta ir}\phi_{y\theta(j+N)s} \sum_{k=1}^{NNP}\sum_{\ell=1}^{NNP} \{-y_{j\ell}[\alpha_{ik}\alpha_{j\ell} S_{\ddot{v}_{yik}\ddot{v}_{xj\ell}}(\omega)+\alpha_{ik}\beta_{xj\ell} S_{\ddot{v}_{yik}\dot{v}_{xj\ell}}(\omega$$

$$+ \beta_{yik}\alpha_{j\ell} S_{\dot{v}_{yik}\ddot{v}_{xj\ell}}(\omega) + \beta_{yik}\beta_{xj\ell} S_{\dot{v}_{yik}\dot{v}_{xj\ell}}(\omega)] + x_{j\ell}[\alpha_{ik}\alpha_{j\ell} S_{\ddot{v}_{yik}\ddot{v}_{xj\ell}}(\omega)$$

$$\alpha_{ik}\beta_{yj\ell} S_{\ddot{v}_{yik}\dot{v}_{yj\ell}}(\omega)+\beta_{yik}\alpha_{j\ell} S_{\dot{v}_{yik}\ddot{v}_{yj\ell}}(\omega)+\beta_{yik}\beta_{yj\ell} S_{\dot{v}_{yik}\dot{v}_{yj\ell}}(\omega)]\}$$

$$+ \sum_{i=1}^{N}\sum_{j=1}^{N} \phi_{y\theta(i+N)r}\phi_{y\theta js} \sum_{k=1}^{NNP}\sum_{\ell=1}^{NNP} \{-y_{ik}[\alpha_{ik}\alpha_{j\ell} S_{\ddot{v}_{xik}\ddot{v}_{yj\ell}}(\omega)+\alpha_{ik}\beta_{yj\ell} S_{\ddot{v}_{xik}\dot{v}_{yj\ell}}(\omega)$$

$$+ \beta_{xik}\alpha_{j\ell}\, S_{\dot{v}_{xik}\ddot{v}_{yj\ell}}(\omega) + \beta_{xik}\beta_{yj\ell}\, S_{\dot{v}_{xik}\dot{v}_{yj\ell}}(\omega)] + x_{ik}[\alpha_{ik}\alpha_{j\ell}\, S_{\ddot{v}_{yik}\ddot{v}_{yj\ell}}(\omega)$$

$$+ \alpha_{ik}\beta_{yj\ell}\, S_{\ddot{v}_{yik}\dot{v}_{yj\ell}}(\omega) + \beta_{yik}\alpha_{j\ell}\, S_{\dot{v}_{yik}\ddot{v}_{yj\ell}}(\omega) + \beta_{yik}\beta_{yj\ell}\, S_{\dot{v}_{yik}\dot{v}_{yj\ell}}(\omega)]\}$$

$$+ \sum_{i=1}^{N}\sum_{j=1}^{N} \phi_{y\theta(i+N)r}\, \phi_{y\theta(i+N)s} \sum_{k=1}^{NNP}\sum_{\ell=1}^{NNP} \{y_{ik}\, y_{j\ell}[\alpha_{ik}\alpha_{j\ell}\, S_{\ddot{v}_{xik}\ddot{v}_{xj\ell}}(\omega)$$

$$+ \alpha_{ik}\beta_{xj\ell}\, S_{\ddot{v}_{xik}\dot{v}_{xj\ell}}(\omega) + \beta_{xik}\alpha_{j\ell}\, S_{\dot{v}_{xik}\ddot{v}_{xj\ell}}(\omega) + \beta_{xik}\beta_{xj\ell}\, S_{\dot{v}_{xik}\dot{v}_{xj\ell}}(\omega)]$$

$$- y_{ik}\, x_{j\ell}[\alpha_{ik}\alpha_{j\ell}\, S_{\ddot{v}_{xik}\ddot{v}_{yj\ell}}(\omega) + \alpha_{ik}\beta_{yj\ell}\, S_{\ddot{v}_{xik}\dot{v}_{yj\ell}}(\omega) + \beta_{xik}\alpha_{j\ell}\, S_{\dot{v}_{xik}\ddot{v}_{yj\ell}}(\omega)$$

$$+ \beta_{xik}\beta_{yj\ell}\, S_{\dot{v}_{xik}\dot{v}_{yj\ell}}(\omega)] - x_{ik}\, y_{j\ell}[\alpha_{ik}\alpha_{j\ell}\, S_{\ddot{v}_{yik}\ddot{v}_{xj\ell}}(\omega) + \alpha_{ik}\beta_{xj\ell}\, S_{\ddot{v}_{yik}\dot{v}_{xj\ell}}(\omega)$$

$$+ \beta_{yik}\alpha_{j\ell}\, S_{\dot{v}_{yik}\ddot{v}_{xj\ell}}(\omega) + \beta_{yik}\beta_{xj\ell}\, S_{\dot{v}_{yik}\dot{v}_{xj\ell}}(\omega)] + x_{ik}\, x_{j\ell}[\alpha_{ik}\alpha_{j\ell}\, S_{\ddot{v}_{yik}\ddot{v}_{yj\ell}}(\omega)$$

$$+ \alpha_{ik}\beta_{yj\ell}\, S_{\ddot{v}_{yik}\dot{v}_{yj\ell}}(\omega) + \beta_{yik}\alpha_{j\ell}\, S_{\dot{v}_{yik}\ddot{v}_{yj\ell}}(\omega) + \beta_{yik}\beta_{yj\ell}\, S_{\dot{v}_{yik}\dot{v}_{yj\ell}}(\omega)]\} \tag{3.85}$$

Integrating Eq. (3.77) over the frequency range, the average product of the responses in the r th and s th modes is obtained in the normal coordinate system as follows:

$$E[Y_r Y_s] = \int_{-\infty}^{\infty} S_{Y_r Y_s}(\omega)\, d\omega \tag{3.86}$$

Having determined these quantities for all necessary modes, the statistics of structural displacements and other linear related quantities are easy to determine.

Examining Eq. (3.66), the expression that optimizes the damping coefficients, it is seen that one has to determine the average product of the structural velocities in normal coordinates for the different modes. Noting that

$$S_{\dot{Y}_r \dot{Y}_s}(\omega) = \omega^2 \, S_{Y_r Y_s}(\omega) \tag{3.87}$$

where $S_{Y_r Y_s}(\omega)$ is given by Eq. (3.77) the average product of the structural velocities in r th and s th mode is

$$E[\dot{Y}_r \dot{Y}_s] = \int_{-\infty}^{\infty} S_{\dot{Y}_r \dot{Y}_s}(\omega) \, d\omega = \int_{-\infty}^{\infty} \omega^2 \, S_{Y_r Y_s}(\omega) \, d\omega \tag{3.88}$$

Substituting Eq. (3.88) into Eq. (3.66) optimizes the model damping coefficients.

For calculation of specific response statistics consider a response quantity $z_i(t)$ that is a linear function of the response in normal coordinates as given by

$$z_i(t) = \sum_{r=1}^{3N} B_{ir} Y_r(t) \tag{3.89}$$

where the B_{ir}'s are known coefficients. Thus the covariance function for $z_i(t)$ and $z_j(t+\tau)$ is

$$R_{z_i z_j}(\tau) = \sum_{r=1}^{3N} \sum_{s=1}^{3N} B_{ir} B_{js} \, E[Y_r(t) \, Y_s(t+\tau)] = \sum_{r=1}^{3N} \sum_{s=1}^{3N} B_{ir} B_{js} \, R_{Y_r Y_s}(\tau) \tag{3.90}$$

Taking the Fourier transform of Eq. (3.90), the cross spectral density function for the responses is obtained, i.e.

$$S_{z_i z_j}(\omega) = \sum_{r=1}^{3N} \sum_{s=1}^{3N} B_{ir} B_{js} S_{Y_r Y_s}(\omega) \qquad (3.91)$$

Thus the average product of the responses is

$$E[z_i\ z_j] = \int_{-\infty}^{\infty} S_{z_i z_j}(\omega)\, d\omega = \sum_{r=1}^{3N} \sum_{s=1}^{3N} B_{ir}\, B_{js}\, E[Y_r\ Y_s] \qquad (3.92)$$

Using Eq. (3.92), the variances of the structural displacements and rotation at the i th level become:

(1) x-direction

$$\sigma^2_{u_{xi}} = \sum_{r=1}^{N} \sum_{s=1}^{N} \phi_{xxir}\, \phi_{xxis}\, E[Y_{xr}\ Y_{xs}] \qquad (3.93)$$

(2) y-direction

$$\sigma^2_{u_{yi}} = \sum_{r=1}^{2N} \sum_{s=1}^{2N} \phi_{y\theta ir}\, \phi_{y\theta is}\, E[Y_{y\theta r}\ Y_{y\theta s}] \qquad (3.94)$$

(3) rotation

$$\sigma^2_{u_{\theta i}} = \sum_{r=1}^{2N} \sum_{s=1}^{2N} \phi_{y\theta (i+N)r}\, \phi_{y\theta (i+N)s}\, E[Y_{y\theta r}\ Y_{y\theta s}] \qquad (3.95)$$

In addition to the quantities given by Eqs.(3.93) through (3.95), the variances of the nodal displacements are of great interest. Using Eqs. (3.1) and (3.2), the covariance function of these displacements are obtained as follows:

(1) x-direction

$$R_{u_{xik}u_{xik}}(\tau) = \langle u_{xik}(t)\, u_{xik}(t+\tau) \rangle$$

$$= R_{u_{xi}u_{xi}}(\tau) + y^2_{ik}\, R_{u_{\theta i}u_{\phi i}}(\tau) - y_{ik}[R_{u_{xi}u_{\theta i}}(\tau) + R_{u_{\theta i}u_{xi}}(\tau)] \qquad (3.96)$$

(2) y-direction

$$R_{u_{yik}u_{yik}}(\tau) = \langle u_{yik}(t)\, u_{yik}(t+\tau) \rangle$$

$$= R_{u_{yi}u_{yi}}(\tau) + x_{ik}^2 R_{u_{\theta i}u_{\theta i}}(\tau) + x_{ik}[R_{u_{yi}u_{\theta i}}(\tau) + R_{u_{\theta i}u_{xi}}(\tau)] \tag{3.97}$$

Taking the Fourier transform of Eqs. (3.96) and (3.97), one obtains the spectral density functions for the nodal displacements as follows:

(1) x-direction

$$S_{u_{xik}u_{xik}}(\omega) = S_{u_{xi}u_{xi}}(\omega) + y_{ik}^2 S_{u_{\theta i}u_{\theta i}}(\omega) - y_{ik}[S_{u_{xi}u_{\theta i}}(\omega) + S_{u_{\theta i}u_{xi}}(\omega)] \tag{3.98}$$

(2) y-direction

$$S_{u_{yik}u_{yik}}(\omega) = S_{u_{yi}u_{yi}}(\omega) + x_{ik}^2 S_{u_{\theta i}u_{\theta i}}(\omega) + x_{ik}[S_{u_{yi}u_{\theta i}}(\omega) + S_{u_{\theta i}u_{xi}}(\omega)] \tag{3.99}$$

Integrating Eqs. (3.98) and (3.99) the variances of the nodal displacements can be written as:

(1) x-direction

$$\sigma_{u_{xik}}^2 = \sigma_{u_{xi}}^2 + y_{ik}^2 \sigma_{u_{\theta i}}^2 - y_{ik}\{E[u_{xi}u_{\theta i}] + E[u_{\theta i}u_{xi}]\} \tag{3.100}$$

(2) y-direction

$$\sigma_{u_{yik}}^2 = \sigma_{u_{yi}}^2 + x_{ik}^2 \sigma_{u_{\theta i}}^2 + x_{ik}\{E[u_{yi}u_{\theta i}] + E[u_{\theta i}u_{yi}]\} \tag{3.101}$$

where $\sigma^2_{u_{xi}}$, $\sigma^2_{u_{yi}}$ and $\sigma^2_{u_{\theta i}}$ are obtained in Eqs. (3.93) through (3.95). The average products of responses in translation and rotation are determined using Eqs. (3.92), i.e.

$$E[u_{xi}u_{\theta i}] = E[u_{\theta i}\ u_{xi}] = \sum_{r=1}^{N}\sum_{s=1}^{2N} \phi_{xxir}\ \phi_{y\theta(j+N)s}\ E[Y_{xr}Y_{y\theta s}] \tag{3.102}$$

$$E[u_{yi}u_{\theta i}] = E[u_{\theta i}\ u_{yi}] = \sum_{r=1}^{2N}\sum_{s=1}^{2N} \phi_{y\theta ir}\ \phi_{y\theta(j+N)s}\ E[Y_{y\theta r}\ Y_{y\theta s}] \tag{3.103}$$

Knowing the structural displacement vector $\{U(t)\}$, shear forces and twisting moments are readily calculated using the transformation

$$\{V(t)\} = [T_s]\ [K]\ \{U(t)\} \tag{3.104}$$

where the transformation matrix $[T_s]$ is

$$[T_s] = \left[\begin{array}{c|c|c} [L] & 0 & 0 \\ \hline 0 & [L] & 0 \\ \hline 0 & 0 & [L] \end{array}\right] \tag{3.105}$$

where $[L]$ is a lower triangular matrix; where $\ell_{ij} = 1 \quad j \le i$ and $\ell_{ij} = 0\ j > i$. Consistent with previous partitions, Eq. (3.104) can be written in the form

$$\left\{\begin{array}{c} \{V_x(t)\} \\ \hline \{V_y(t)\} \\ \hline \{M_t(t)\} \end{array}\right\} = \left[\begin{array}{c|c|c} [L] & 0 & 0 \\ \hline 0 & [L] & 0 \\ \hline 0 & 0 & [L] \end{array}\right] \left[\begin{array}{c|c|c} [K_{xx}] & 0 & 0 \\ \hline 0 & [K_{yy}] & [K_{y\theta}] \\ \hline 0 & [K_{\theta y}] & [K_{\theta\theta}] \end{array}\right] \left[\begin{array}{c|c} [\phi_{xx}] & 0 \\ \hline 0 & [\phi_{y\theta}] \end{array}\right] \left\{\begin{array}{c} \{Y_x\} \\ \hline \{Y_{y\theta}\} \end{array}\right\} \tag{3.106}$$

Thus the coefficients for transforming the response in normal coordinates into the following response quantities at the i th level

of structure are:

(1) shear force in x-direction

$$B_{V_{xir}} = \sum_{j=1}^{N} \phi_{xxjr} \sum_{\ell=1}^{i} k_{xx\ell j} \tag{3.107}$$

(2) shear force in y-direction

$$B_{V_{yir}} = \sum_{j=1}^{N} \phi_{y\theta jr} \sum_{\ell=1}^{i} k_{yy\ell j} + \sum_{j=1}^{N} \phi_{y\theta(j+N)r} \sum_{\ell=1}^{i} k_{y\theta\ell j} \tag{3.108}$$

(3) twisting moment

$$B_{M_{tir}} = \sum_{j=1}^{N} \phi_{y\theta jr} \sum_{\ell=1}^{i} k_{\theta y\ell j} + \sum_{j=1}^{N} \phi_{y\theta(j+N)r} \sum_{\ell=1}^{i} k_{\theta\theta\ell j} \tag{3.109}$$

Substituting Eqs. (3.107) through (3.109) into Eqs. (3.92), one obtains for the i th level of the structure:

(1) shear force variance in x-direction

$$\sigma^2_{V_{xi}} = \sum_{r=1}^{N} \sum_{s=1}^{N} B_{V_{xir}} B_{V_{xis}} E[Y_{xr} Y_{xs}] \tag{3.110}$$

(2) shear force variance in y-direction

$$\sigma^2_{V_{yi}} = \sum_{r=1}^{2N} \sum_{s=1}^{2N} B_{V_{yir}} B_{V_{yis}} E[Y_{y\theta r} Y_{y\theta s}] \tag{3.111}$$

(3) twisting moment variance

$$\sigma^2_{M_{ti}} = \sum_{r=1}^{2N} \sum_{s=1}^{2N} B_{M_{tir}} B_{M_{tis}} E[Y_{y\theta r} Y_{y\theta s}] \tag{3.112}$$

Bending moments in the structure are obtained by integrating

the shear forces; thus the bending moments at level i(i=2,3,---,N+1) are:

(1) x-direction

$$M_{b_{xi}}(t) = \sum_{j=1}^{i-1} (z_{j+1} - z_j)\, V_{xj}(t) = \sum_{j=1}^{i-1} (z_{j+1} - z_j) \sum_{r=1}^{N} B_{V_{xjr}}\, Y_{xr}(t) \tag{3.113}$$

where z_j is the vertical coordinate of the j th level.

(2) y-direction

$$M_{b_{yi}}(t) = \sum_{j=1}^{i-1} (z_{j+1} - z_j)\, V_{yj}(t) = \sum_{j=1}^{i-1} (z_{j+1} - z_j) \sum_{r=1}^{2N} B_{V_{yjr}}\, Y_{y\theta r}(t) \tag{3.114}$$

Examining Eqs. (3.113) and (3.114) it is easily seen that the transformation coefficients are for bending moments in x-direction

$$B_{M_{bxir}} = \sum_{j=1}^{i-1} (z_{j+1} - z_j)\, B_{V_{xjr}} = \sum_{j=1}^{i-1} (z_{j+1} - z_j) \sum_{m=1}^{N} \phi_{xxmr} \sum_{\ell=1}^{j} k_{xx\ell m} \tag{3.115}$$

and for bending moments in y-direction

$$B_{M_{byir}} = \sum_{j=1}^{i-1} (z_{j+1} - z_j)\, B_{V_{yjr}} = \sum_{j=1}^{i-1} (z_{j+1} - z_j) \sum_{m=1}^{N} \{\phi_{y\theta mr} \sum_{\ell=1}^{j} k_{yy\ell m} + \phi_{y\theta(m+N)r} \sum_{\ell=1}^{j} k_{y\theta\ell m}\} \tag{3.116}$$

Substituting Eqs. (3.115) and (3.116) into Eq. (3.92), the bending moment variances are readily determined to be:

(1) x-direction

$$\sigma^2_{M_{bxi}} = \sum_{r=1}^{N} \sum_{s=1}^{N} B_{M_{bxir}}\, B_{M_{bxis}}\, E[Y_{xr}\, Y_{xs}] \tag{3.117}$$

(2) y-direction

$$\sigma^2_{M_{byi}} = \sum_{r=1}^{2N} \sum_{s=1}^{2N} B_{M_{byir}} B_{M_{byis}} E[Y_{y\theta r} Y_{y\theta s}] \qquad (3.118)$$

Even though shear force and bending moment variances are determined by Eqs. (3.110), (3.111), (3.117) and (3.118), no effect of rotation of the structure has been included in these formulas. This effect varies linearly with the distance from the vertical z-axis, see Fig. 3.1. Numbering the tower legs 1, 2, 3, and 4, consistent with the node numbering on the idealized tower with 4 legs, it is seen that the effect of rotation is largest in the frames consisting of the following legs and their interconnections:

FRAME	LEG NOS.	STIFFNESS MATRIX	ARM AT LEVEL I
A	1 and 2	$[KF_{AB}]$	$a_{ABi} = \frac{\lvert y_{i1}+y_{i2}\rvert}{2}$
B	3 and 4		
C	1 and 3	$[KF_C]$	$a_{Ci} = \lvert x_{i1}\rvert$
D	2 and 4	$[KF_D]$	$a_{Di} = \lvert x_{i2}\rvert$

Table 3.1 FRAMES CONSISTING OF TOWER LEGS

It should be noted that Frames A and B are not always parallel to the x-axis, but they are in this part of the investigation considered to be parallel to the x-axis. The arms used for taking the rotational effects into account are the mean distances from the xz-plane at each level.

The shear force in any of the frames can be written as:

$$\{V_F(t)\} = [L]\ [KF]\ \{U_F(t)\} \tag{3.119}$$

where [L] is defined in Eq. (3.105); [KF] represents the frame stiffness coefficients; and $\{U_F(t)\}$ represents the frame displacements. Referring to Fig. 3.2 and Table 3.1, the displacements at level i are as follows:

(1) frame A

$$u_{F_{Ai}}(t) = u_{xi}(t) + a_{ABi}\ \ u_{\theta i}(t) \tag{3.120}$$

(2) frame B

$$u_{F_{Bi}}(t) = u_{xi}(t) - a_{ABi}\ \ u_{\theta i}(t) \tag{3.121}$$

(3) frame C

$$u_{F_{Ci}}(t) = u_{yi}(t) - a_{Ci}\ u_{\theta i}(t) \tag{3.122}$$

(4) frame D

$$u_{F_{Di}}(t) = u_{yi}(t) + a_{Di}\ u_{\theta i}(t) \tag{3.123}$$

Thus the shear force at level can be expressed as follows:

(1) frame A

$$V_{F_{Ai}}(t) = \sum_{r=1}^{N} B_{V_{ABxir}} Y_{xr}(t) + \sum_{r=1}^{2N} B_{V_{AB\theta ir}} Y_{y\theta r}(t) \tag{3.124}$$

where

$$B_{V_{ABxir}} = \sum_{j=1}^{N} \phi_{xxjr} \sum_{\ell=1}^{i} kf_{AB\ell j} \tag{3.125}$$

where the kf's are the stiffness coefficients of the frame and

where

$$B_{V_{AB\theta ir}} = \sum_{j=1}^{N} \phi_{y\theta(j+N)r}\, a_{ABj} \sum_{\ell=1}^{i} kf_{AB\ell j} \tag{3.126}$$

(2) frame B

$$V_{F_{Bi}}(t) = \sum_{r=1}^{N} B_{V_{ABxir}} Y_{xr}(t) - \sum_{r=1}^{2N} B_{V_{AB\theta ir}} Y_{y\theta r}(t) \tag{3.127}$$

(3) frame C

$$V_{F_{Ci}}(t) = \sum_{r=1}^{2N} B_{V_{Cir}} Y_{y\theta r}(t) \tag{3.128}$$

where

$$B_{V_{Cir}} = \sum_{j=1}^{N} [\phi_{y\theta jr} - \phi_{y\theta(j+N)r}\, a_{Cj}] \sum_{\ell=1}^{i} kf_{C\ell j} \tag{3.129}$$

(4) frame D

$$V_{F_{Di}}(t) = \sum_{r=1}^{2N} B_{V_{Dir}} Y_{y\theta r}(t) \tag{3.130}$$

where

$$B_{V_{Dir}} = \sum_{j=1}^{N} [\phi_{y\theta jr} + \phi_{y\theta(j+N)r}\, a_{Dj}] \sum_{\ell=1}^{i} kf_{D\ell j} \tag{3.131}$$

Substituting Eqs. (3.124), (3.127), (3.128) and (3.130) into Eq. (3.92) the variances of shear forces caused by combined translation and rotation are obtained as follows:

(1) frame A

$$\sigma^2_{V_{FAi}} = E[V_1^2] + 2E[V_1\, V_2] + E[V_2^2] \tag{3.132}$$

where

$$E[V_1^2] = \sum_{r=1}^{N} \sum_{s=1}^{N} B_{V_{ABxir}} B_{V_{ABxis}} E[Y_{xr}\, Y_{xs}] \tag{3.133}$$

$$E[V_1\ V_2] = \sum_{r=1}^{N} \sum_{s=1}^{2N} B_{V_{ABxir}} B_{V_{AB\theta is}} E[Y_{xr}\ Y_{y\theta s}] \tag{3.134}$$

$$E[V_2^2] = \sum_{r=1}^{2N} \sum_{s=1}^{2N} B_{V_{AB\theta ir}} B_{V_{AB\theta is}} E[Y_{y\theta r}\ Y_{y\theta s}] \tag{3.135}$$

(2) frame B

$$\sigma^2_{V_{FBi}} = E[V_1^2] - 2E[V_1\ V_2] + E[V_2^2] \tag{3.136}$$

(3) frame C

$$\sigma^2_{V_{FCi}} = \sum_{r=1}^{2N} \sum_{s=1}^{2N} B_{V_{Cir}} B_{V_{Cis}} E[Y_{y\theta r}\ Y_{y\theta s}] \tag{3.137}$$

(4) frame D

$$\sigma^2_{V_{FDi}} = \sum_{r=1}^{2N} \sum_{s=1}^{2N} B_{V_{Dir}} B_{V_{Dis}} E[Y_{y\theta r}\ Y_{y\theta s}] \tag{3.138}$$

Bending moments in these frames are obtained by integrating the shear forces, thus the transformation coefficients for bending moments at level i(i = 2,3,---,N+1) are obtained, i.e.

(1) frames A and B

$$B_{M_{ABxir}} = \sum_{j=1}^{i-1} (z_{j+1} - z_j)\, B_{V_{ABxjr}} \tag{3.139}$$

where z_j is the vertical coordinate of level j and $B_{V_{ABxjr}}$ is given by Eq. (3.125) and

$$B_{M_{AB\theta ir}} = \sum_{j=1}^{i-1} (z_{j+1} - z_j)\, B_{V_{AB\theta jr}} \tag{3.140}$$

where $B_{V_{AB\theta jr}}$ is given by Eq. (3.126)

(2) frame C

$$B_{M_{Cir}} = \sum_{j=1}^{i-1} (z_{j+1} - z_j) B_{V_{Cjr}} \tag{3.141}$$

where $B_{V_{Cjr}}$ is given by Eq. (3.129)

(3) frame D

$$B_{M_{Dir}} = \sum_{j=1}^{i-1} (z_{j+1} - z_j) B_{V_{Djr}} \tag{3.142}$$

where $B_{V_{Djr}}$ is given by Eq. (3.131).

Using Eq. (3.92) and Eqs. (3.139) through (3.142) and noting the expressions for the shear force, Eqs. (3.124), (3.127), (3.128) and (3.130), the variances of the bending moments caused by combined translation and rotation are obtained:

(1) frame A

$$\sigma^2_{M_{FAi}} = E[M_1^2] + 2E[M_1 M_2] + E[M_2^2] \tag{3.143}$$

where

$$E[M_1^2] = \sum_{r=1}^{N} \sum_{s=1}^{N} B_{M_{ABxir}} B_{M_{ABxis}} E[Y_{xr} Y_{xs}] \tag{3.144}$$

$$E[M_1 M_2] = \sum_{r=1}^{N} \sum_{s=1}^{2N} B_{M_{ABxir}} B_{M_{AB\theta is}} E[Y_{xr} Y_{y\theta s}] \tag{3.145}$$

$$E[M_2^2] = \sum_{r=1}^{2N} \sum_{s=1}^{2N} B_{M_{AB\theta ir}} B_{M_{AB\theta is}} E[Y_{y\theta r} Y_{y\theta s}] \tag{3.146}$$

(2) frame B

$$\sigma^2_{M_{FBi}} = E[M_1^2] - 2E[M_1 M_2] + E[M_2^2] \tag{3.147}$$

(3) frame C

$$\sigma^2_{M_{FCi}} = \sum_{r=1}^{2N} \sum_{s=1}^{2N} B_{M_{Cir}} B_{M_{Cis}} E[Y_{y\theta r} Y_{y\theta s}] \quad (3.148)$$

(4) frame D

$$\sigma^2_{M_{FDi}} = \sum_{r=1}^{2N} \sum_{s=1}^{2N} B_{M_{Dir}} B_{M_{Dis}} E[Y_{y\theta r} Y_{y\theta s}] \quad (3.149)$$

E. STATISTICS OF RELATIVE VELOCITIES BETWEEN WATER PARTICLES AND STRUCTURE

Referring to the linearization procedure for the drag force, section B, it is mentioned that it is necessary to calculate the variances of the relative velocities between water particles and structure at the nodes where the wave forces are applied. At node k at level i these relative velocities are:

(1) x-direction

$$\dot{v}_{rxik}(t) = \dot{v}_{xik}(t) - \dot{u}_{xik}(t) \quad (3.150)$$

(2) y-direction

$$\dot{v}_{ryik}(t) = \dot{v}_{yik}(t) - \dot{u}_{yik}(t) \quad (3.151)$$

Substituting Eq. (3.1) into Eq. (3.150) and Eq. (3.2) into Eq. (3.151), the relative velocities become

$$\dot{v}_{rxik}(t) = \dot{v}_{xik}(t) - \dot{u}_{xi} + y_{ik}\,\dot{u}_{\theta i} \quad (3.152)$$

$$\dot{v}_{ryik}(t) = \dot{v}_{yik}(t) - \dot{u}_{yi} - x_{ik}\,\dot{u}_{\theta i} \quad (3.153)$$

Thus the auto-covariance functions for the relative velocities are:

(1) x-direction

$$R_{\dot{v}_{rxik}\dot{v}_{rxik}}(\tau) = \langle \dot{v}_{rxik}(t)\ \dot{v}_{rxik}(t+\tau) \rangle$$

$$= R_{\dot{v}_{xik}\dot{v}_{xik}}(\tau) + R_{\dot{u}_{xi}\dot{u}_{xi}}(\tau) + y_{ik}^2\ R_{\dot{u}_{\theta i}\ \dot{u}_{\theta i}}(\tau)$$

$$- R_{\dot{v}_{xik}\dot{u}_{xi}}(\tau) - R_{\dot{u}_{xi}\ \dot{v}_{xik}}(\tau) + y_{ik}[R_{\dot{v}_{xik}\dot{u}_{\theta i}}(\tau)$$

$$+ R_{\dot{u}_{\theta i}\ \dot{v}_{xik}}(\tau) - R_{\dot{u}_{xi}\dot{u}_{\theta i}}(\tau) - R_{\dot{u}_{\theta i}\ \dot{u}_{xi}}(\tau)] \qquad (3.154)$$

(2) y-direction

$$R_{\dot{v}_{ryik}\dot{v}_{ryik}}(\tau) = \langle \dot{v}_{ryik}(t)\ \dot{v}_{ryik}(t+\tau) \rangle$$

$$= R_{\dot{v}_{yik}\dot{v}_{yik}}(\tau) + R_{\dot{u}_{yi}\dot{u}_{yi}}(\tau) + x_{ik}^2\ R_{\dot{u}_{\theta i}\ \dot{u}_{\theta i}}(\tau)$$

$$- R_{\dot{v}_{yik}\dot{u}_{yi}}(\tau) - R_{\dot{u}_{yi}\dot{v}_{yik}}(\tau) - x_{ik}[R_{\dot{v}_{yik}\dot{u}_{\theta i}}(\tau)$$

$$+ R_{\dot{u}_{\theta i}\dot{v}_{yik}}(\tau) - R_{\dot{u}_{yi}\dot{u}_{\theta i}}(\tau) - R_{\dot{u}_{\theta i}\dot{u}_{yi}}(\tau)] \qquad (3.155)$$

Taking the Fourier transforms of Eq. (3.154) and Eq. (3.155) one obtains the spectral density functions for the relative velocities:

(1) x-direction

$$S_{\dot{v}_{rxik}\dot{v}_{rxik}}(\omega) = S_{\dot{v}_{xik}\dot{v}_{xik}}(\omega) + S_{\dot{u}_{xi}\dot{u}_{xi}}(\omega)$$

$$+ y_{ik}^2\ S_{\dot{u}_{\theta i}\dot{u}_{\theta i}}(\omega) - S_{\dot{v}_{xik}\dot{u}_{xi}}(\omega) - S_{\dot{u}_{xi}\dot{v}_{xik}}(\omega) \qquad (3.156)$$

$$+ y_{ik}[S_{\dot{v}_{xik}\dot{u}_{\theta i}}(\omega) + S_{\dot{u}_{\theta i}\dot{v}_{xik}}(\omega) - S_{\dot{u}_{xi}\dot{u}_{\theta i}}(\omega) - S_{\dot{u}_{\theta i}\dot{u}_{xi}}(\omega)]$$

(2) y-direction

$$S_{\dot{v}_{ryik}\dot{v}_{ryik}}(\omega) = S_{\dot{v}_{yik}\dot{v}_{yik}}(\omega) + S_{\dot{u}_{yi}\dot{u}_{yi}}(\omega) + x_{ik}^2 S_{\dot{u}_{\theta i}\dot{u}_{\theta i}}(\omega)$$

$$- S_{\dot{v}_{yik}\dot{u}_{yi}}(\omega) - S_{\dot{u}_{yi}\dot{v}_{yik}}(\omega) - x_{ik}[S_{\dot{v}_{yik}\dot{u}_{\theta i}}(\omega)$$

$$+ S_{\dot{u}_{\theta i}\dot{v}_{yik}}(\omega) - S_{\dot{u}_{yi}\dot{u}_{\theta i}}(\omega) - S_{\dot{u}_{\theta i}\dot{u}_{yi}}(\omega)] \qquad (3.157)$$

Thus the variances of the relative velocities are obtained as:

(1) x-direction

$$\sigma^2_{\dot{v}_{rxik}} = \sigma^2_{\dot{v}_{xik}} + \sigma^2_{\dot{u}_{xi}} + y_{ik}^2 \sigma^2_{\dot{u}_{\theta i}} - 2E[\dot{v}_{xik}\dot{u}_{xi}]$$

$$+ 2\, y_{ik}\{E[\dot{v}_{xik}\dot{u}_{\theta i}] - E[\dot{u}_{xi}\,\dot{u}_{\theta i}]\} \qquad (3.158)$$

(2) y-direction

$$\sigma^2_{\dot{v}_{ryik}} = \sigma^2_{\dot{v}_{yik}} + \sigma^2_{\dot{u}_{yi}} + x_{ik}^2 \sigma^2_{\dot{u}_{\theta i}} - 2E[\dot{v}_{yik}\dot{u}_{yi}]$$

$$- 2\, x_{ik}\{E[\dot{v}_{yik}\dot{u}_{\theta i}] - E[\dot{u}_{yi}\dot{u}_{\theta i}]\} \qquad (3.159)$$

In Eqs. (3.158) and (3.159) $\sigma^2_{\dot{v}_{xik}}$ and $\sigma^2_{\dot{v}_{yik}}$ are obtained by integrating the spectral density functions for water particle velocities, Eq. (4.47), over the frequency range. Using Eqs. (3.88) and (3.92) one obtains these expressions:

$$\sigma^2_{\dot{u}_x} = \sum_{r=1}^{N}\sum_{s=1}^{N} \phi_{xxir}\,\phi_{xxis}\,E[\dot{Y}_{xr}\,\dot{Y}_{xs}] \qquad (3.160)$$

$$\sigma^2_{\dot{u}_y} = \sum_{r=1}^{2N}\sum_{s=1}^{2N} \phi_{y\theta ir}\,\phi_{y\theta is}\,E[\dot{Y}_{y\theta r}\,\dot{Y}_{y\theta s}] \qquad (3.161)$$

$$\sigma^2_{\dot{u}_\theta} = \sum_{r=1}^{2N} \sum_{s=1}^{2N} \phi_{y\theta(i+N)r}\, \phi_{y\theta(i+N)s}\, E[\dot{Y}_{y\theta r}\, \dot{Y}_{y\theta s}] \qquad (3.162)$$

$$E[\dot{u}_{xi}\, \dot{u}_{\theta i}] = \sum_{r=1}^{N} \sum_{s=1}^{2N} \phi_{xxir}\, \phi_{y\theta(i+N)s}\, E[\dot{Y}_{xr}\, \dot{Y}_{y\theta s}] \qquad (3.163)$$

$$E[\dot{u}_{yi}\, \dot{u}_{\theta i}] = \sum_{r=1}^{2N} \sum_{s=1}^{2N} \phi_{y\theta ir}\, \phi_{y\theta(i+N)s}\, E[\dot{Y}_{y\theta r}\, \dot{Y}_{y\theta s}] \qquad (3.164)$$

It is necessary, however, to derive expressions for the average products of water particle velocities and structural velocities in order to determine all terms in Eqs. (3.158) and (3.159). For this purpose, consider the covariance function for water particle velocity and structural velocity, namely

$$R_{\dot{v}_{xik}\dot{u}_{xi}}(\tau) = \frac{\partial}{\partial t} R_{\dot{v}_{xik}u_{xi}}(\tau) \qquad (3.165)$$

Thus one can determine the covariance function for water particle velocity and structural displacement, i.e.

$$R_{\dot{v}_{xik}u_{xi}}(\tau) = \langle \dot{v}_{xik}(t)\, u_{xi}(t+\tau) \rangle = \langle \dot{v}_{xik}(t-\tau)\, u_{xi}(t) \rangle \qquad (3.166)$$

Substituting Eqs. (3.50) and (3.71) into Eq. (3.166) gives:

$$R_{\dot{v}_{xik}u_{xi}}(\tau) = \langle \dot{v}_{xik}(t-\tau) \sum_{r=1}^{N} \phi_{xxir} \int_{-\infty}^{t} P^*_{xr}(\gamma)\, h_{xr}(t-\gamma)\, d\gamma \rangle \qquad (3.167)$$

where γ is a dummy time variable. Substituting the value of P^*_{xr}, Eq. (3.62), into Eq. (3.167), gives

$$R_{\dot{v}_{xik}u_{xi}}(\tau) = \sum_{r=1}^{N}\sum_{j=1}^{N}\phi_{xxir}\,\phi_{xxjr}\sum_{\ell=1}^{NNP}\int_{-\infty}^{t}\left[\alpha_{j\ell}\,R_{\dot{v}_{xik}\ddot{v}_{xj\ell}}(\gamma-t+\tau)\right.$$

$$\left.+\,\beta_{xj\ell}\,R_{\dot{v}_{xik}\dot{v}_{xj\ell}}(\gamma-t+\tau)\right]h_{xr}(t-\gamma)\,d\gamma \qquad (3.168)$$

Taking the Fourier transform of Eq. (3.168), the cross spectral density function for water particle velocity and structural displacement is obtained. For this purpose, consider the typical transformation

$$S_0(\omega) = \frac{1}{2\pi}\int_{-\infty}^{\infty}\int_{-\infty}^{t} R_i(\gamma-t+\tau)\,h\,(t-\gamma)\,d\gamma\,e^{-i\omega\tau}\,d\tau \qquad (3.169)$$

Holding γ constant while integrating with respect to τ by introducing a new variable $\gamma_1 = \gamma-t+\tau$, Eq. (3.169) can be expressed in the form

$$S_0(\omega) = \int_{-\infty}^{t} h(t-\gamma)e^{-i\omega(t-\gamma)}\,d\gamma\,\frac{1}{2\pi}\int_{-\infty}^{\infty} R_i(\gamma_1)\,e^{-i\omega\gamma_1}\,d\gamma_1$$

$$= H(i\omega)\,S_i(\omega) \qquad (3.170)$$

since $h(t-\gamma) = 0$ for $\gamma > t$.

Substituting Eq. (3.168) into Eq. (3.169) the cross spectral density function for water particle and structural velocities in the x-direction is obtained in the form:

$$S_{\dot{v}_{xik}\dot{u}_{xi}}(\omega) = i\omega\,S_{\dot{v}_{xik}u_{xi}}(\omega) = \sum_{r=1}^{N}\phi_{xir}\,i\omega\,H_{xr}(i\omega)$$

$$\sum_{j=1}^{N}\phi_{xxjr}\sum_{\ell=1}^{NNP}\left[\alpha_{j\ell}\,S_{\dot{v}_{xik}\ddot{v}_{xj\ell}}(\omega)+\beta_{xj\ell}\,S_{\dot{v}_{xik}\dot{v}_{xj\ell}}(\omega)\right] \qquad (3.171)$$

The cross spectral density functions for water particle and structural velocities in other directions are readily obtained by

substituting the appropriate terms into Eq. (3.169), i.e.

$$S_{\dot{v}_{xik}\dot{u}_{\theta i}}(\omega) = \sum_{r=1}^{2N} \phi_{y\theta(i+N)r}\, i\omega\, H_{y\theta r}(i\omega)$$

$$\{\sum_{j=1}^{N} \phi_{y\theta jr} \sum_{\ell=1}^{NNP} [\alpha_{j\ell}\, S_{\dot{v}_{xik}\ddot{v}_{yj\ell}}(\omega) + \beta_{yj\ell}\, S_{\dot{v}_{xik}\dot{v}_{yj\ell}}(\omega)]$$

$$+ \sum_{j=1}^{N} \phi_{y\theta(j+N)r} \sum_{\ell=1}^{NNP} [-y_{j\ell}\,(\alpha_{j\ell}\, S_{\dot{v}_{xik}\ddot{v}_{xj\ell}}(\omega) + \beta_{xj\ell}\, S_{\dot{v}_{xik}\dot{v}_{xj\ell}}(\omega))$$

$$+ x_{j\ell}\,(\alpha_{j\ell}\, S_{\dot{v}_{xik}\ddot{v}_{yj\ell}}(\omega) + \beta_{yj\ell}\, S_{\dot{v}_{xik}\dot{v}_{yj\ell}}(\omega))]\} \qquad (3.172)$$

$$S_{\dot{v}_{yik}\dot{u}_{yi}} = \sum_{r=1}^{2N} \phi_{y\theta ir}\, S^{*}_{ir}(\omega) \qquad (3.173)$$

$$S_{\dot{v}_{yik}\dot{u}_{\theta i}} = \sum_{r=1}^{2N} \phi_{y\theta(i+N)r}\, S^{*}_{ir}(\omega) \qquad (3.174)$$

where

$$S^{*}_{ir}(\omega) = i\omega\, H_{y\theta r}(i\omega)\, \{\sum_{j=1}^{N} \phi_{y\theta jr} \sum_{\ell=1}^{NNP} [\alpha_{j\ell}\, S_{\dot{v}_{yik}\ddot{v}_{yj\ell}}(\omega)$$

$$+ \beta_{yj\ell}\, S_{\dot{v}_{yik}\dot{v}_{yj\ell}}(\omega)] + \sum_{j=1}^{N} \phi_{y\theta(j+N)r} \sum_{\ell=1}^{NNP} [-y_{j\ell}(\alpha_{j\ell}\, S_{\dot{v}_{yik}\ddot{v}_{xj\ell}}(\omega)$$

$$+ \beta_{xj\ell}\, S_{\dot{v}_{yik}\dot{v}_{xj\ell}}(\omega)) + x_{j\ell}(\alpha_{j\ell}\, S_{\dot{v}_{yik}\ddot{v}_{yj\ell}}(\omega) + \beta_{yj\ell}\, S_{\dot{v}_{yik}\dot{v}_{yj\ell}}(\omega))]\} \qquad (3.175)$$

Integrating Eqs. (3.171) through (3.174) over the frequency range, all terms in Eqs. (3.158) and (3.159) are obtained, since

$$E[x_1\, x_2] = \int_{-\infty}^{\infty} S_{x_1\, x_2}(\omega)\, d\omega \qquad (3.176)$$

Thus, the variances of the relative velocities between water particles and structures are obtained as needed for linearization of the drag force.

CHAPTER IV

STATISTICAL EXPRESSIONS FOR WATER PARTICLE MOTIONS

A. DIRECTIONAL SPECTRA

The directional spectrum specifies the distribution of wave energy with respect to frequency and direction. Because ocean waves are rather irregular, they cannot be specified by a single function like a sinusoid. A general accepted assumption, however, is to consider the sea surface elevation to be the sum of a large number of small harmonic waves of various frequencies and travelling in different directions. This is the reason why one is interested in the distribution of energy with respect to frequency and direction.

The contribution to the surface elevation at a fixed location from the i th sinusoid may be expressed as

$$\eta_i = a_i \sin (\omega_i t + \psi_i) \qquad (4.1)$$

where a_i is the amplitude, ω_i is the frequency, and ψ_i is the phase angle.

The phase angle ψ_i is random and is assumed to have uniform probability density between 0 and 2π radians. It is also assumed that all ψ_i's are statistical independent, and that none of the harmonics dominates the wave profile. Letting the number of these harmonics go to infinity, the individual amplitudes must go to zero in order to maintain finite wave height. Applying the central limit theorem, the random wave process can be considered to be Gaussian. It may be noted that it is generally accepted to consider random ocean waves as a zero

mean stationary and ergodic Gaussian process [34, pg. 343].

The ocean surface elevation may therefore be described by a power spectrum, $S_{\eta\eta}(\omega,\theta)$, which is called the directional spectrum. Figure 4.1 shows a 3-dimensional plot of this spectrum. Considering the prism indicated in Fig. 4.1, the directional spectral density, $S_{\eta\eta}(\omega,\theta)$, has the property that $S_{\eta\eta}(\omega,\theta)\Delta\omega\Delta\theta$ is the mean square amplitude of the waves with frequencies and directions within the $\Delta\omega\Delta\theta$ rectangle. The volume enclosed by the directional spectrum and the ω - θ plane is therefore equal to the mean square wave amplitude.

Although the importance of the directional distribution of ocean waves is acknowledged, the use of directional spectra in design of structures in the ocean environment have been rather limited. The major reason for this is lack of measured directional spectra, and therefore computational techniques using directional spectra have not been developed to any extent. Some directional spectra, however, have been obtained in the laboratory and in the ocean.[1]

In computations it is desirable to express the directional spectrum as a product of a function of frequency and a function of direction, i.e.

$$S_{\eta\eta}(\omega,\theta) = D_{\omega}(\theta)\, S_{\eta\eta}(\omega) \qquad (4.2)$$

where $D_{\omega}(\theta)$ is the directional distribution of energy at frequency ω and where $S_{\eta\eta}(\omega) = \int_0^{2\pi} S_{\eta\eta}(\omega,\theta)\, d\theta$ is the one-dimensional wave spectral density function. It may be noted that $D_{\omega}(\theta)$ is always positive and that

$$\int_0^{2\pi} D_{\omega}(\theta)\, d\theta = \frac{1}{S_{\eta\eta}(\omega)} \int_0^{2\pi} S_{\eta\eta}(\omega,\theta)\, d\theta = 1 \qquad (4.3)$$

---

[1] An extensive biography may be found in [36].

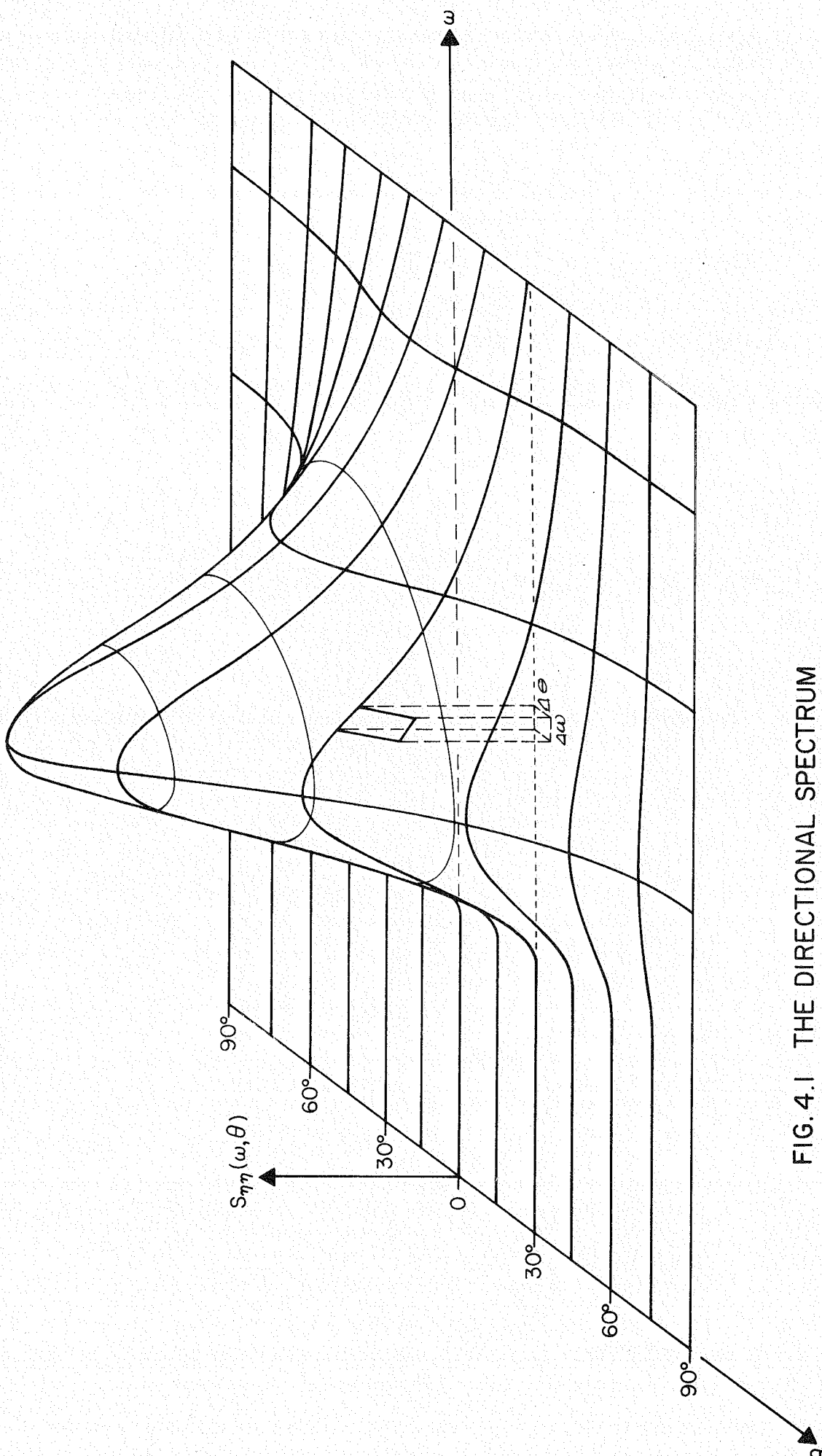

FIG. 4.1 THE DIRECTIONAL SPECTRUM

The subscript ω indicates that the directional distribution $D_\omega(\theta)$ pertains to a frequency ω. Normally low frequency waves have directional distributions that are fairly concentrated about the mean direction of wave advance, while the angular spread tends to be wider toward higher frequencies.

Borgman [35] and Panicker [36] have described several possible forms for $D_\omega(\theta)$ as follows:

(1) a finite Fourier series

$$D(\theta) = \frac{a_0}{2} + \sum_{n=1}^{N} (a_n \cos n\theta + b_n \sin n\theta) \qquad (4.4)$$

where a_0, a_n and b_n are the Fourier coefficients,

(2) a weighted modification of the finite Fourier series [37]

$$D(\theta) = c_0 \frac{a_0}{2} + \sum_{n=1}^{N} c_n (a_n \cos n\theta + b_n \sin n\theta) \qquad (4.5)$$

where c_0 and c_n are the weights on the Fourier coefficients.

(3) the circular normal [38]

$$D_\omega(\theta) = \frac{1}{2\pi I_0(a)} \exp [a \cos (\theta - \alpha)] \qquad (4.6)$$

where $I_0(a)$ is a modified Bessel function of zero order and a is a measure of the concentration about the mean angle, α. This distribution is shown in Fig. 4.2 for α=0 and different values of a.

(4) the wrapped-around Gaussian

$$D(\theta) = \sum_{k=-\infty}^{\infty} \frac{1}{\sqrt{2\pi}\,\sigma} \exp \left(- \frac{(\theta - 2\pi k - \alpha)^2}{2\sigma^2} \right) \qquad (4.7)$$

(5) a wrapped-around Hermite series expansion

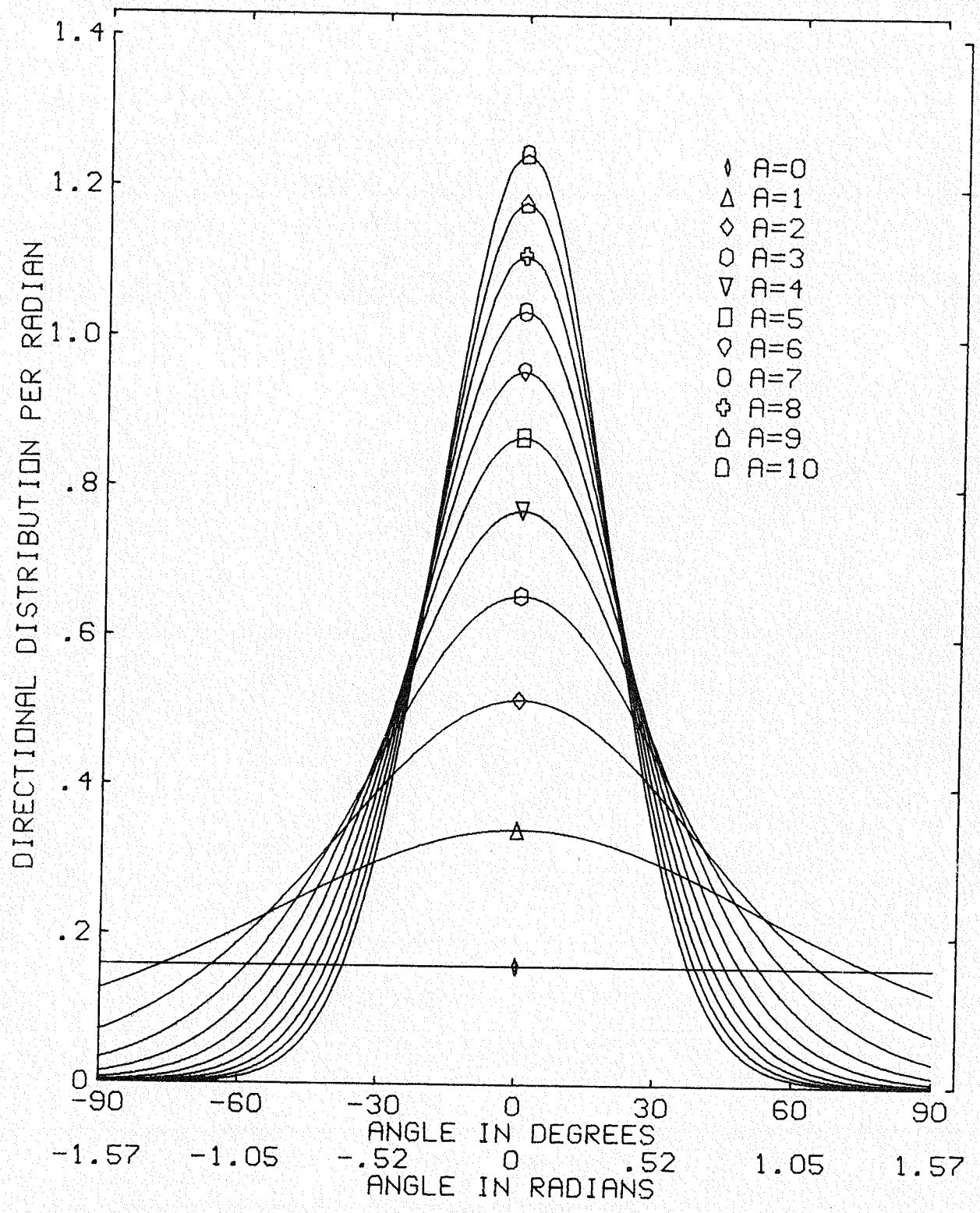

FIG. 4.2 CIRCULAR NORMAL DISTRIBUTION

$$D(\theta) = \sum_{k=-\infty}^{\infty} \left[\sum_{n=0}^{N} a_n H_n(\theta - 2\pi k - \alpha) \right] \frac{1}{\sqrt{2\pi}\,\sigma} \exp\left(-\frac{\theta - 2\pi k - \alpha}{2\sigma^2}\right) \tag{4.8}$$

where $H_n(x)$ are Hermite polynomials.

At the International Ship Structures Congress in Tokyo in 1970 [39] the following formula was proposed to be used for the directional distribution

$$D(\theta) = A \cos^n(\theta - \alpha) \quad -\frac{\pi}{2} \leq (\theta - \alpha) \leq \frac{\pi}{2} \tag{4.9}$$

where the exponent n is normally taken as 2 or 4.

The analysis procedure developed in this investigation does not set restrictions to the form of the directional distribution, $D(\theta)$. In the computational examples reasonable directional distributions are used, given by the circular normal distribution, Eq. (4.6).

B. SPECTRAL DENSITY FUNCTIONS FOR WATER PARTICLE MOTIONS

The derivation of the expressions for the water particle motions is based upon linear wave theory and that the sea state is specified by the directional spectrum. This is possible since the directional spectrum is based upon linear superposition of component waves of various frequencies and directions.

Consider a two dimensional progressive harmonic wave having the following equation for the surface ordinate η (positive upwards, base at still water level)

$$\eta = a \cos(\kappa r - \omega t) \tag{4.10}$$

where a is the amplitude, r is the horizontal distance from origin, ω is the frequency in rad/sec and κ is the radian wave number,

given by

$$\omega^2 = g \kappa \quad \tanh [\kappa d] \tag{4.11}$$

where g is the acceleration of gravity and d is the depth of water.

It is possible to derive the following velocity potential for the wave [40, pp 11-64]

$$\phi(r,z,t) = \frac{ga}{\omega} \frac{\cosh [\kappa(-z+d)]}{\cosh [\kappa d]} \sin [\kappa r - \omega t] \tag{4.12}$$

where z is the distance from the still water level (positive downwards).

If the ocean waves are considered to be the sum of a large number of harmonic waves of various frequencies and directions, the velocity potential for the harmonic wave with frequency ω_i and direction θ_j is

$$\phi_{\omega_i\theta_j}(r,z,t) = \frac{g}{\omega_i} \sqrt{2 S_{\eta\eta}(\omega_i,\theta_j) \Delta\omega\Delta\theta} \frac{\cosh [\kappa_i(-z+d)]}{\cosh [\kappa_i d]}$$

$$\sin [\kappa_i r - \omega_i t + \psi(\omega_i,\theta_j)] \tag{4.13}$$

where $\sqrt{2 S_{\eta\eta}(\omega_i,\theta_j) \Delta\omega\Delta\theta}$ is the amplitude and $\psi(\omega_i,\theta_j)$ is the phase angle.

The phase angle $\psi(\omega_i,\theta_j)$ is random and has uniform probability density between 0 and 2π radians and is statistically independent for all i and j.

Adding contributions from all harmonics in direction θ_j, and letting their number go to infinity, i.e. $\Delta\omega$ goes to zero, eliminating the acceleration of gravity term by using Eq. (4.11), the velocity

potential for waves in this direction becomes

$$\phi_{\theta_j}(r,z,t) = \int_0^\infty \frac{\omega}{\kappa} \sqrt{2\, S_{\eta\eta}(\omega,\theta_j)\, d\omega\Delta\theta}\ \frac{\cosh\,[\kappa(-z+d)]}{\sinh\,[\kappa\, d]}$$

$$\sin\,[\kappa\, r - \omega t + \psi(\omega,\theta_j)] \qquad (4.14)$$

The horizontal component of the water particle velocity for waves in direction θ_j is obtained by the partial derivative

$$\dot{v}_{\theta_j}(r,z,t) = \frac{\partial \phi_{\theta_j}(r,z,t)}{\partial r} = \int_0^\infty \omega \sqrt{2\, S_{\eta\eta}(\omega,\theta_j)\, d\omega\Delta\theta}\ \frac{\cosh\,[\kappa(-z+d)]}{\sinh\,[\kappa\, d]}$$

$$\cos\,[\kappa\, r - \omega t + \psi(\omega,\theta_j)] \qquad (4.15)$$

Likewise, the water particle acceleration is given by

$$\ddot{v}_{\theta_j}(r,z,t) = \frac{\partial \dot{v}_{\theta_j}(r,z,t)}{\partial t} = \int_0^\infty \omega^2 \sqrt{2\, S_{\eta\eta}(\omega,\theta_j)\, d\omega\Delta\theta}\ \frac{\cosh\,[\kappa(-z+d)]}{\sinh\,[\kappa\, d]}$$

$$\sin\,[\kappa\, r - \omega t + \psi(\omega,\theta_j)] \qquad (4.16)$$

The velocity and acceleration components in the orthogonal horizontal directions are

$$\dot{v}_{x_j} = \dot{v}_{\theta_j} \cos\,\theta_j \qquad (4.17)$$

$$\ddot{v}_{x_j} = \ddot{v}_{\theta_j} \cos\,\theta_j \qquad (4.18)$$

$$\dot{v}_{y_j} = \dot{v}_{\theta_j} \sin\,\theta_j \qquad (4.19)$$

$$\ddot{v}_{y_j} = \ddot{v}_{\theta_j} \sin\,\theta_j \qquad (4.20)$$

The horizontal distance from the origin in the direction of the wave, r, may be expressed by the coordinates of the considered point and the angle between the direction of the wave and the x-axis. Examining Fig. 4.3, it is easily seen that

$$r = x \cos\theta + y \sin\theta \tag{4.21}$$

Adding contributions from all directions and letting their number go to infinity, i.e. $\Delta\theta$ tends to zero, substituting Eq. (4.21) for r into Eqs. (4.15) and (4.16), expressions for water particle motions are obtained in the form

$$\dot{v}(x,y,z,t) = \int_0^{\infty} \int_0^{2\pi} \omega\, C(\theta) \sqrt{2\, S_{\eta\eta}(\omega,\theta)\, d\omega d\theta}\, \frac{\cosh[\kappa(-z+d)]}{\sinh[\kappa\, d]}$$

$$\cos[\kappa\,(x\cos\theta + y\sin\theta) - \omega t + \psi(\omega,\theta)] \tag{4.22}$$

$$\ddot{v}(z,y,z,t) = \int_0^{\infty} \int_0^{2\pi} \omega^2 C(\theta) \sqrt{2\, S_{\eta\eta}(\omega,\theta)\, d\omega d\theta}\, \frac{\cosh[\kappa(-z+d)]}{\sinh[\kappa\, d]}$$

$$\sin[\kappa\,(x\cos\theta + y\sin\theta) - \omega t + \psi(\omega,\theta)] \tag{4.23}$$

where

$$C(\theta) = \begin{cases} \cos\theta & \text{component in x direction} \\ \sin\theta & \text{component in y direction} \end{cases}$$

If desired, vertical components of water particle motions may be obtained by a partial derivative, similar to Eqs. (4.15) and (4.16), i.e. $\dot{v}_z = \partial\phi/\partial z$ and $\ddot{v}_z = \partial\dot{v}_z/\partial t$. Only horizontal components of water particle motions are of interest in this investigation, since the

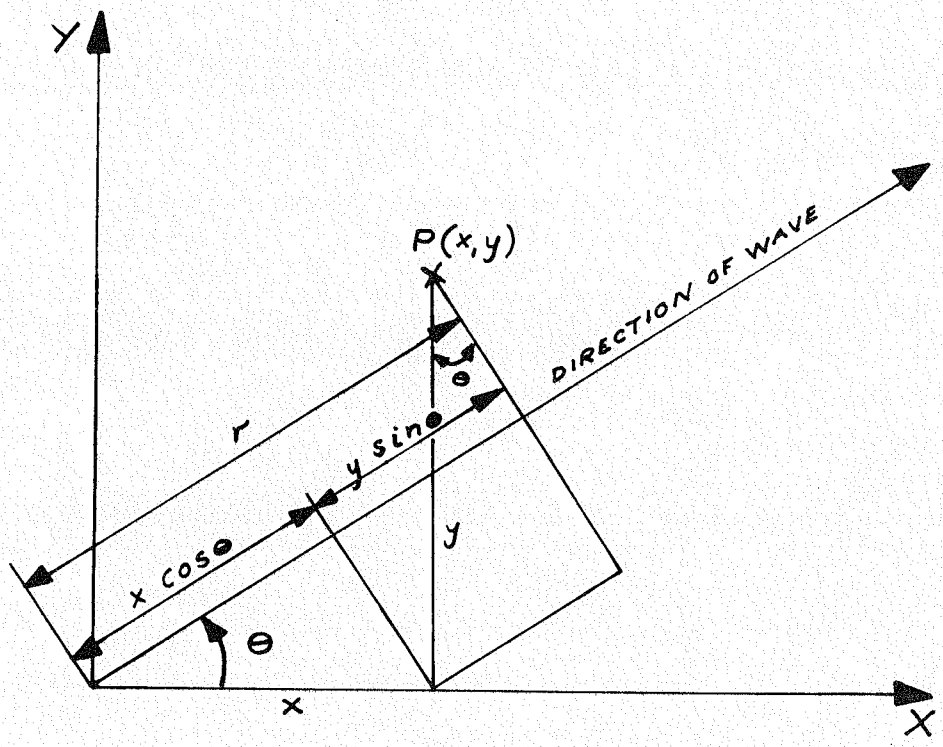

FIG. 4.3 TRANSFORMATION OF DISTANCE r IN DIRECTION OF WAVE INTO x AND y COORDINATES

structural vibration in the vertical direction can be neglected.

Given Eq. (4.22), the covariance function for horizontal water particle velocity components at point $P_i(x_i,y_i,z_i)$ at time t and at point $P_j(x_j,y_j,z_j)$ at time $t+\tau$ is

$$R_{\dot{v}_i\dot{v}_j}(\tau) = \int_0^{\infty} \int_0^{2\pi} \omega^2 \, C_1(\theta) \, S_{\eta\eta}(\omega,\theta) \, \frac{\cosh\,[\kappa(-z_i+d)]\,\cosh\,[\kappa(-z_j+d)]}{\sinh^2\,[\kappa\, d]}$$

$$\cos\,\{\kappa[(x_i-x_j)\,\cos\,\theta + (y_i-y_j)\,\sin\,\theta] + \omega\tau\}\, d\theta d\omega \tag{4.24}$$

where

$$C_1(\theta) = \begin{cases} \cos^2\,\theta & \text{components in x direction} \\ \sin\,\theta\,\cos\,\theta & \text{components in x and y direction} \\ \sin^2\,\theta & \text{components in y direction} \end{cases} \tag{4.25}$$

Covariance functions for velocity - acceleration and accelerations at two points can be obtained similarly from Eqs. (4.22) and (4.23), or more easily by taking a partial derivative of the covariance function for water particle velocities with respect to τ, noting that

$$R_{\dot{v}\ddot{v}}(\tau) = -R_{\ddot{v}\dot{v}}(\tau) = \frac{\partial R_{\dot{v}\dot{v}}(\tau)}{\partial\tau} \tag{4.26}$$

$$R_{\ddot{v}\ddot{v}}(\tau) = -\frac{\partial^2 R_{\dot{v}\dot{v}}(\tau)}{\partial\tau^2} \tag{4.27}$$

In practical computations it is preferable to solve this kind of dynamic problem in the frequency domain rather than in the time

domain. Spectral density functions must therefore be derived for the water particle motions. These functions are, however, Fourier transforms of the corresponding covariance functions, Eq. (2.11).

In order to use two sided (positive and negative frequencies) Fourier transforms, the directional spectrum is redefined as:

$$S^*_{\eta\eta}(\omega,\theta) = S^*_{\eta\eta}(-\omega,\theta) \quad = \tfrac{1}{2}\, S_{\eta\eta}(\omega,\theta) \quad \omega \geq 0 \tag{4.28}$$

Thus the cross spectral density function for water particle velocities at point P_i and point P_j is the Fourier transform of Eq. (4.24), i.e.

$$S_{\dot{v}_i \dot{v}_j}(\omega) = \frac{1}{2\pi} \int_{-\infty}^{\infty} \{ \int_{-\infty}^{\infty} \int_{0}^{2\pi} \sigma^2\, C_1(\theta)\, S^*_{\eta\eta}(\sigma,\theta)\, \frac{\cosh[\kappa_\sigma(-z_i+d)]}{\sinh^2[\kappa_\sigma d]}$$

$$\cosh[\kappa_\sigma(-z_j+d)]\cos\{\kappa_\sigma[(x_i-x_j)\cos\theta + (y_i-y_j)\sin\theta] + \sigma\tau\}\, d\theta d\sigma$$

$$\exp(-i\omega\tau)\, d\tau \tag{4.29}$$

where σ is a dummy frequency variable, κ_σ is the corresponding wave number and $C_1(\theta)$ is given by Eq. (4.25).

Consider first integration with respect to τ by setting

$$I = \int_{-\infty}^{\infty} \cos\{\kappa_\sigma[(x_i-x_j)\cos\theta + (y_i-y_j)\sin\theta]+\sigma\tau\} \exp(-i\omega\tau)\, d\tau \tag{4.30}$$

Introducing a new variable, β, in Eq. (4.30), given by

$$\beta = \frac{\kappa_\sigma}{\sigma}[(x_i-x_j)\cos\theta + (y_i-y_j)\sin\theta] + \tau \tag{4.31}$$

Equation (4.30) can then be rewritten as

$$I = \int_{-\infty}^{\infty} \cos\sigma\beta \exp(-i\omega\beta)d\beta \exp\left\{\frac{i\kappa_\sigma \omega}{\sigma}[(x_i-x_j)\cos\theta + (y_i-y_j)\sin\theta]\right\}$$

$$= \pi[\delta(\omega+\sigma) + \delta(\omega-\sigma)] \exp\left\{\frac{i\kappa_\sigma \omega}{\sigma}[(x_i-x_j)\cos\theta + (y_i-y_j)\sin\theta]\right\} \quad (4.32)$$

where $\delta[\ \ ]$ is the Dirac delta function. The integration with respect to β is consistent with similar previous integration [41, pg.148], [42, pg. 70].

Substituting Eq. (4.32) into Eq. (4.29) gives the cross spectral density function for water particle velocities at point P_i and point P_j

$$S_{\dot{v}_i\dot{v}_j}(\omega) = \int_0^{2\pi} \omega^2 C_1(\theta) S^*_{\eta\eta}(\omega,\theta) \frac{\cosh[\kappa(-z_i+d)]\cosh[\kappa(-z_j+d)]}{\sinh^2[\kappa d]}$$

$$\exp\{i\kappa[(x_i-x_j)\cos\theta + (y_i-y_j)\sin\theta]\} \quad (4.33)$$

where $C_1(\theta)$ is as in Eq. (4.25).

Spectral densities of velocity-acceleration and accelerations may be obtained similarly, or easier by noting that

$$S_{\dot{v}\ddot{v}}(\omega) = -S_{\ddot{v}\dot{v}}(\omega) = i\omega S_{\dot{v}\dot{v}}(\omega) \quad (4.34)$$

$$S_{\ddot{v}\ddot{v}}(\omega) = \omega^2 S_{\dot{v}\dot{v}}(\omega) \quad (4.35)$$

C. INTEGRATION OF SPECTRAL DENSITY FUNCTIONS OVER THE ANGULAR RANGE

In order to compute numerical values of the spectral density functions as given in Eq. (4.33), integration over the angular range is necessary.

A typical spectral density function for water particle motion is

$$S_{ij}(\omega) = \int_0^{2\pi} F_\omega(\theta)\, G_{ij}(\omega) \exp\{i\kappa[(x_i-x_j)\cos\theta + (y_i-y_j)\sin\theta]\}\, d\theta \tag{4.36}$$

where

$$F_\omega(\theta) = C_1(\theta)\, D_\omega(\theta) \tag{4.37}$$

where $C_1(\theta)$ is given in Eq. (4.25), and where

$$G_{ij}(\omega) = G_1(\omega)\, \frac{\cosh[\kappa(-z_i+d)]\cosh[\kappa(-z_j+d)]}{\sinh^2[\kappa d]} \tag{4.38}$$

where

$$G_1(\omega) = \begin{cases} \omega^2 S^*_{\eta\eta}(\omega) & \text{velocities} \\ i\omega^3 S^*_{\eta\eta}(\omega) & \text{velocity-acceleration} \\ -i\omega^3 S^*_{\eta\eta}(\omega) & \text{acceleration-velocity} \\ \omega^4 S^*_{\eta\eta}(\omega) & \text{accelerations} \end{cases}$$

Note that in Eq. (4.36) the directional spectrum is expressed as a product of the directional distribution function $D_\omega(\theta)$ and the one-dimensional spectral density function $S_{\eta\eta}(\omega)$ which is consistent with Eq. (4.2).

By simple trigonometric manipulation, Eq. (4.36) can be written in the form

$$S_{ij}(\omega) = G_{ij}(\omega) \int_0^{2\pi} F_\omega(\theta) \exp[i\kappa A_{ij}\cos(\theta-\alpha_{ij})]\, d\theta \tag{4.39}$$

where

$$A_{ij} = \sqrt{(x_i-x_j)^2 + (y_i-y_j)^2} \tag{4.40}$$

$$\alpha_{ij} = \tan^{-1}\left[\frac{y_i - y_j}{x_i - x_j}\right] \tag{4.41}$$

$F_\omega(\theta)$ can be expanded in Fourier series

$$F_\omega(\theta) = \sum_{n=-\infty}^{\infty} c_n \exp(in\theta) \tag{4.42}$$

where the Fourier coefficients c_n are

$$c_n = \frac{1}{2\pi} \int_0^{2\pi} F_\omega(\theta) \exp(in\theta)\, d\theta \tag{4.43}$$

where $F_\omega(\theta)$ is defined in Eq. (4.37). Substituting Eq. (4.42) into Eq. (4.39) gives

$$\begin{aligned} S_{ij}(\omega) &= G_{ij}(\omega) \sum_{n=-\infty}^{\infty} c_n \int_0^{2\pi} \exp[in\theta + i\kappa A_{ij} \cos(\theta-\alpha)]\, d\theta \\ &= G_{ij}(\omega) \sum_{n=-\infty}^{\infty} c_n \exp(in\alpha_{ij}) \int_0^{2\pi} \exp[in(\theta-\alpha_{ij}) + i\kappa A_{ij} \cos(\theta-\alpha_{ij})]\, d\theta \\ &= G_{ij}(\omega) \sum_{n=-\infty}^{\infty} c_n \exp(in\alpha_{ij}) \int_{-\pi}^{\pi} \exp(i\kappa A_{ij} \cos\theta)(\cos n\theta + i \sin n\theta)\, d\theta \end{aligned} \tag{4.44}$$

Since $\exp(i\kappa A_{ij} \cos\theta)$ and $\cos n\theta$ are even functions and $\sin n\theta$ is an odd function with respect to θ, Eq. (4.44) may be simplified to the form

$$S_{ij}(\omega) = G_{ij}(\omega) \sum_{n=-\infty}^{\infty} c_n \exp(in\alpha)\, 2 \int_0^{\pi} \exp(i\kappa A_{ij} \cos\theta) \cos n\theta\, d\theta \tag{4.45}$$

Since [43, pg. 360, Eq.(9.1.21)]

$$\int_0^{\pi} \exp(i\kappa A_{ij} \cos\theta) \cos n\theta\, d\theta = \pi i^n J_n(\kappa A_{ij}) \tag{4.46}$$

where $J_n(\,)$ is a Bessel function of first kind and order n. Noting that $i^n = \exp(i\, n\frac{\pi}{2})$ and substituting Eq. (4.46) into Eq. (4.45),

the cross spectral density function for water particle motions at point P_i and point P_j can be expressed as

$$S_{ij}(\omega) = 2\pi\, G_{ij}(\omega) \sum_{n=-\infty}^{\infty} c_n \exp\left[in\left(\alpha_{ij} + \frac{\pi}{2}\right)\right] J_n(\kappa A_{ij}) \quad (4.47)$$

where $G_{ij}(\omega)$ is given by Eq. (4.38), c_n by Eq. (4.43), α_{ij} by Eq. (4.41) and A_{ij} is given by Eq. (4.40).

Using Eq. (4.47) spectral densities of water particle motions for discrete frequencies can be calculated as needed for the determination of the spectral densities of the generalized forces in Chapter III.

CHAPTER V

COMPUTER APPLICATION

For the purpose of using the theory that is developed in Chapters III and IV in practical applications, two computer programs have been developed. One program is for structures that are symmetric about a vertical plane and the other is for structures that are symmetric about two vertical planes. Thus, full advantage of symmetry is always taken. Symmetry about two vertical planes uncouples translational and rotational modes and due to complex conjugation only half of the cross spectral density functions have to be determined. Since these spectral density functions are expressed by a series expansion, Eq. (4.47), they have to be computed and stored in the computer for discrete frequencies. This implies that is is necessary to deal with a large number of spectral densities and that mean products must be obtained by numerical integration of the corresponding spectral density functions. The substantial saving in computer storage obtained for structures symmetric about two vertical planes may be used to make the analysis more accurate by increasing the number of degrees of freedom and/or the number of discrete frequencies used in defining the directional spectrum.

A flowchart for the solution process is shown in Fig. 5.1.

A. DYNAMIC SPECIFICATION OF STRUCTURE

To describe the dynamic model of the structure, Fig. 3.1, the following data are required: structural mass, damping and stiffness (or flexibility) matrices; coordinates of the nodal points; and mem-

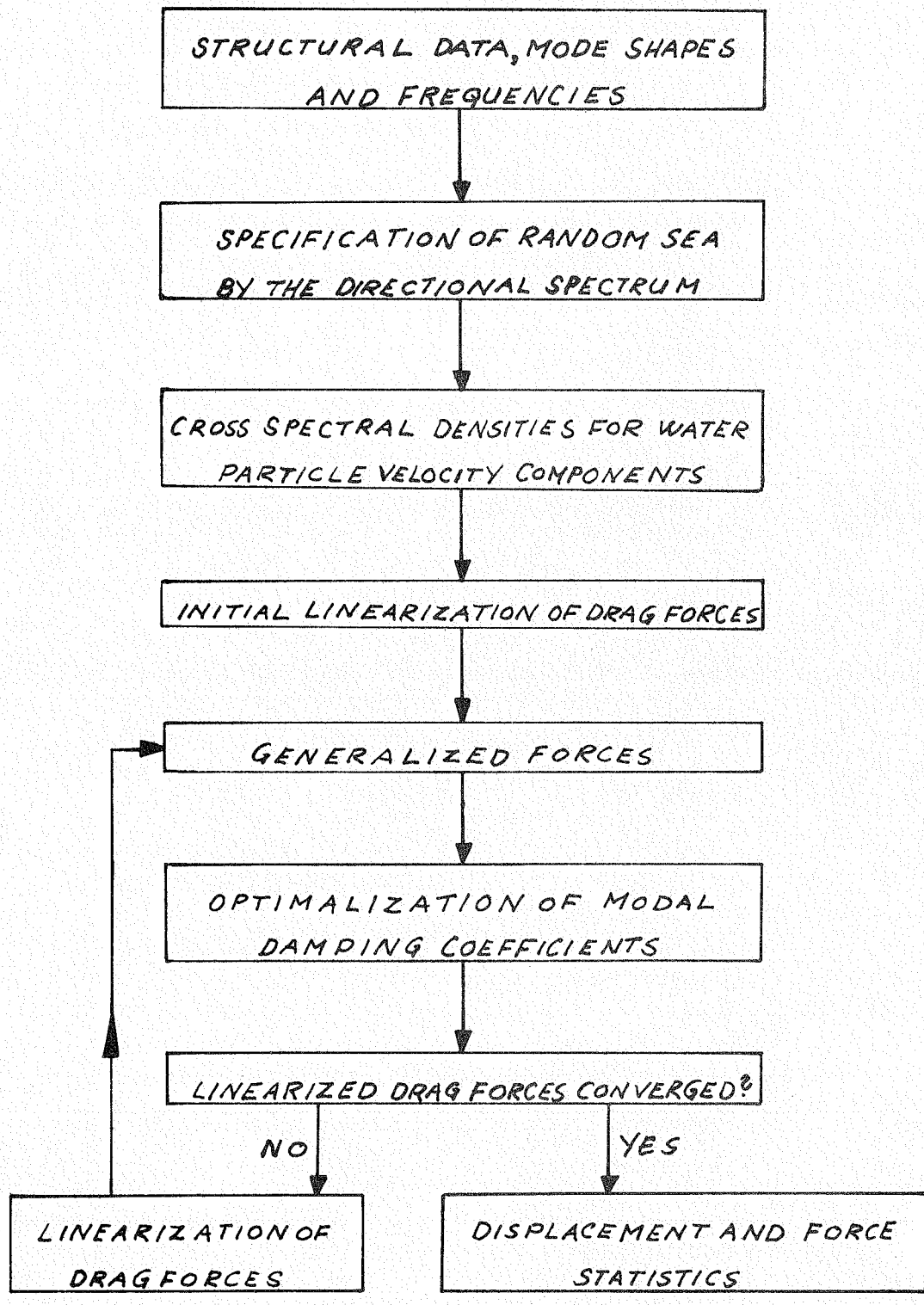

FIG. 5.1 FLOW CHART FOR COMPUTER SOLUTION

ber volumes and projected areas (perpendicular to the x and y directions) associated with the submerged nodal points. The coefficient of inertia C_M and the coefficient of drag C_D have to be assigned numerical values.

The mass matrix (including hydrodynamic mass) in Eq. (3.32) is calculated using Eqs. (3.33) through (3.37). The damping of the dynamic system, however, cannot be determined at this stage of the calculation, because the hydrodynamic damping depends on the linearized drag forces, and thus only the structural damping is known (normally given in percent of critical for the normal modes).

The equations of motions are solved using the normal mode superposition, which requires that mode shapes and frequencies are determined. This is done by solving the generalized eigenvalue problem given by Eq. (3.51), i.e.

$$[K]\ [\phi] = [M]\ [\phi]\ [\Omega]^2 \qquad (5.1)$$

In this type of analysis the number of degrees of freedom is normally in the range of 15 to 30. The eigenvalue problem is therefore solved very efficient by the generalized Jacobi iteration method [44].

The modal matrix (eigenvectors) obtained by solving Eq. (5.1) may be normalized as desired. For the purpose of comparing the various mode shapes, it is normal to make the largest element of each modal vector equal to unity. The calculation of the structural response, however, is simplest when the modal matrix is normalized such that the generalized mass matrix is an identity matrix. Calling the modal matrix obtained by solving Eq. (5.1) $[\phi]$ and the corresponding

generalized mass matrix [M*], an identity matrix is obtained by pre- and post-multiplying the generalized mass matrix [M*] by $[M^*]^{-\frac{1}{2}}$, i.e.

$$[I] = [M^*]^{-\frac{1}{2}} [M^*] [M^*]^{-\frac{1}{2}} = [M^*]^{-\frac{1}{2}} [\phi]^T [M] [\phi] [M^*]^{-\frac{1}{2}}$$

$$= [\tilde{\phi}]^T [M] [\tilde{\phi}] \qquad (5.2)$$

where

$$[\tilde{\phi}] = [\phi] [M^*]^{-\frac{1}{2}} \qquad (5.3)$$

is the modal matrix normalized such that the generalized mass matrix is an identity matrix.

B. SPECTRAL DENSITIES FOR WATER PARTICLE MOTIONS

As mentioned in Chapter IV, the ocean waves are described by the directional spectrum $S_{\eta\eta}(\omega,\theta)$, which is given by the spectral density $S_{\eta\eta}(\omega)$ (assuming waves in one direction) and the corresponding directional distribution $D_\omega(\theta)$ of the waves for discrete frequencies (see Eq. (4.2)). Only the spectral densities for the water particle velocity components are computed according to Eq. (4.47) due to the simple relations that exist between spectral density functions for velocities, velocity - acceleration and accelerations, Eq. (4.34) and (4.35).

Examining Eq. (4.47) reveals that the spectral densities for water particle velocities can be computed quite efficiently. For discussion of this computation, Eq. (4.47) is rewritten for water particle velocity components at node k at level i and at node ℓ at level j as:

$$S_{\dot{v}_{ik}\dot{v}_{j\ell}}(\omega) = 2\pi\, G_{ij}(\omega) \sum_{n=-\infty}^{\infty} c_n \exp\left[in\left(\alpha_{ikj\ell} + \frac{\pi}{2}\right)\right] J_n(\kappa A_{ikj\ell}) \tag{5.4}$$

Due to the following relations that exist for the terms in Eq. (5.4) for positive and negative n's:

(1) Fourier coefficients

$$c_{-n} = \bar{c}_n \tag{5.5}$$

where $\bar{c}_n$ is the complex conjugate of c_n

(2) Bessel functions of even order

$$J_n(z) = J_{-n}(z) \tag{5.6}$$

(3) Bessel functions of odd order

$$J_n(z) = -J_{-n}(z) \tag{5.7}$$

Eq. (5.4) may be rewritten as:

(1) The real part

$$\text{Real}\left[S_{\dot{v}_{ik}\dot{v}_{j\ell}}(\omega)\right] = G_{ij}(\omega)\ 2\pi \left\{c_0 J_0(\kappa A_{ikj\ell}) + 2 \sum_{n=1}^{\infty} \text{Real}\left[c_{2n} \exp\left\{i\, 2n\left(\alpha_{ikj\ell} + \frac{\pi}{2}\right)\right\}\right] J_{2n}(\kappa A_{ikj\ell})\right\} \tag{5.8}$$

(2) The imaginary part

$$\text{Imag.}\left[S_{\dot{v}_{ik}\dot{v}_{j\ell}}(\omega)\right] = G_{ij}(\omega)\ 4\pi \sum_{n=1}^{\infty} \text{imag.}\left[c_{2n-1} \exp\left\{i(2n-1)\left(\alpha_{ikj\ell} + \frac{\pi}{2}\right)\right\}\right] J_{2n-1}(\kappa A_{ikj\ell}) \tag{5.9}$$

The function $G_{ij}(\omega)$, given by Eq. (4.38) is independent of the summation in Eq. (5.4), and is therefore computed separately for the frequencies where the spectral densities $S_{\eta\eta}(\omega)$ are given. It is seen from Eq. (4.38) that the part"$\cosh[\kappa(-z_i+d)]\cosh[\kappa(-z_j+d)]/\sinh^2[\kappa d]$"indicates that $G_{ij}(\omega)$ needs to be computed only when $i \leq j$. It also indicates that $G_{ij}(\omega)$ decreases as the distances from the surface z_i and z_j increase, especially for high wave numbers κ (frequency dependent). For the purpose of saving computational effort, $G_{ij}(\omega)$ is only calculated when the above hyperbolic expression is larger than a certain value (in the computer programs this value is set equal to 0.01), thus taking advantage of the fact that high frequency waves have insignificant effect at large distances beneath the water surface.

Before calculating $G_{ij}(\omega)$, the radian wave number κ must be determined. For this purpose Eq. (4.11) is rewritten in the form

$$\kappa = \frac{\omega^2}{g} \operatorname{cotanh} (\kappa d) \qquad (5.10)$$

This implicit equation is solved iteratively by initially setting $\operatorname{cotanh} (\kappa d) = 1$ (deep water assumption) for calculation of an initial value for κ and substituting this value into Eq. (5.10) to obtain a new value for κ. This procedure is then continued until sufficient convergence is reached.

The Fourier coefficients in Eq. (5.4), given by Eq. (4.43) depend only on the directional distribution $D_\omega(\theta)$ and the directions of the water particle velocity components. These coefficients are obtained by numerical integration over the angular range where the directional distribution is given for $n=0,1,---,N_1$, where N_1 is

selected such that $|c_{N_1}|$ is small compared to $|c_0|$. A limit for N_1 is set because the arguments of the Bessel functions in this analysis are small, thus taking advantage of the fact that Bessel functions of non-zero order can be considered to be zero for arguments whose absolute value is less than a value z_0, which increases with the order n.

The calculations of the angle $\alpha_{ikj\ell}$ and the Bessel functions $J_n(\kappa A_{ikj\ell})$ are performed in connection with the summations in Eqs. (5.8) and (5.9). The arguments of the Bessel functions, $\kappa A_{ikj\ell} = \kappa \sqrt{(x_{ik}-x_{j\ell})^2 + (y_{ik}-y_{j\ell})^2}$, depend on the wave numbers and the horizontal distance between the nodes. For the considered nodal point combinations, the Bessel functions are calculated only for the frequencies where $G_{ij}(\omega)$ are considered non-zero, and for $n=0,1,---,N_1$, except when the arguments are small compared to the order such that the value of the Bessel functions can be considered to be zero. For the spectral densities when i=j and k=ℓ, the arguments for the Bessel functions are zero, and these functions become

$$S_{\dot{v}_{ik}\dot{v}_{ik}}(\omega) = 2\pi\, G_{ii}(\omega)\, c_0 \qquad (5.11)$$

C. CALCULATION OF STRUCTURAL RESPONSE

Referring to Fig. 5.1, it is seen that the next step is to determine the initial linearized drag forces. This is done by calculating the variances of the water particle velocities, i.e. integrating the corresponding spectral densities, and then substituting the standard deviations into Eq. (3.22).

The spectral densities for the generalized forces are obtained using Eqs. (3.83) through (3.85). Because only spectral densities

for water particle velocities are stored in the computer, all terms are calculated as if they were dependent upon velocities, after which they are multiplied by the appropriate relations that exist between spectral densities of velocities and spectral densities of accelerations, etc., Eqs. (4.34) and (4.35).

The modal hydrodynamic damping coefficients can now be optimized. (Structural damping is selected in percent of critical in the normal modes.) The hydrodynamic damping coefficients depend on the linearized drag force, and they are computed using Eqs. (3.40) through (3.42) and Eqs.(3.44) and (3.45). The generalized damping matrix is obtained from Eq. (3.58), and it is diagonalized using Eq. (3.66). It is seen from this equation that it is necessary to calculate the mean products of the structural velocities in the generalized coordinate system, which is done using Eq. (3.88). Initially the modal damping coefficients are selected as the diagonal terms of the generalized damping matrix, Eq.(3.58), and the generalized structural velocities are computed. The generalized damping matrix is then diagonalized using Eq. (3.66). This procedure is continued until satisfactory convergence is obtained.

To linearize drag forces the variances of the relative velocities between water particles and structure must be computed, as given by Eqs.(3.158) and (3.159). In these equations, the computation of the mean products of the structure and water particle velocities caused most of the numerical work. The corresponding spectral densities for these quantities are given by Eqs.(3.171) through (3.174). Having determined these variances, the drag forces are linearized using Eq. (3.22). Because present linearized drag forces are based

upon previous linearized drag forces, the cyclic procedure of calculating the generalized forces, etc., must be continued until acceptable convergence is obtained.

Final generalized forces and optimized damping coefficients are now calculated such that the statistics of structural response can be obtained. See Chapter III, section D, for the calculation of variances of displacements, rotations, shear forces and twisting and bending moments. Mean peak values, based upon storm duration, of these quantities are also determined using Eq. (2.39).

Calculation of the response of a 7 level tower (21 degrees of freedom), symmetric about one vertical plane, requires approximately 1 minute central processor time on a CDC 6400 computer when 11 frequencies are used in the numerical integration of the spectral density functions.

CHAPTER VI

CASE STUDIES

A. DATA

Seven deep water towers have been selected for this investigation. Six of the towers are symmetric about a vertical plane, and have heights of 475 (Tower 1, 5, and 6), 675 (Tower 2), 875 (Tower 3) and 1075ft (Tower 4), corresponding to water depths of 400, 600, 800, and 1000ft, respectively. The torsional stiffness of Tower 5 is 75% of the stiffness of Tower 1. Tower 6 has leg spacings that are twice the leg spacing of Tower 1 (rotational inertias and stiffnesses are scaled accordingly). Tower 7 is symmetric about two vertical planes and has a height of 475ft, corresponding to a water depth of 400ft.

Data describing the 7 levels models of the towers are given in Appendix A; see Fig. 3.1, pg.17, for a sketch of a typical structure. These data are generated from preliminary design data for two-dimensional models of towers that have been supplied by the Standard Oil Company of California. The towers have 4 cylindrical legs that are tapered stepwise and interconnected by extensive bracings. Due to this complexity, the towers are described only by the data needed for the dynamic analysis. In this investigation structural damping ratios of 5 percent [1] of critical are assumed for all normal modes of the towers vibrating in water. Six normal modes are included in the calculation of the structural response; two for vibration in the x-direction and four for coupled translational (in the y-direction) - rotational

---

[1] Except for a few examples that were calculated with 2 per cent damping to investigate the effect of structural damping.

vibrations. For Tower 7, which is symmetric about two vertical planes the vibrations in the x-direction, y-direction and rotation are uncoupled; therefore, two modes of vibration are included in each direction. The coefficients of inertia C_M and the coefficient of drag C_D are assigned values of 2.0 and 1.4, respectively.[1]

The ocean waves have been described by several directional spectra in order to investigate systematically the response of the structures. The directional spectra are given by one-dimensional spectral densities and their directional distributions for discrete frequencies, corresponding to Eq. (4.3). For most examples, the spectral densities are calculated by the Pierson - Moskowitz formula [45] for the wave height spectrum, namely

$$S_{\eta\eta}(\omega) = \frac{.0081g^2}{\omega^5} \exp\left[- .74 \left(\frac{g}{\omega W}\right)^4 \right] \qquad 0 \leq \omega < \infty \tag{6.1}$$

where g is the acceleration of gravity and W is the mean wind speed at a height of 64ft above the sea surface. Table 6.1 gives the spectral densities at 11 discrete frequencies for the various one-dimensional spectra. Equation (6.1) is used to calculate the values for spectra A,B and C, while the spectral densities for spectrum D are selected to investigate the effect of two storms coming from different directions. The circular normal distribution, Eq. (4.6), is used to describe the directional distributions. The higher the value of a, the more concentrated is the distribution about the mean direction. Figure 4.2, pg.61, shows the circular normal distribution for constants a = 1

---

[1] A few examples were calculated using $C_D = 1.0$ in order to investigate the effect of variation in the drag coefficient.

WAVE SPECTRUM		A	B	C	D
Wind speed in Pierson-Moskowitz form.		50ft/sec	75ft/sec	100ft/sec	N.A.
Lowest frequency [rad/sec]		.4518	.3012	.2259	.3
Frequency increment [rad/sec]		.0932	.06213	.0466	.065
	Freq.No.				
	1	21	160	673	130
	2	41.3	313	1321	270
Spectral	3	36.8	280	1178	240
	4	25.7	195	823	175
Densities	5	16.7	127	535	100
	6	10.8	81.9	345	120
ft^2 sec	7	7.04	53.5	225	100
	8	4.7	35.7	150	80
	9	3.21	24.4	103	50
	10	2.24	17	71.7	30
	11	1.6	12.1	51.2	20

Table 6.1 One-dimensional Wave Spectral Densities

through 10. The various directional distributions used are summarized in Table 6.2.

Directional Distribution	Constant a in circular normal distribution	Mean angle of flow frequency dependent ?
A	See Table 6.3	No
B	10	No
C	100	No
D	See Table 6.3	Yes, see Table 6.3
E	10	Yes, see Table 6.4 Tower 1. Spectrum D.

Table 6.2 Directional distributions

Frequency No.	1-2	3-4	5-6	7-8	9-10	11
Constant in a circular normal distribution	6	5.6	5.2	4.8	4.4	4
Angle between mean direction of wave advance and x-axis. Distribution D only	45°	54°	63°	72°	81°	90°

Table 6.3 Additional Data for Distribution A and D

Various examples are summarized in Table 6.4. The angles in the table are the angles between the mean directions of wave advance and the positive x-axis (in plane of symmetry).

Tower No.	One-Dimensional Wave Spectrum Table 6.1	Directional Distribution: see Table 6.2 Angles between mean direction of wave advance and x-axis
1	A	A; 90°*
	B	A; 0°, 22.5°, 45°, 67.5°, 90°*, 135°, 180° B; 0°, 45°, 90° C; 0°, 45°, 90°, 135°, 180° D
	C	A; 90°*
	D	E; Lowest 5 frequencies: 90° Highest 6 frequencies: 0°, 45° or 90° (3 cases)
2,3, and 4	B	A; 0°, 45°, 90°** D
5 and 6	B	A; 0°, 45°, 90°
7	B	A; 0°, 22.5°, 45°, 67.5°, 90° B; 0°, 45°, 90° D

* C_D = 1.4: Calculated with 5% and 2% structural modal damping
C_D = 1.0: 5% structural modal damping
** Tower 4 only: Calculated with 5% and 2% structural modal damping.

Table 6.4 Test Examples

B. RESULTS

1. Mode Shapes and Frequencies

The mode shapes and frequencies are determined for the towers vibrating in water, which mean that an added hydrodynamic mass is included in the mass matrix. Figures 6.1 through 6.5 show the mode shapes for Towers 1 through 5, respectively. In these figures each coupled mode shape for vibrations in the y-direction and rotation is drawn as two separate curves; one for the component in y-direction and the other for the component in rotation. The rotational components shown in these figures are 40 times their real magnitude relative to the translational components. Figure 6.1 shows also the mode shapes for Tower 6, but here the above mentioned factor is 80. The reason for this relative decrease of the rotational component for Tower 6 is that the tower has twice the leg spacings of Tower 1, and even though the translational stiffness is held constant, the torsional stiffness is quadrupled. Figures 6.1 through 6.4 show that the coupled modes 1 and 2 have similar shapes, but that the rotational component of mode 2 is larger than that of mode 1 relative to the translational component. This applies also to modes 3 and 4. For Tower 5, Fig. 6.5, this relationship has changed, such that the rotational components of modes 1 and 3 have increased significantly compared to those of Tower 1, Fig. 6.1. This is because the rotational stiffness of Tower 5 is 75% of that of Tower 1; therefore the mode shapes indicate that the torsional response for Tower 5 will be larger than for Tower 1.

Figure 6.6 shows mode shapes for Tower 7. This tower is symmetric about two vertical planes, and therefore there is no coupling between the modes in the various directions.

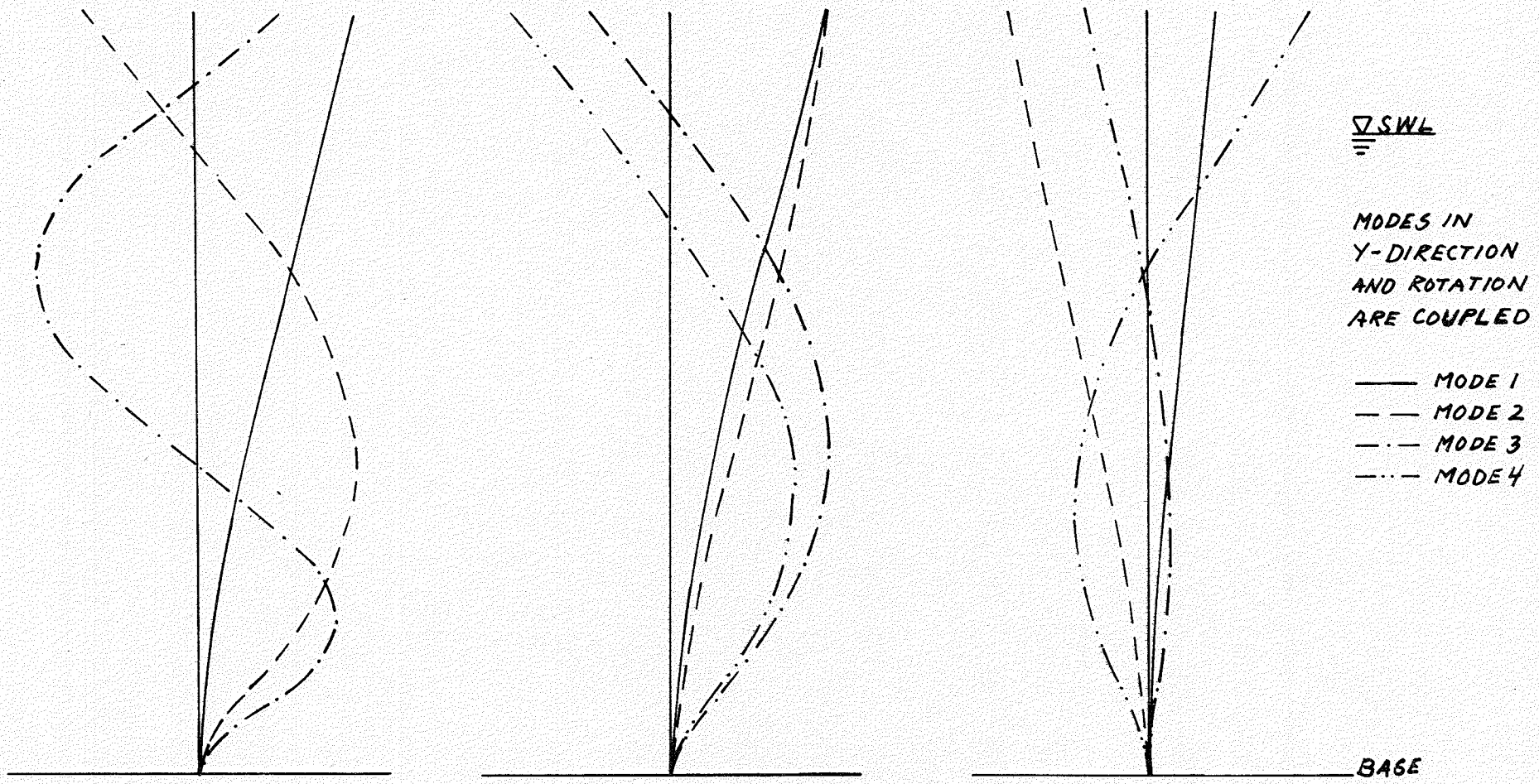

FIG. 6.1 MODESHAPES. TOWERS 1 AND 6

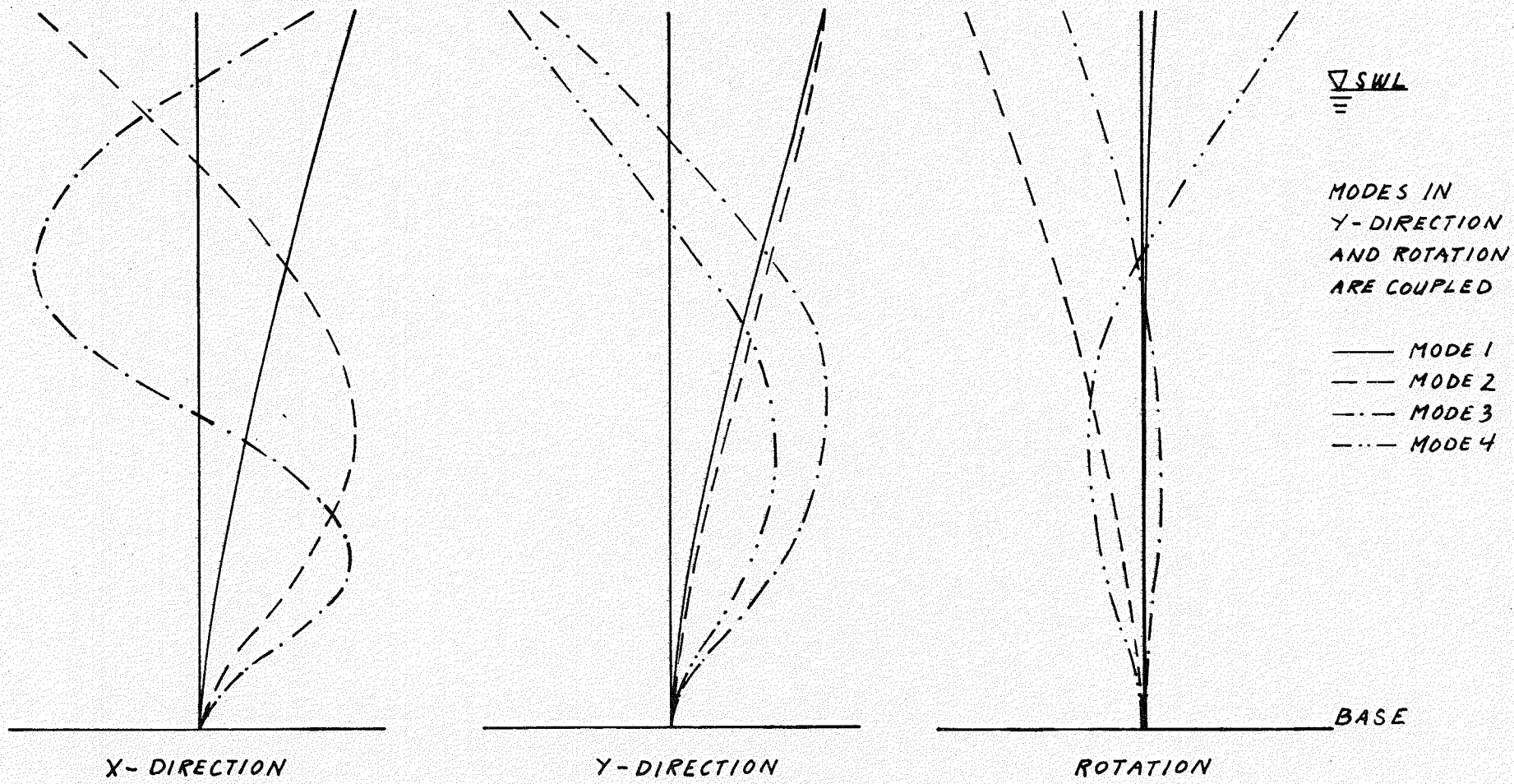

FIG. 6.2 MODESHAPES. TOWER 2

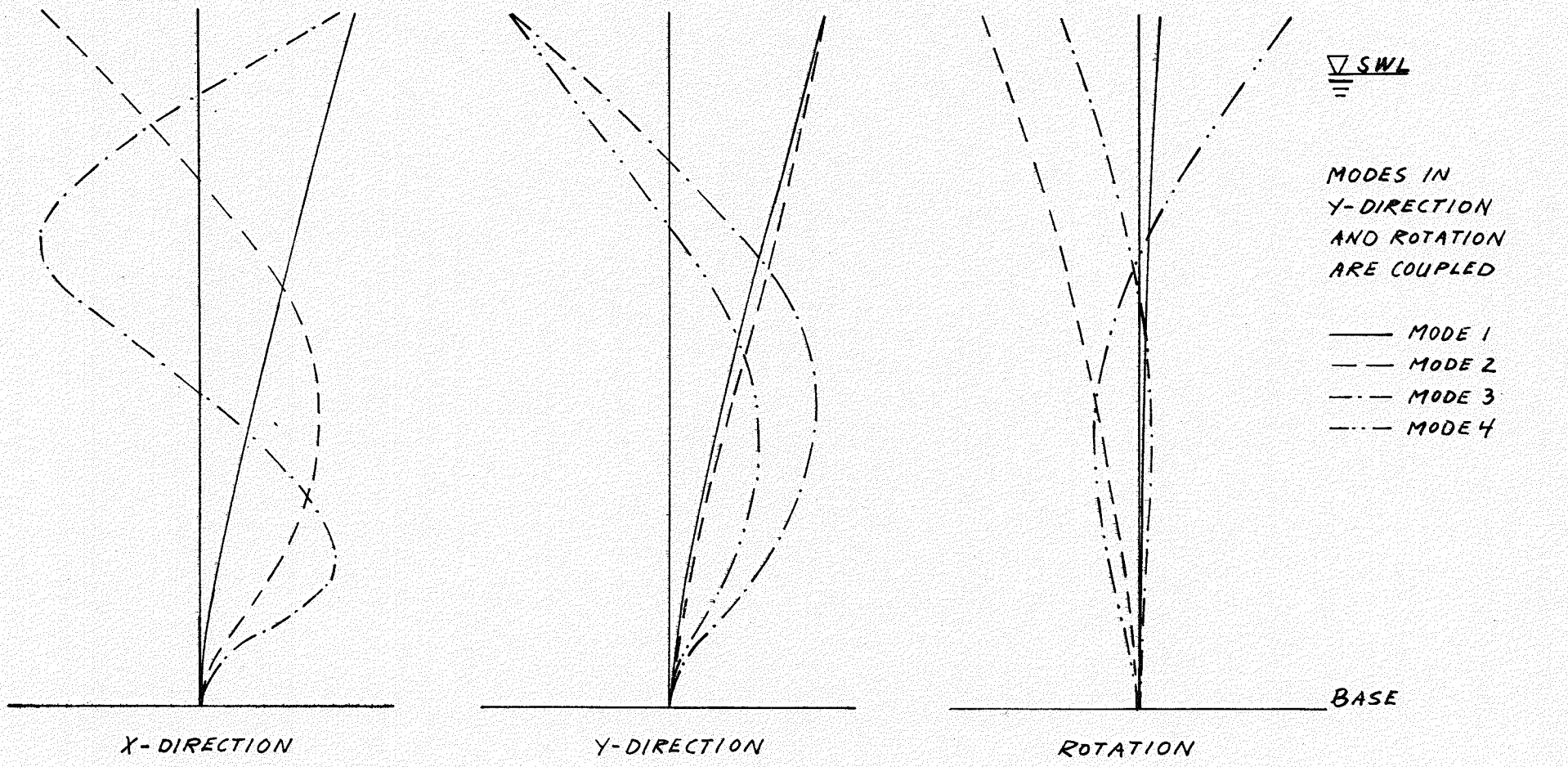

FIG. 6.3 MODESHAPES. TOWER 3

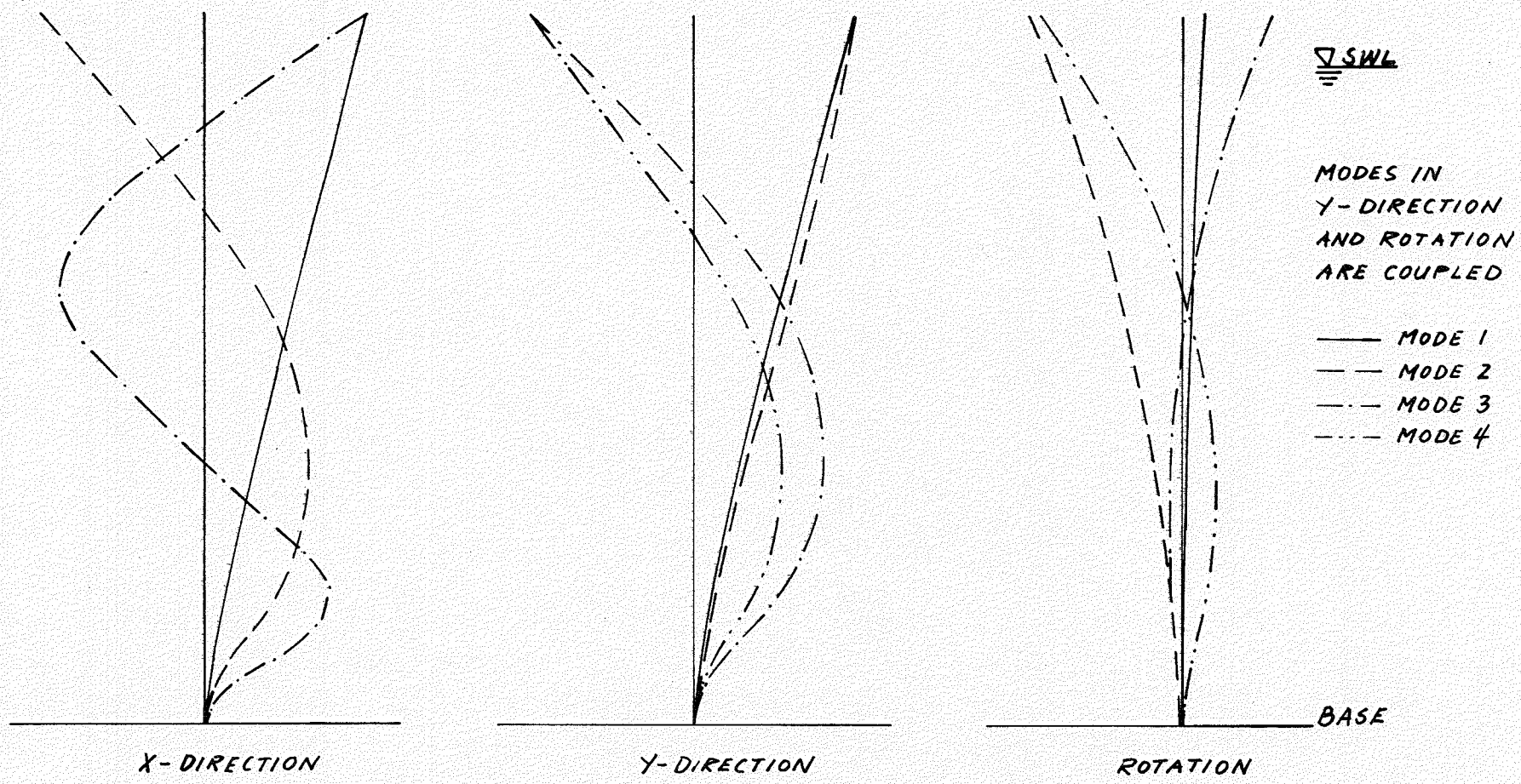

FIG. 6.4 MODESHAPES. TOWER 4

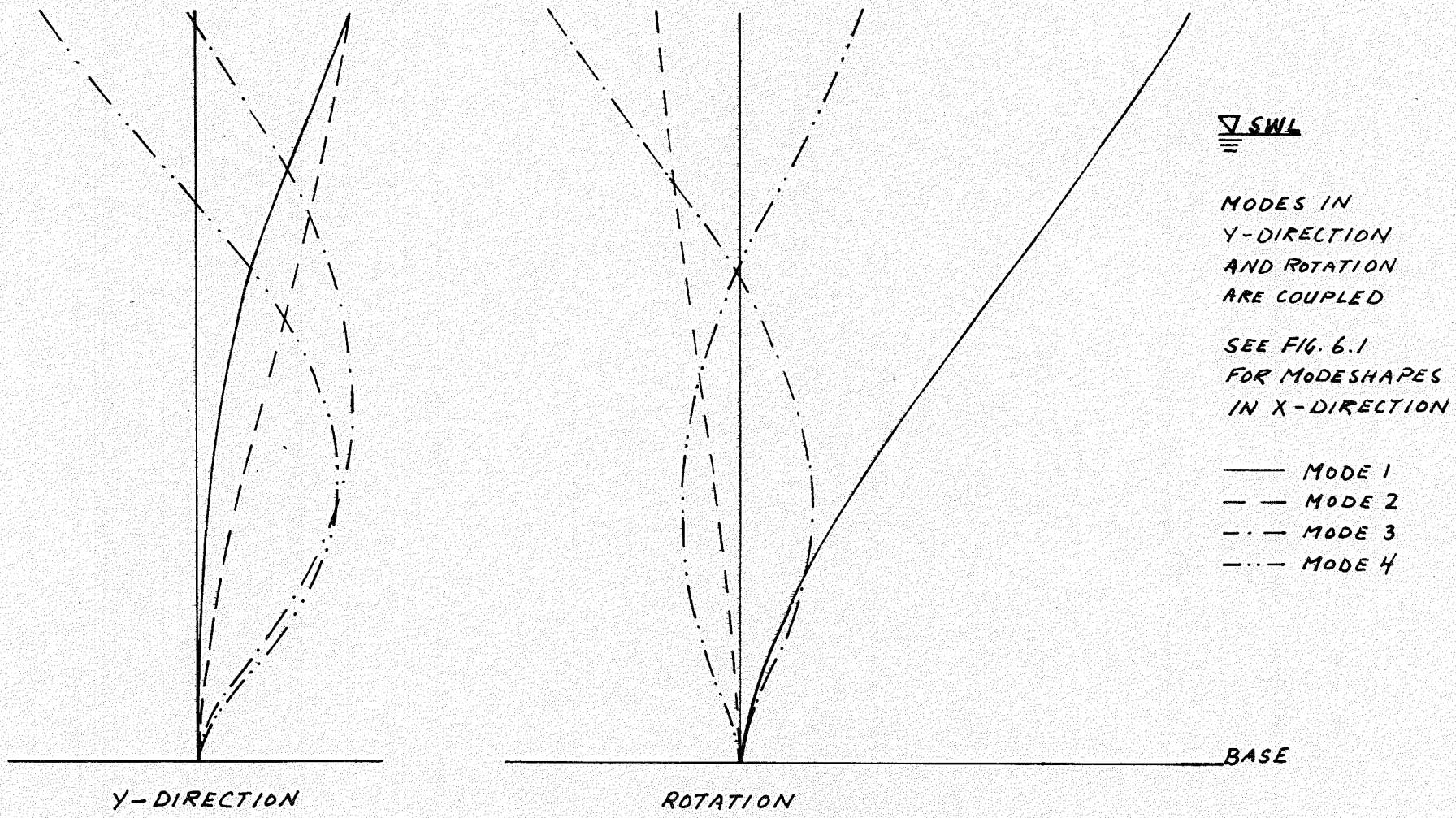

FIG. 6.5 MODESHAPES. TOWER 5

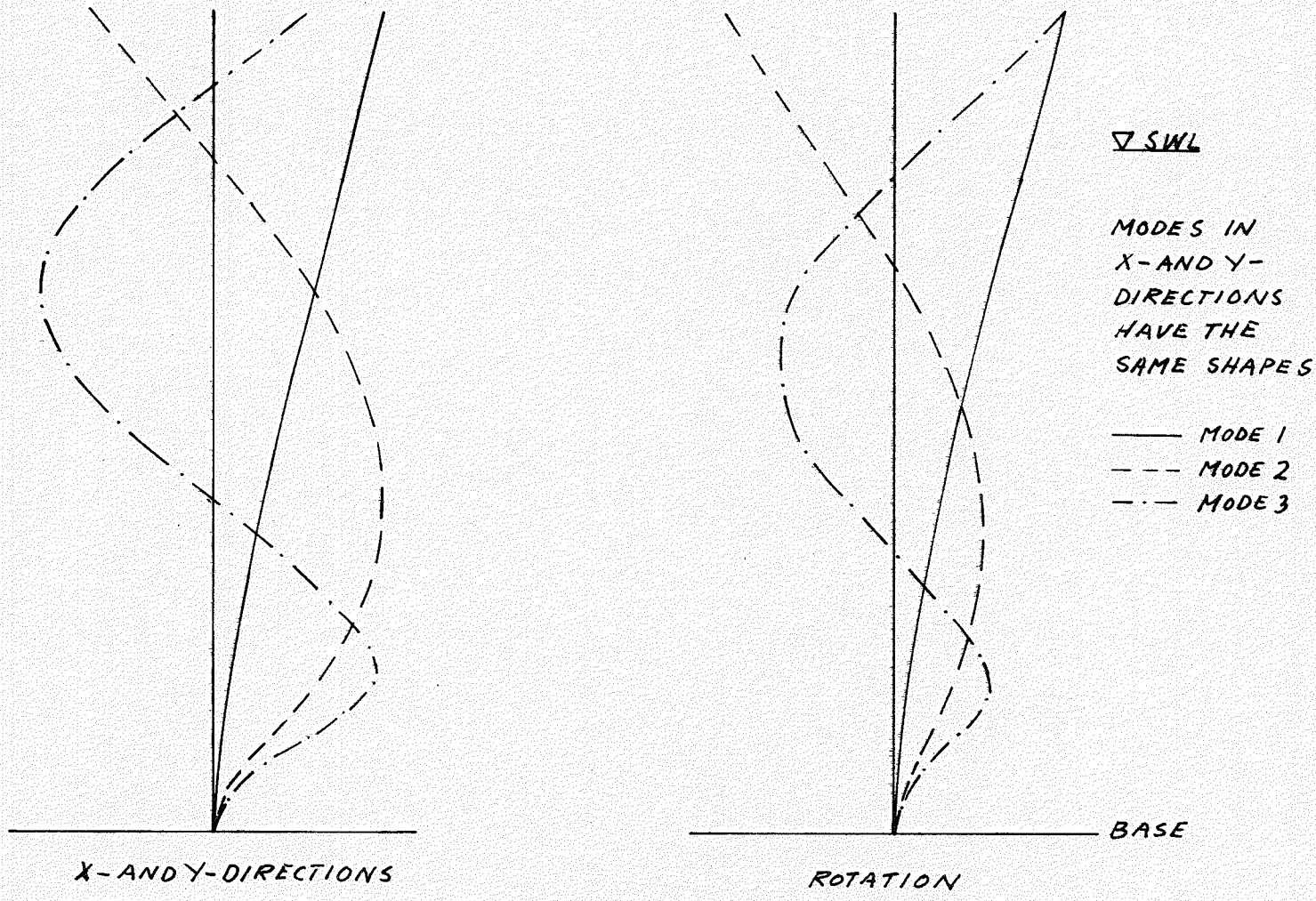

FIG. 6.6 MODESHAPES. TOWER 7

The natural frequencies for the 3 lowest normal modes in each direction are given in Table 6.6. For towers 1 through 6 the 6 lowest frequencies are given for the coupled modes.

Tower No	Modes in x-direction			Coupled modes in y-direction and rotation					
	1	2	3	1	2	3	4	5	6
1 and 6	2.57	6.07	10.5	2.26	2.71	5.32	6.89	9.22	11.3
2	1.85	3.96	7.28	1.65	2.14	3.48	4.5	6.38	7.86
3	1.41	2.9	5.31	1.26	1.63	2.56	3.25	4.66	5.63
4	1.16	2.2	3.66	1.02	1.3	1.93	2.42	3.19	3.93
5	2.57	6.07	10.5	2.07	2.57	5.02	6.33	8.55	10.5
				Modes in y-direction			Modes in rotation		
	1	2	3	1	2	3	1	2	3
7	2.59	6.07	10.5	2.32	5.43	9.43	3.86	7.96	13.3

Table 6.5 Natural Frequencies in rad/sec

2. Response Statistics

Table 6.4 summarizes the various test examples in this investigation, but due to their large number, only selective results are presented.

Figure 6.7 shows how the standard deviations of the rotations at deck for Tower 1, 5, 6, and 7 depend on different directional spectra, summarized in the following table (see next page). Curves A, B and C show that the largest rotational response is obtained when the mean direction of flow is nearly perpendicular to the plane of symmetry (xz-plane), and that the response increases as the directional distribution of the waves becomes more narrow. When the mean direction of flow is parallel to the plane of symmetry the rotational response increases with increasing directional spread. This behavior is expected

SEE TABLE 6.6 AND TEXT FOR EXPLANATION OF THE DIFFERENT CURVES

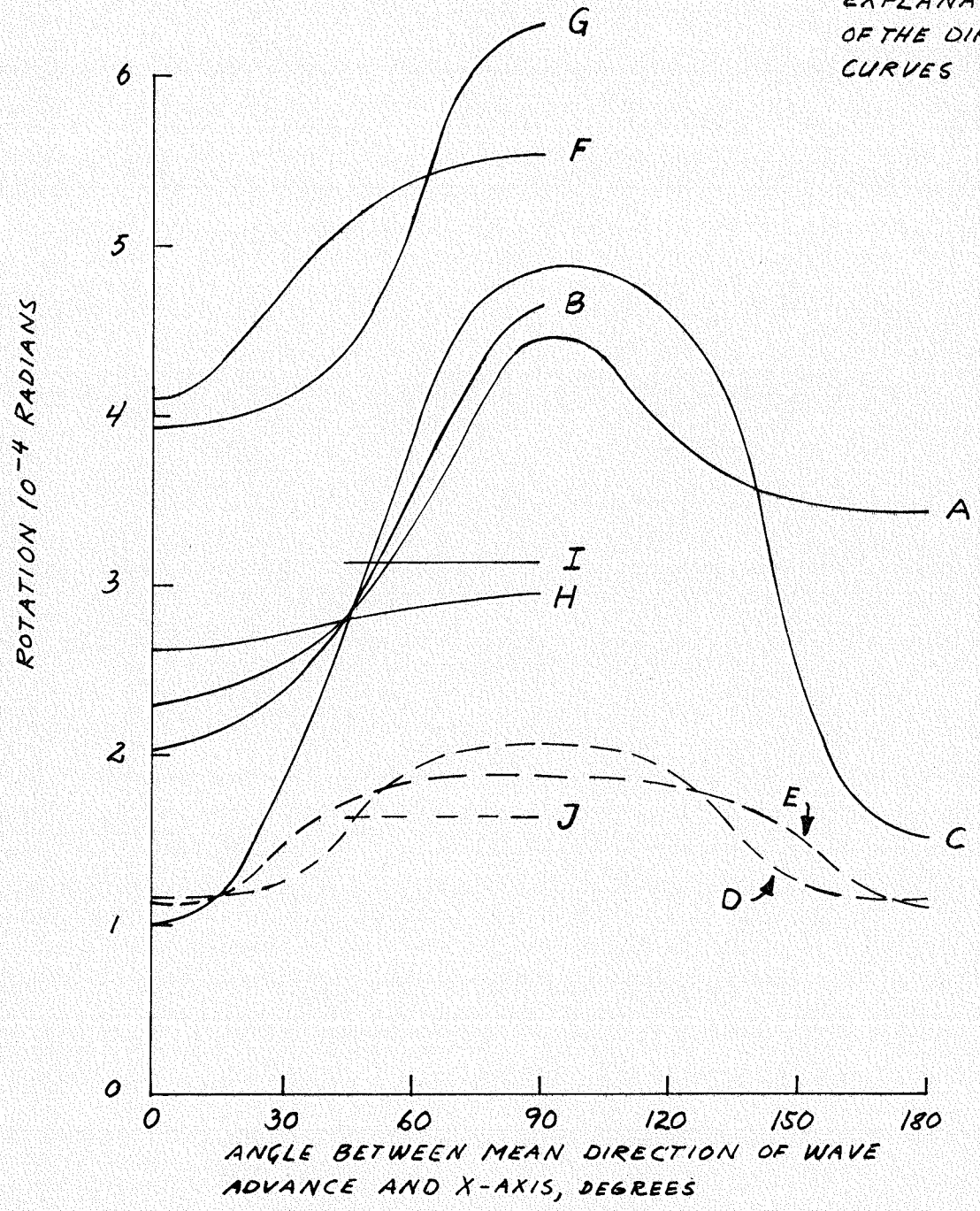

FIG. 6.7 STANDARD DEVIATION OF ROTATION OF DECK VS. DIRECTION OF WAVE ADVANCE

Curve	Tower	One-dimensional Wave Spectrum*	Directional Distribution**
A	1	B	A
B	1	B	B
C	1	B	C
D	7	B	A
E	7	B	B
F	1	D	E
G	5	B	A
H	6	B	A
I	1	B	D
J	7	B	D

* see Table 6.1 pg. 84

** See Table 6.2 pg. 84

Table 6.6 Reference for Figure 6.7

because waves parallel to the plane of symmetry do not exitate the structure in torsion. Since inertia forces and drag force are not in phase (drag forces are $\pi/2$ radians behind the inertia forces), curves A and C are not symmetric for mean angles of wave advance symmetric about the perpendicular to the plane of symmetry. Curves D and E show that rotational responses for towers symmetric about two vertical planes are very small. Curve F shows the effect of two storms containing waves of different frequencies and coming from two different directions. The storm with the low frequency waves has a mean direction of wave advance perpendicular to the plane of symmetry, while the rotational response is shown versus the mean direction of the storm with the high frequency waves.(Note that the one-dimensional wave spectrum used in this case is not the same as those used in the other

cases.) Thus, for Tower 1, the rotational response is largest when the mean directions of wave advance for both storms are perpendicular to the plane of symmetry. Comparing curve G with curve A, the effect of a 25% reduction in torsional stiffness can be seen. Curve H is for a tower where the distances between the legs are doubled. Even though the translational stiffness is held constant, the rotational stiffness for this tower is quadrupled compared to the original tower. This increase is reflected in the torsional response which is less than that for Tower 1, curve A, except when the angle between the mean direction of wave advance and the plane of symmetry is between 0 and 45 degrees. This is due to increased effect of the directional spread of the waves as the leg spacings increase when the mean direction of wave advance is nearly parallel to the plane of symmetry. Lines I and J represent the rotational responses of Tower 1 and 7, respectively, for a directional spectrum with mean direction of wave advance for the component waves at discrete frequencies varying between 45 and 90 degrees angle with the plane of symmetry.

Figure 6.8 shows the rotation of the deck as a function of the depth of the water. The one-dimensional wave spectrum used is spectrum B, and except for curve D, where directional distribution D is used, directional distribution A is used. The large increase in response between towers in 600ft and 800ft of water is due to stepwise changes in tower properties, which are mainly caused by stepwise tapering of the tower legs. The variation of the rotational response with the mean direction of wave advance is shown for Towers 1 through 4 in Fig. 6.9. Wave spectrum B and direction distribution A are used in the generation of these curves to show that the rotational responses

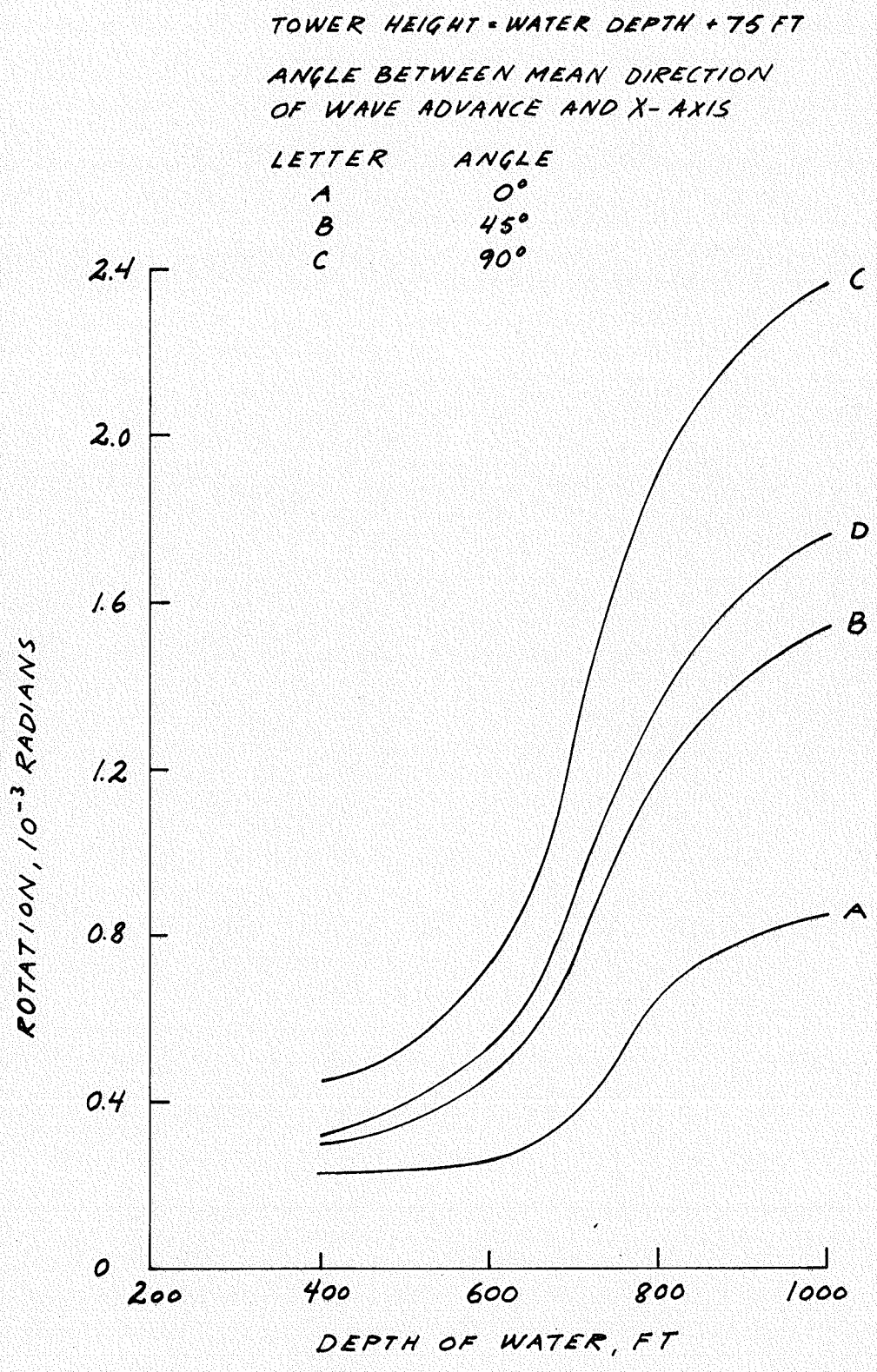

FIG. 6.8 STANDARD DEVIATION OF ROTATION OF DECK VS. DEPTH OF WATER

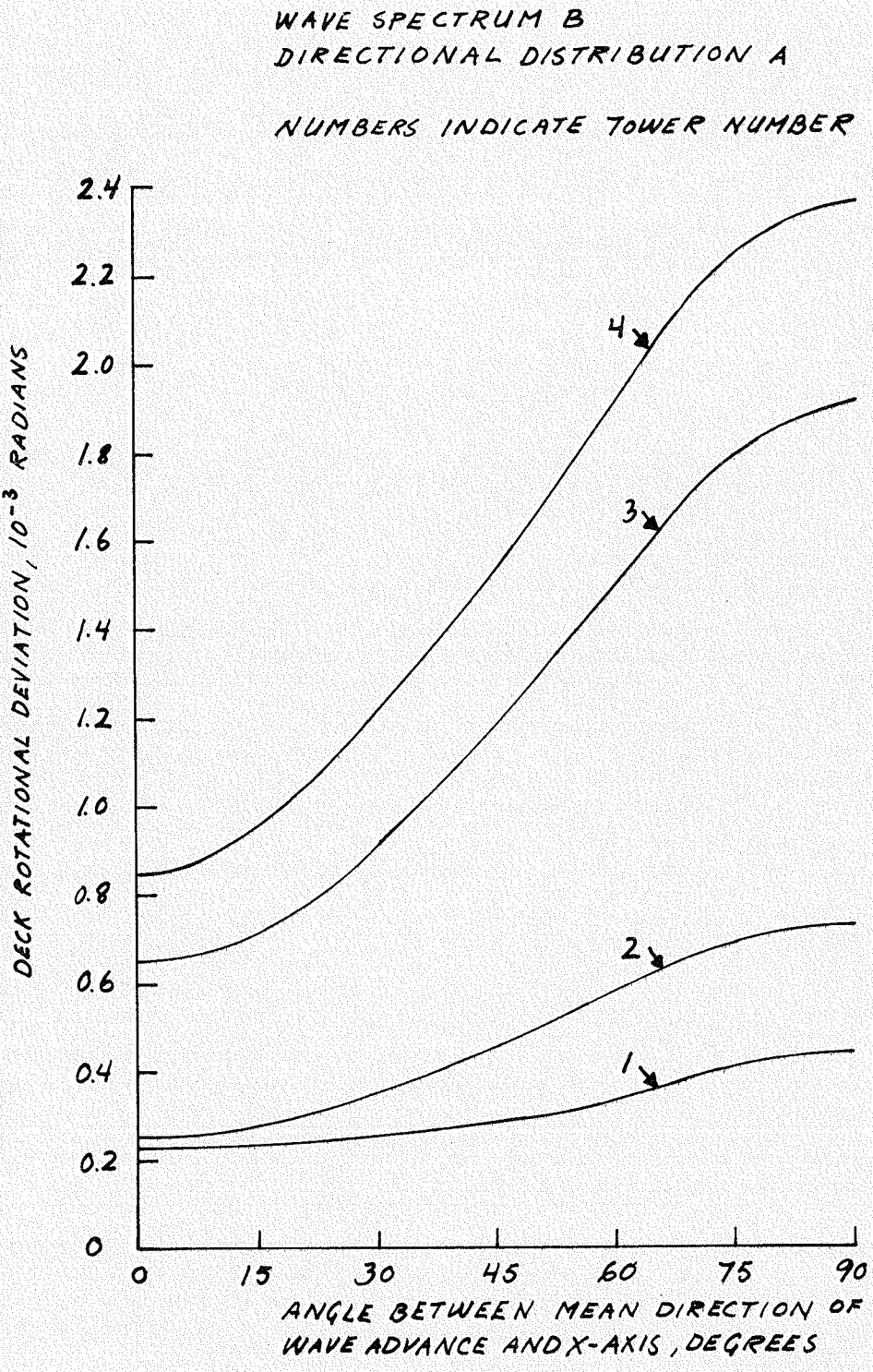

FIG. 6.9 STANDARD DEVIATION OF DECK ROTATION.
TOWERS 1, 2, 3 AND 4

for towers of various heights depend similarly on the mean direction of wave advance. Deck displacements for these towers due to the above mentioned directional spectrum are plotted in Fig. 6.10 versus mean direction of wave advance.

The relation between storm intensity and structural response is shown in Fig. 6.11, where the displacements in the y-direction and the rotations for Tower 1 are plotted for frequency wave spectra A, B and C, corresponding to wind speeds of 50, 75 and 100ft/sec. Mean direction of wave advance is in the y-direction and directional distribution A is used. It is interesting to notice the high ratio of rotation to translation for 50ft/sec wind speed relative to the same ratio for 75 and 100ft/sec wind speeds. The reason for this is that the phase difference of the wave forces over the horizontal extension of the structure has a decreasing effect on the translation of the structure while it often might have an increasing effect on the rotation. This phase difference decreases with increasing wave lengths, and the wave lengths increases with the severity of the storm.

The importance of the including rotation of the structure in the dynamic analysis can best be studied by considering its effect on the displacement of the tower legs, i.e. where the rotations about the vertical z-axis have the largest effects. Figures 6.12 through 6.18 are plotted for this purpose. They show leg displacements for Towers 1 through 6. All curves are based on wave spectrum B and directional distribution A, except some curves in Figs. 6.12 and 6.13, where directional distribution C is used. These figures show that the effect of the rotation on the leg displacements is very small; a maximum of 16% difference between the leg displacements in y-direction for

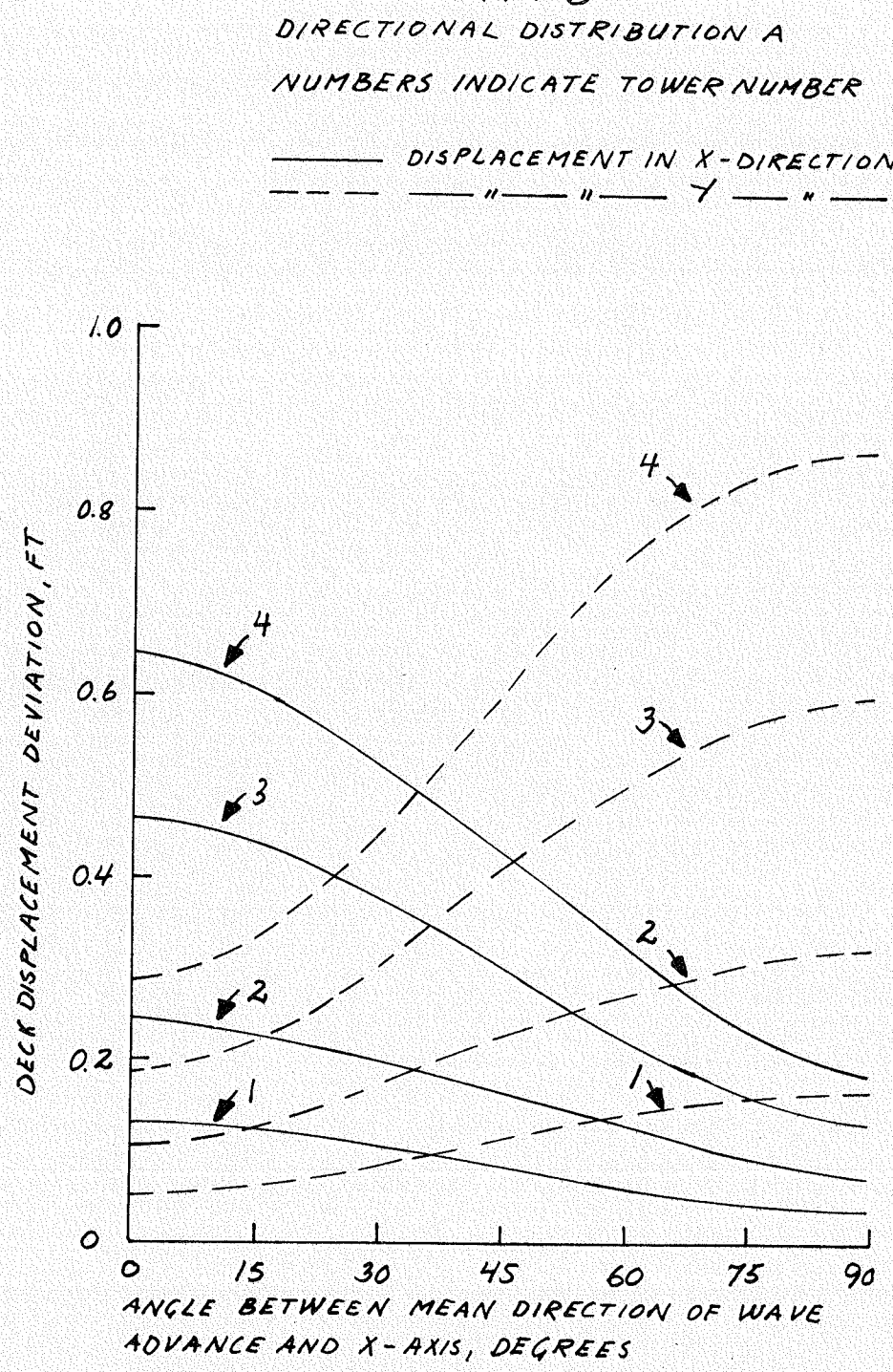

FIG. 6.10 STANDARD DEVIATION OF DECK DISPLACEMENT VS. MEAN DIRECTION OF WAVE ADVANCE. TOWERS 1, 2, 3 AND 4

DIRECTIONAL DISTRIBUTION A
MEAN DIRECTION OF WAVE ADVANCE: Y-DIRECTION

LETTER	WAVE SPECTRUM	WIND SPEED
A	A	50 FT/SEC
B	B	75 FT/SEC
C	C	100 FT/SEC

——— DISPLACEMENT IN Y-DIRECTION
– – – – ROTATION

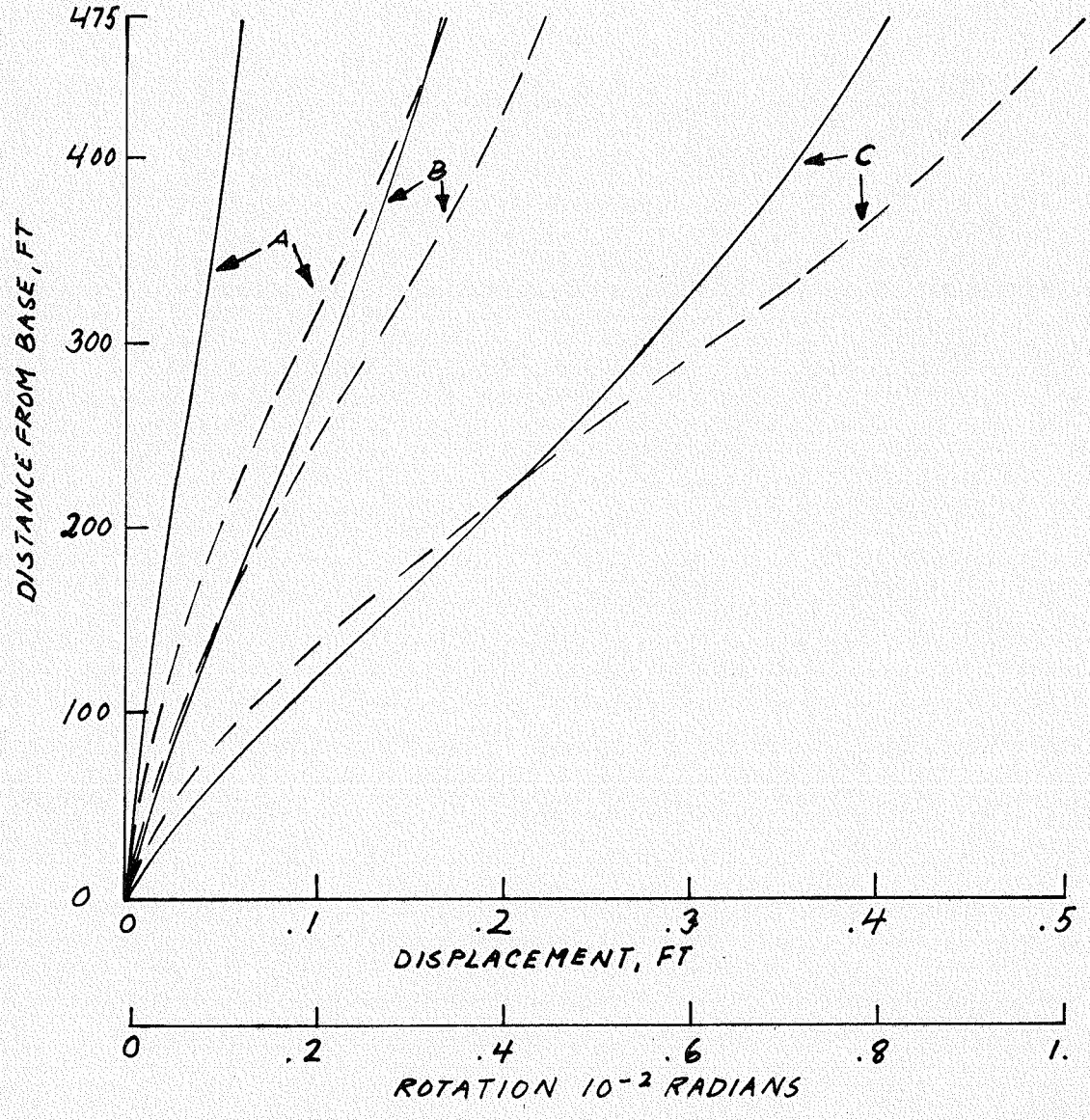

FIG. 6.11 STANDARD DEVIATIONS OF DISPLACEMENTS IN Y-DIRECTION AND OF ROTATIONS FOR DIFFERENT STORM INTENSITIES. TOWER 1

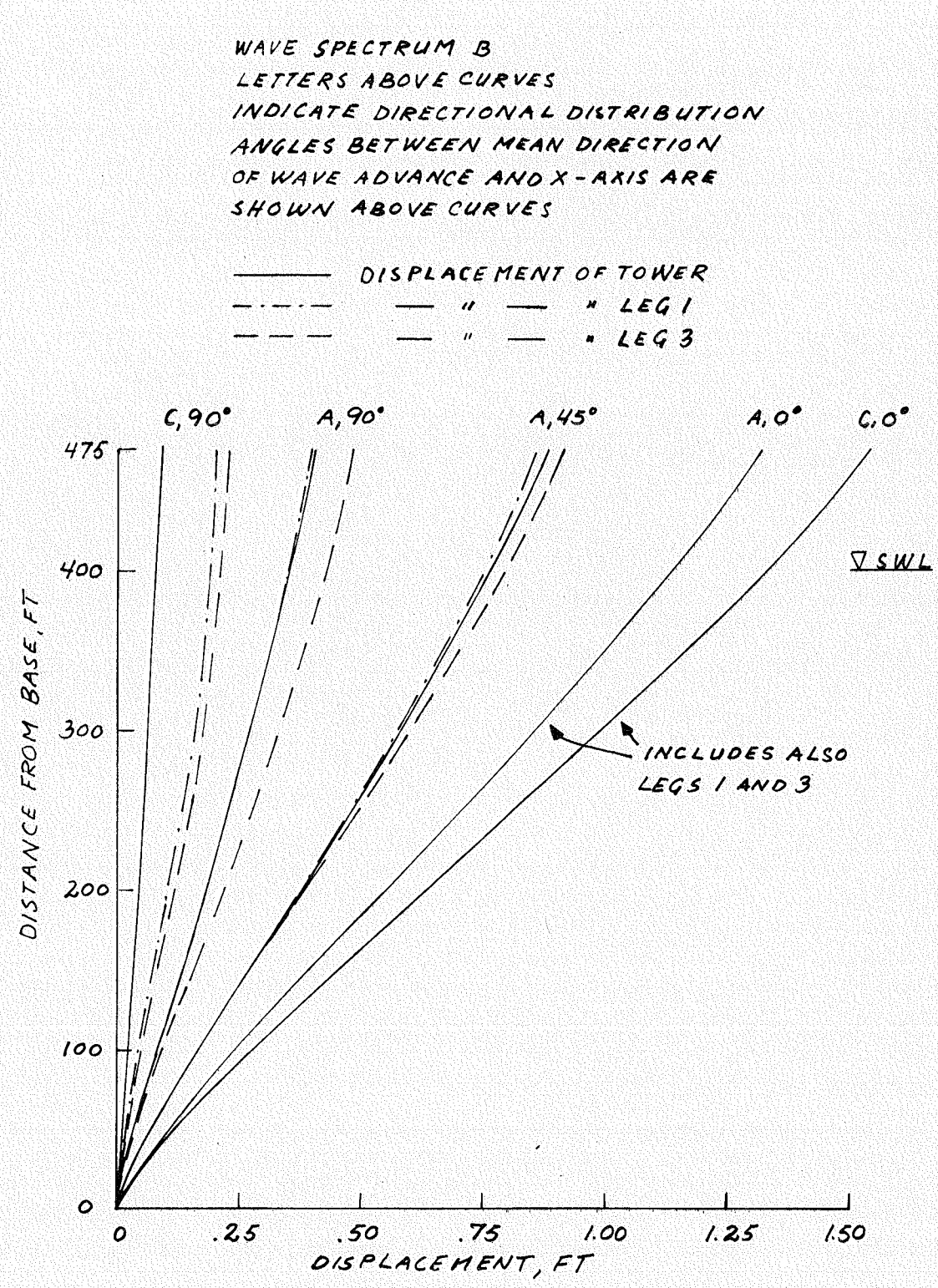

FIG. 6.12 STANDARD DEVIATIONS OF DISPLACEMENTS AND LEG DISPLACEMENTS IN X-DIRECTION TOWER 1

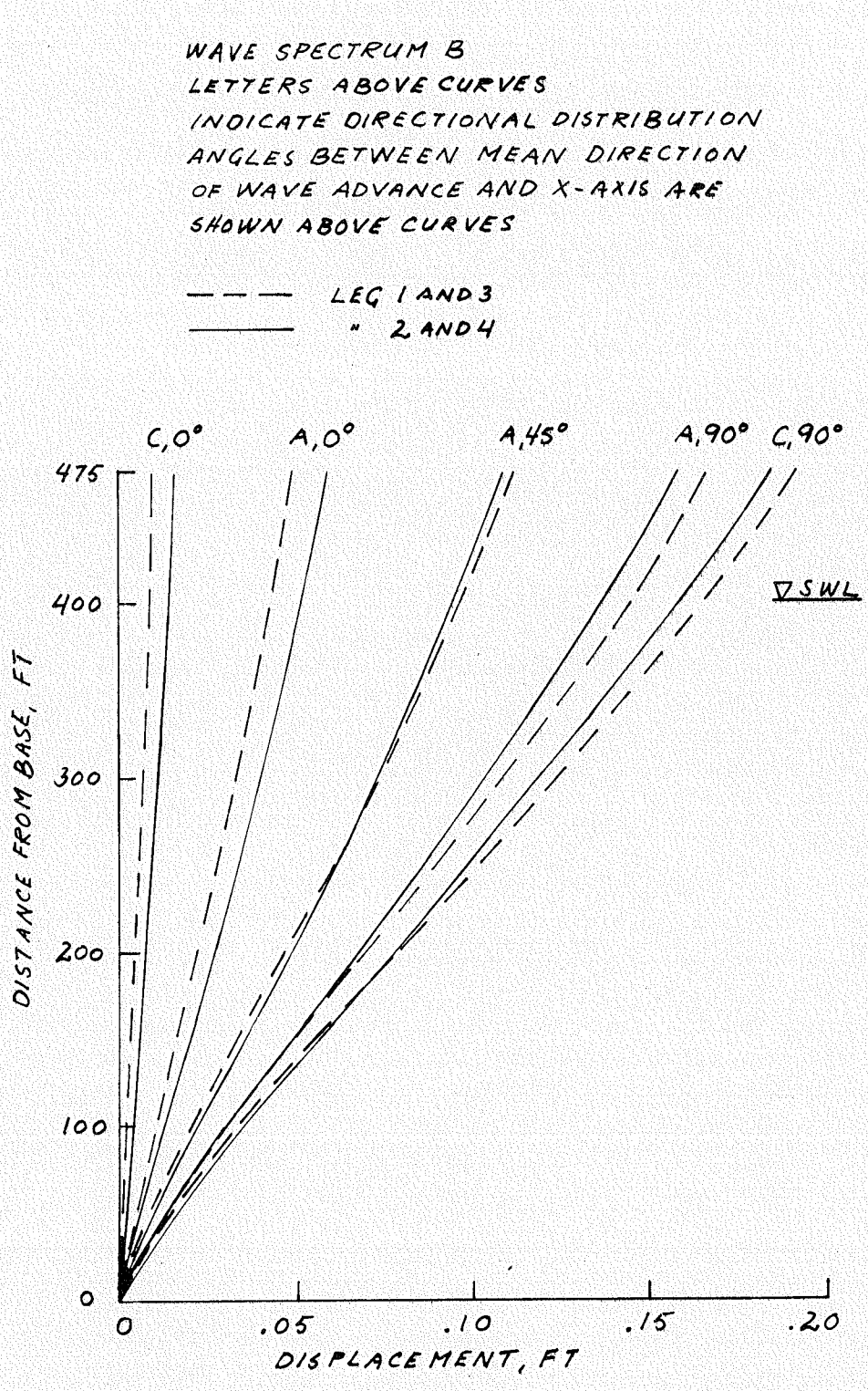

FIG. 6.13 LEG DISPLACEMENT DEVIATIONS IN Y-DIRECTION. TOWER 1

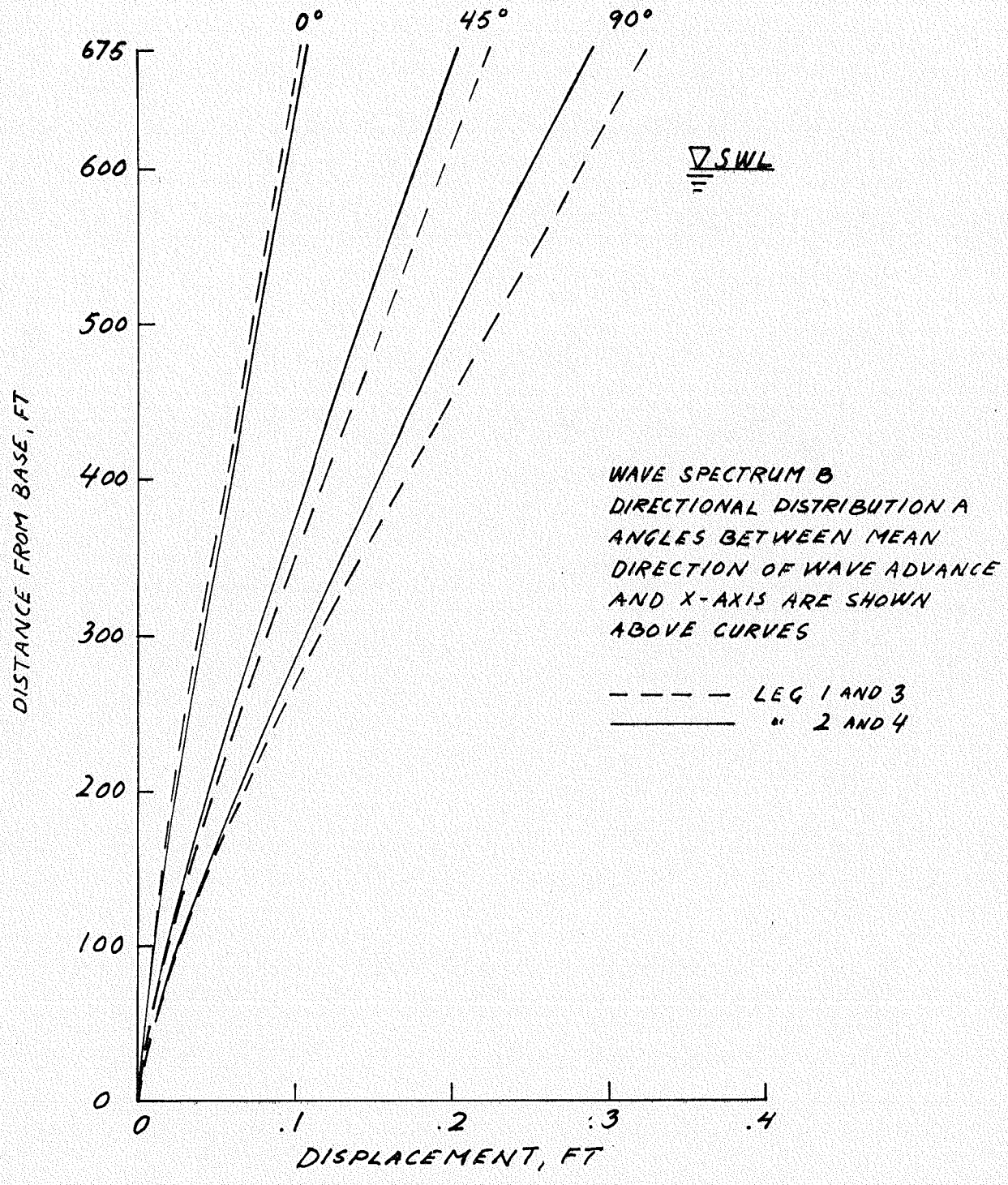

FIG. 6.14 LEG DISPLACEMENT DEVIATIONS IN Y-DIRECTION. TOWER 2

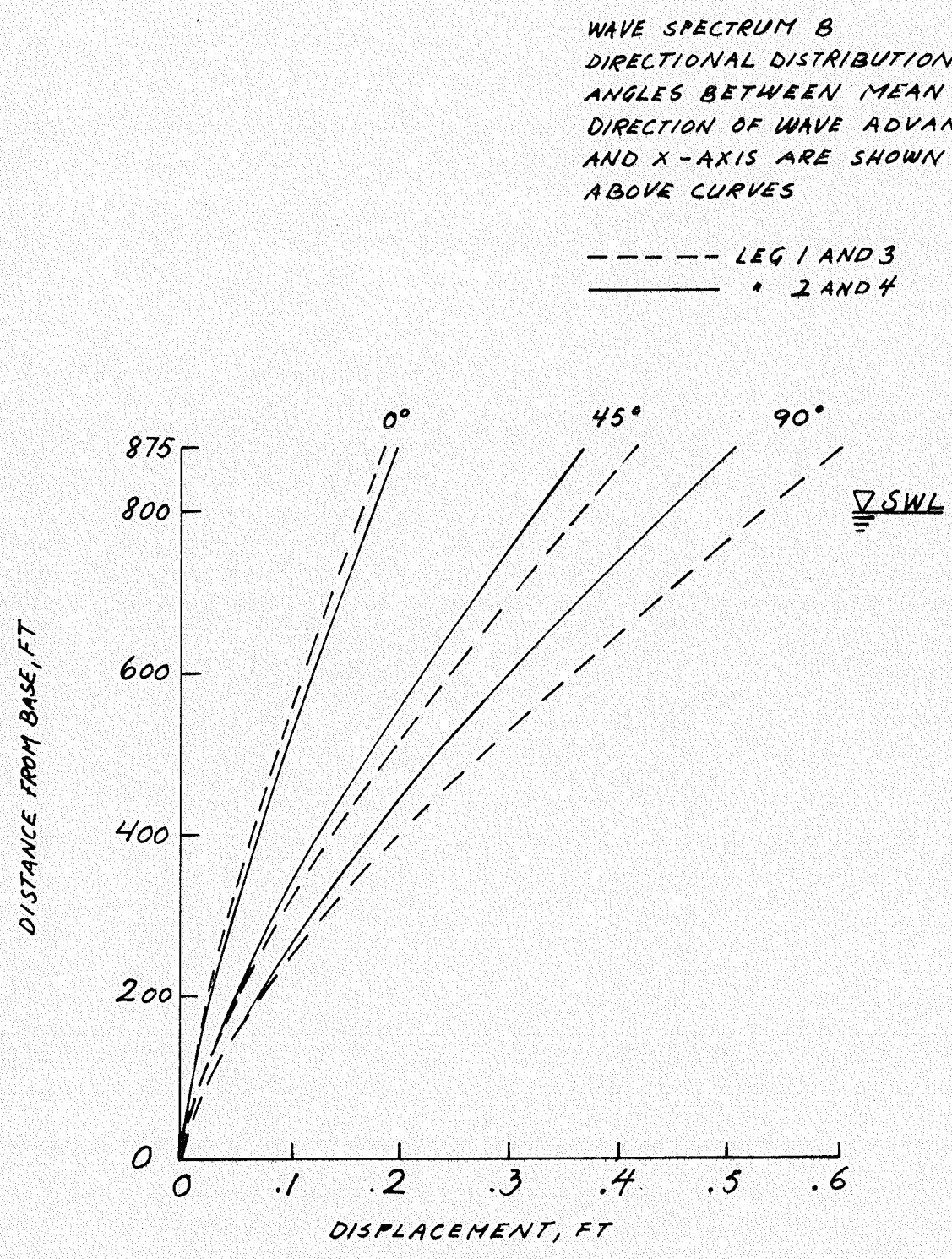

FIG. 6.15 LEG DISPLACEMENT DEVIATIONS IN Y-DIRECTION. TOWER 3

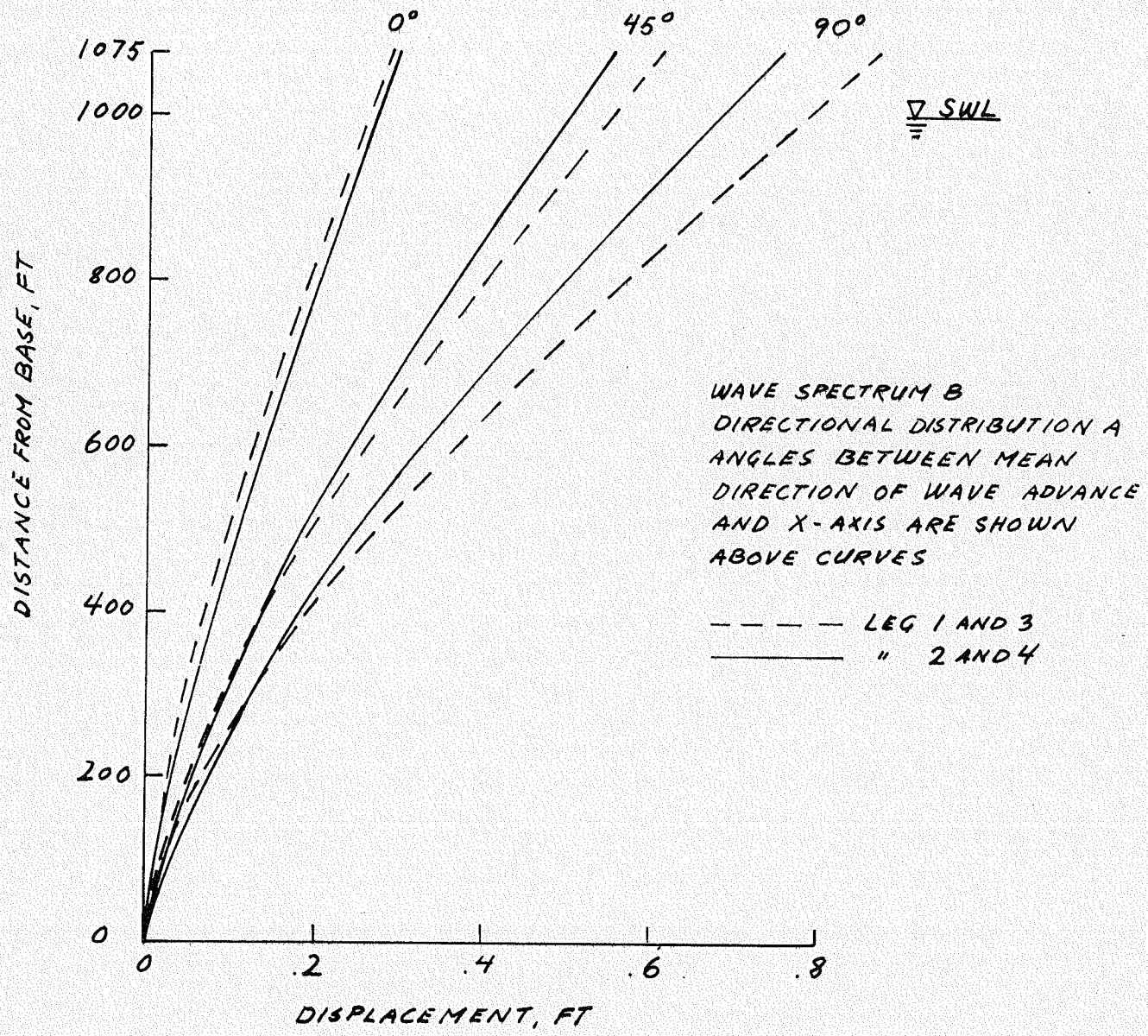

FIG. 6.16 LEG DISPLACEMENT DEVIATIONS IN Y-DIRECTION. TOWER 4

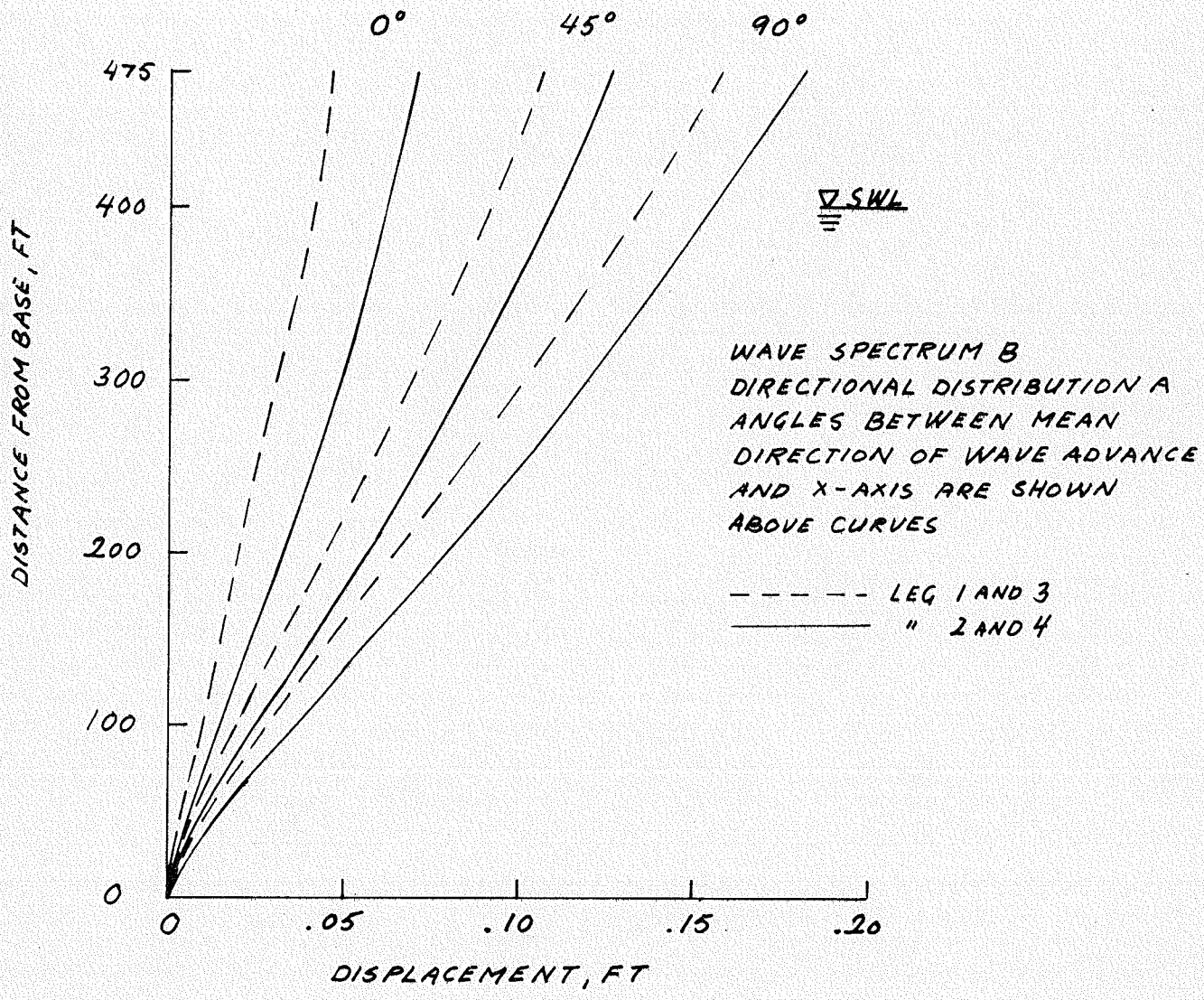

FIG. 6.17 LEG DISPLACEMENT DEVIATIONS IN Y-DIRECTION, TOWER 5

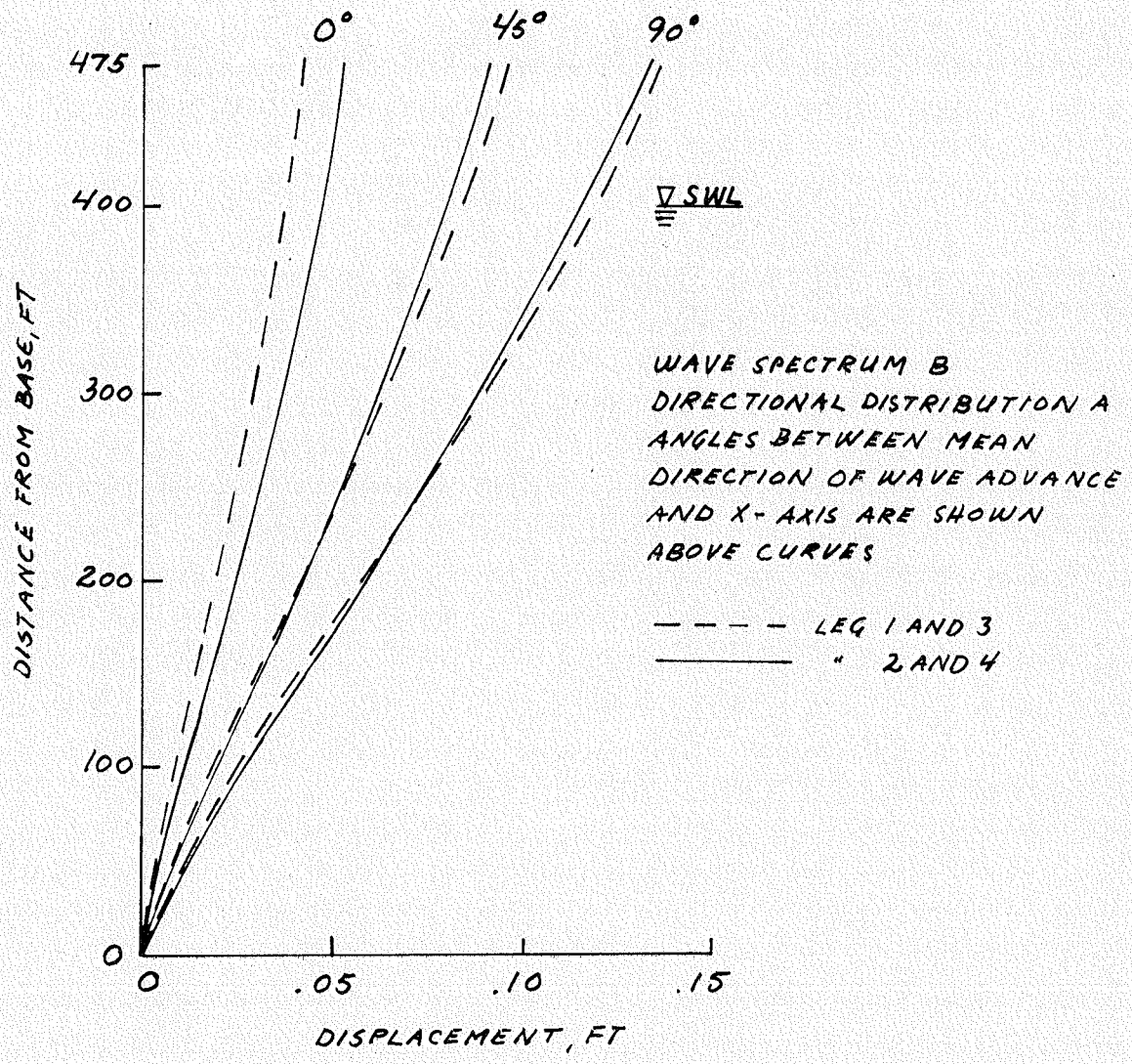

FIG. 6.18 LEG DISPLACEMENT DEVIATIONS IN Y-DIRECTION. TOWER 6

Tower 3, Fig. 6.15, when the mean direction of wave advance is perpendicular to the plane of symmetry. The effect of reduced torsional stiffness is illustrated by comparing the rotations for Tower 5, Fig. 6.17, with the corresponding rotations for Tower 1, Fig. 6.13. Doubling the leg spacings of Tower 1 does not have a significant effect on the contribution from the rotation to the nodal displacement; see Figs. 6.18 and 6.13.

The data discussed so far have been standard deviations of response quantities. While these are important statistical quantities, the designer is more interested in the maximum values that might occur during future storms. Figure 2.2, pg.15, shows how mean peak values measured in standard deviations varies with process duration for Tower 1. (For this tower the frequency ν takes values around 0.1 cps.) The mean peak values for deck displacement in the y-direction and deck rotation are plotted versus storm duration in Fig. 6.19 for 3 different wind velocities.

Twisting moment distributions for Tower 1 through 4 and 7 are shown in Figs. 6.20 through 6.25. These curves give standard deviations and mean peak values for 0.2, 1.5 and 10 hour storms. All distributions in these figures are for directional spectra described by wave spectrum B and directional distribution A, except for Fig. 6.21 where directional distribution B is used. The mean direction of wave advance is in the y-direction. A comparison of Figs. 6.20 and 6.21 reveals that the twisting moment increases slightly as the directional wave spectra become more narrow when the mean direction of wave advance is perpendicular to the plane of symmetry. The twisting moment in Tower 7 (symmetric about two vertical planes) is very small, Fig. 6.25.

DIRECTIONAL DISTRIBUTION A
MEAN DIRECTION OF WAVE ADVANCE: Y-DIRECTION

LETTER	WAVE SPECTRUM	WIND SPEED
A	A	50 FT/SEC
B	B	75 "
C	C	100 "

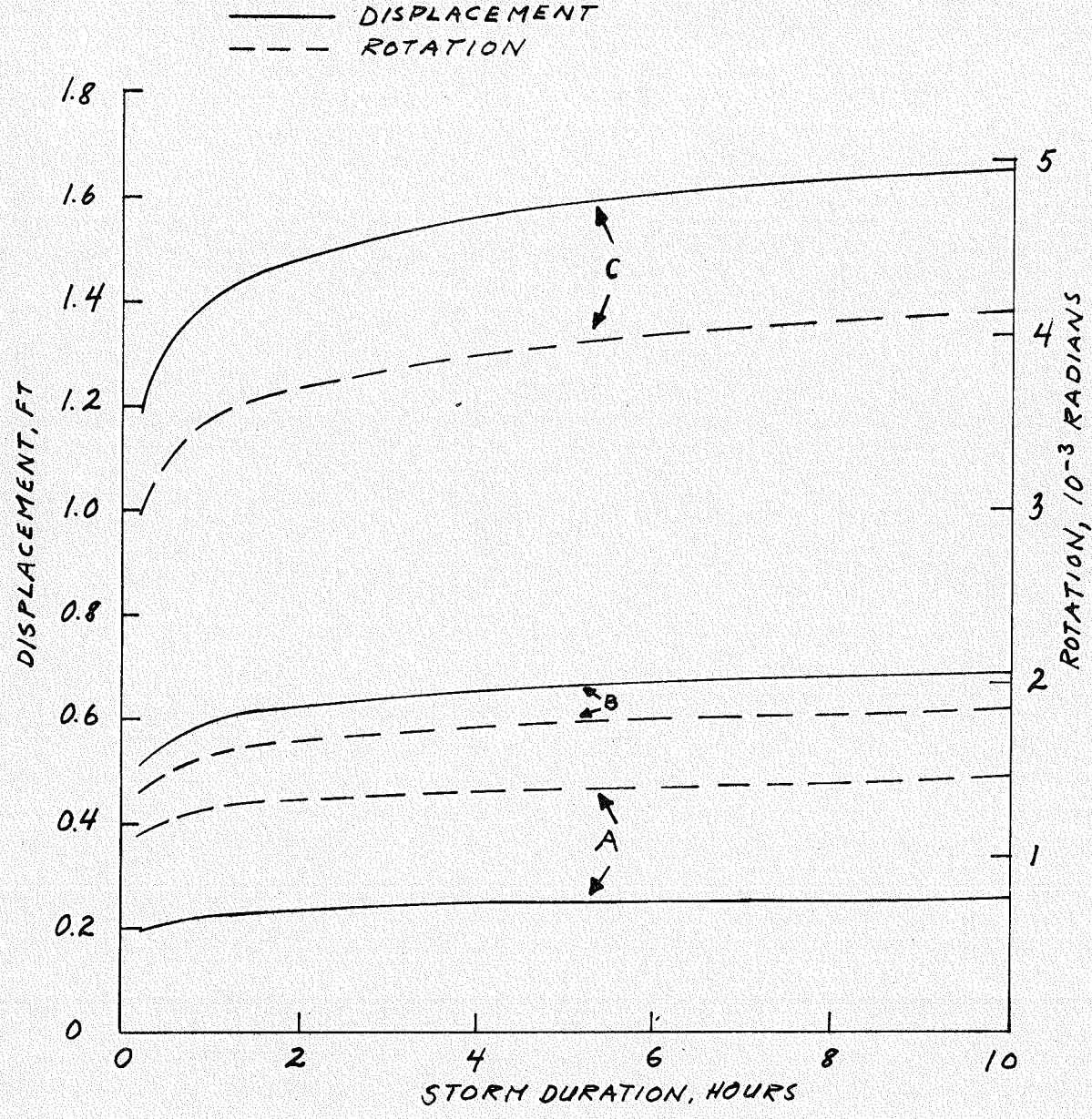

FIG. 6.19 MEAN PEAK VALUES FOR DECK DISPLACEMENT IN Y-DIRECTION AND FOR DECK ROTATION VS. STORM DURATION. TOWER 1

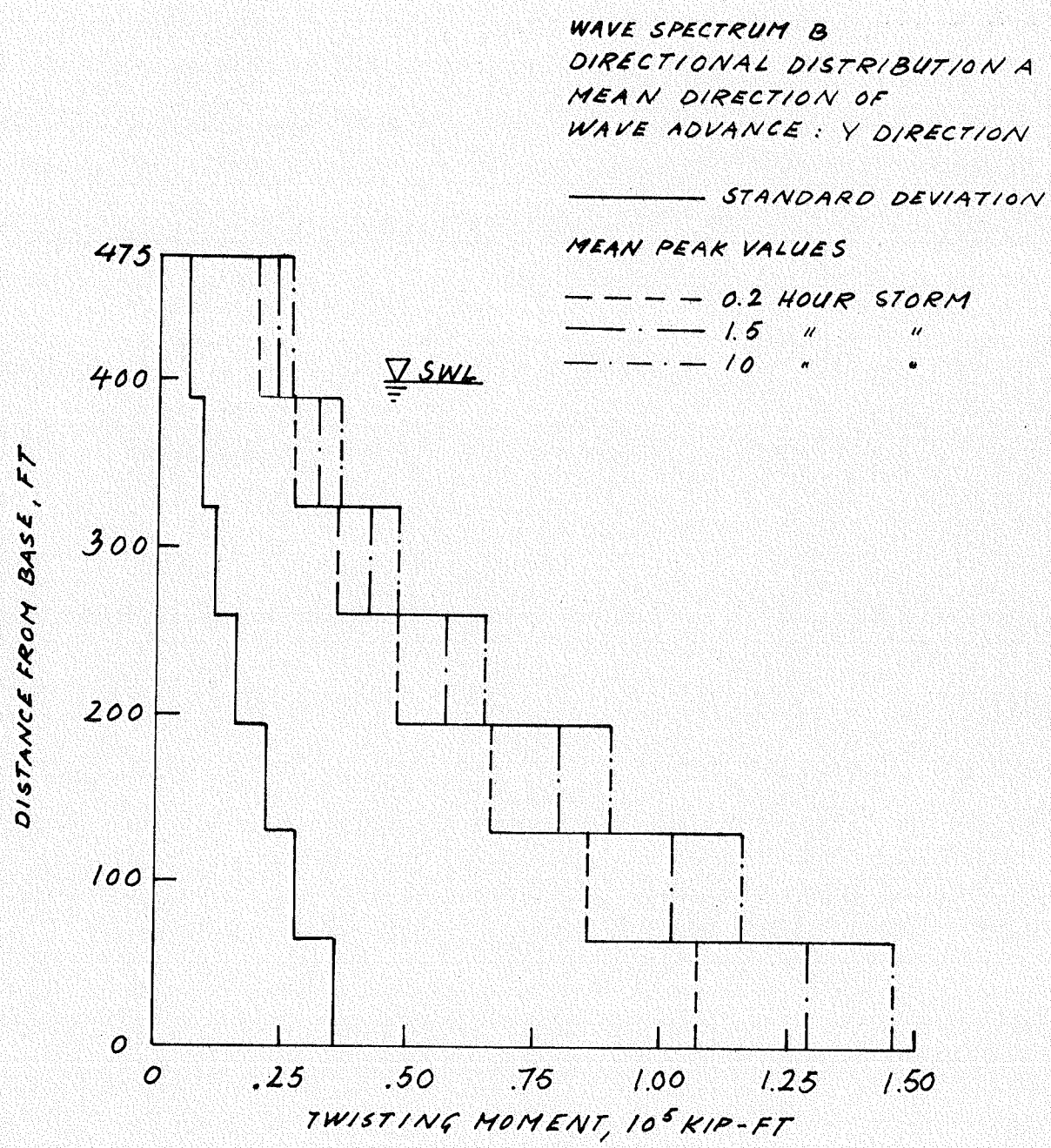

FIG. 6.20 TWISTING MOMENT DISTRIBUTION FOR TOWER 1

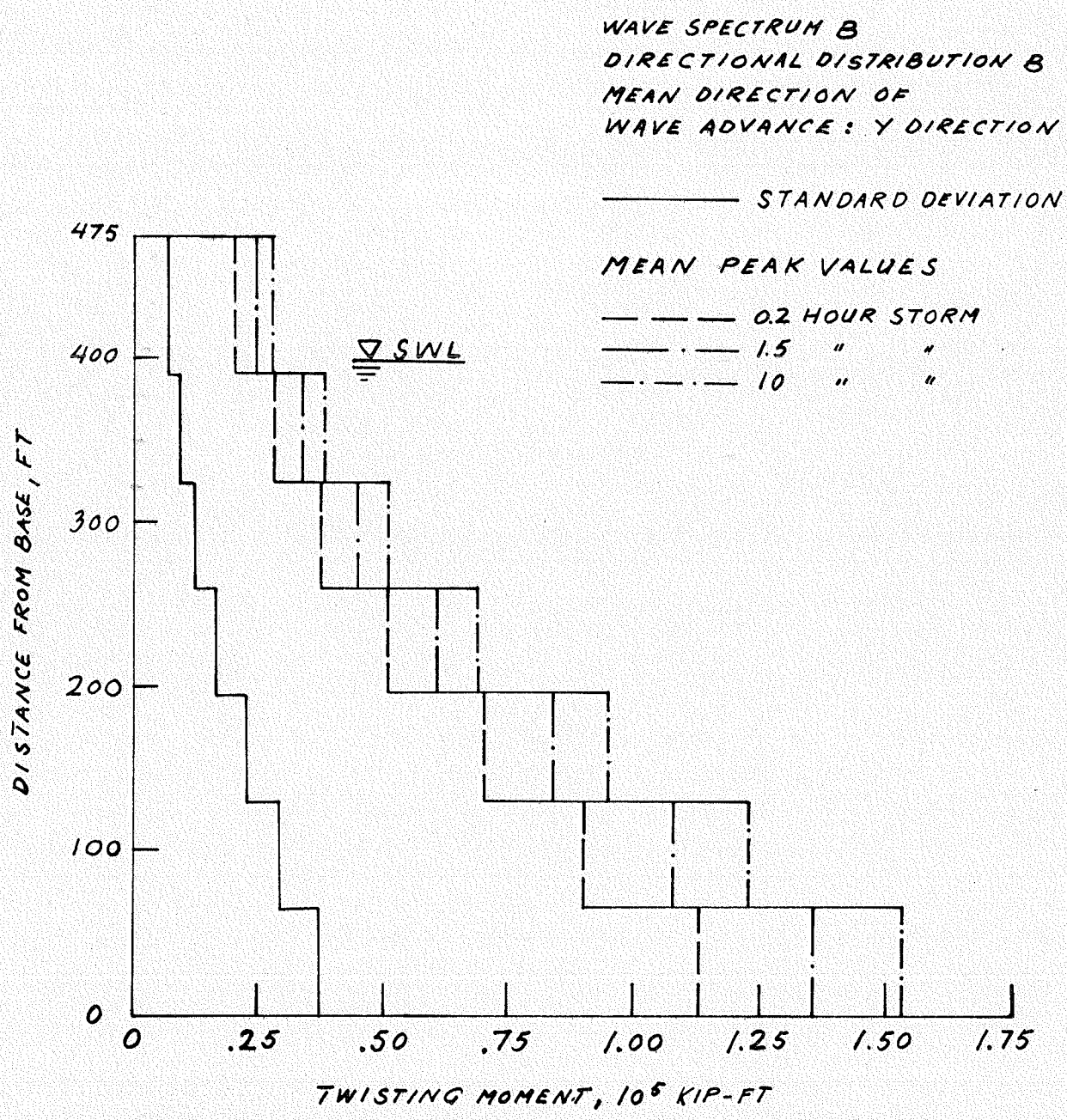

FIG. 6.21 TWISTING MOMENT DISTRIBUTION FOR TOWER 1

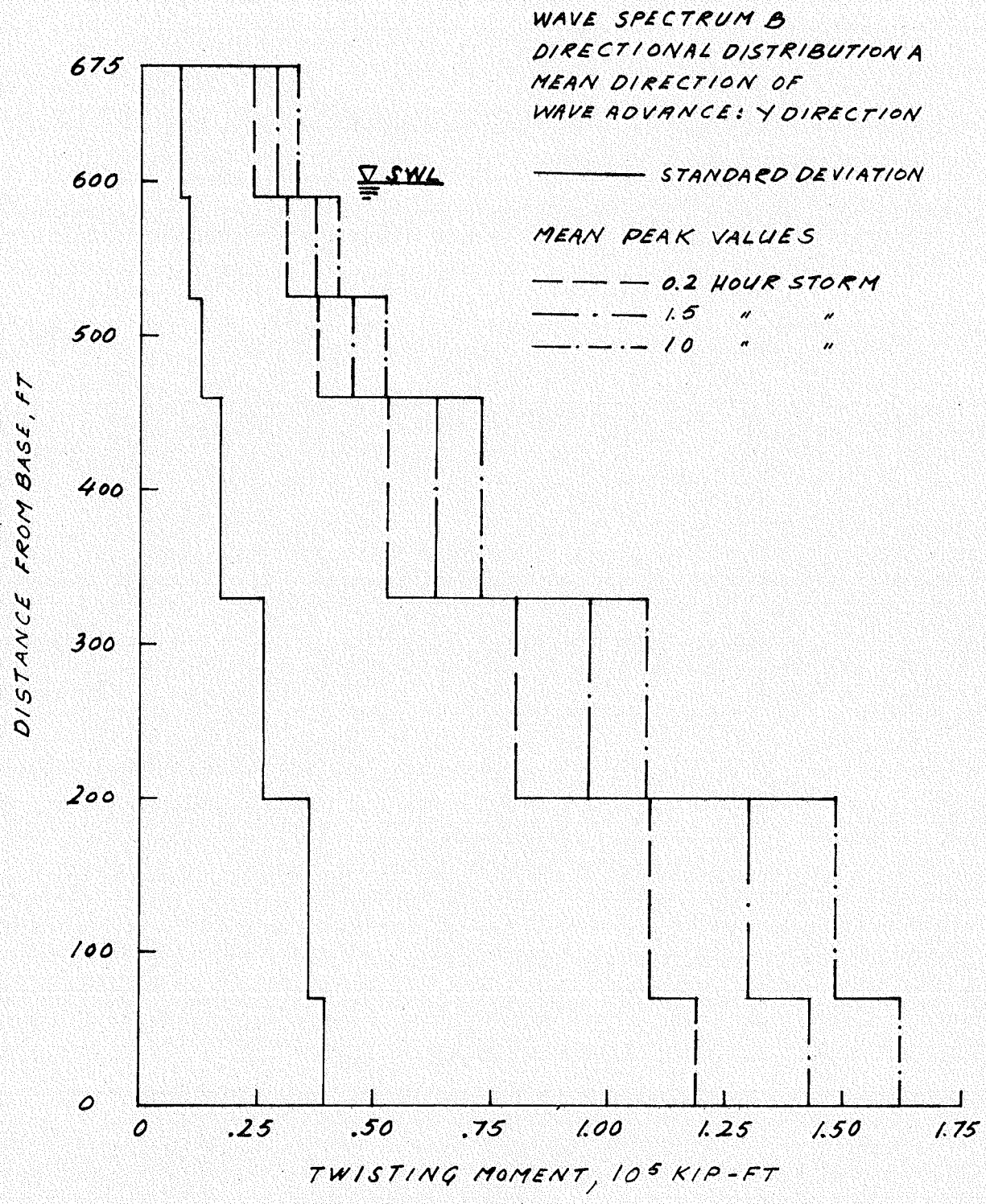

FIG. 6.22 TWISTING MOMENT DISTRIBUTION FOR TOWER 2

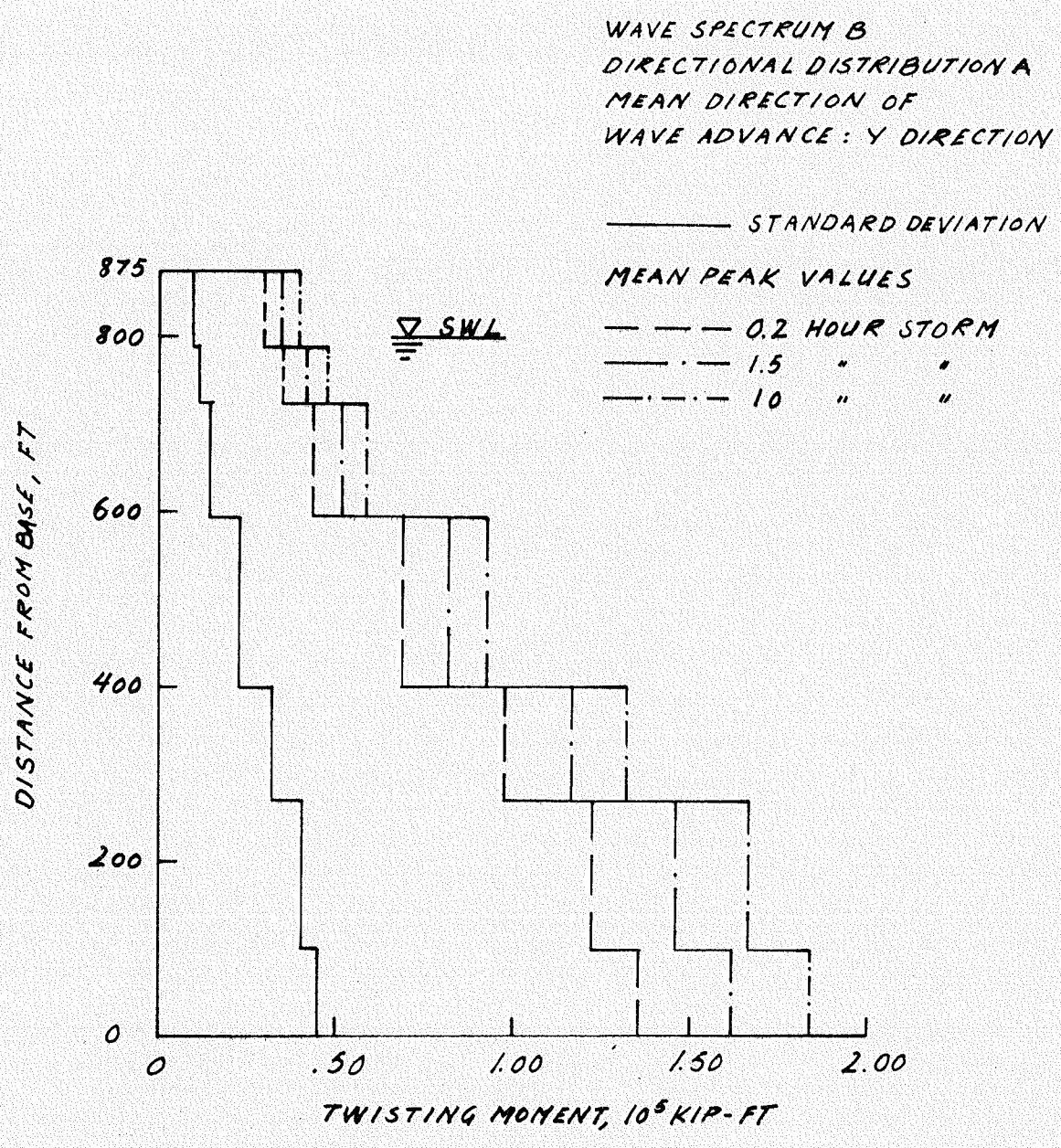

FIG. 6.23 TWISTING MOMENT DISTRIBUTION FOR TOWER 3

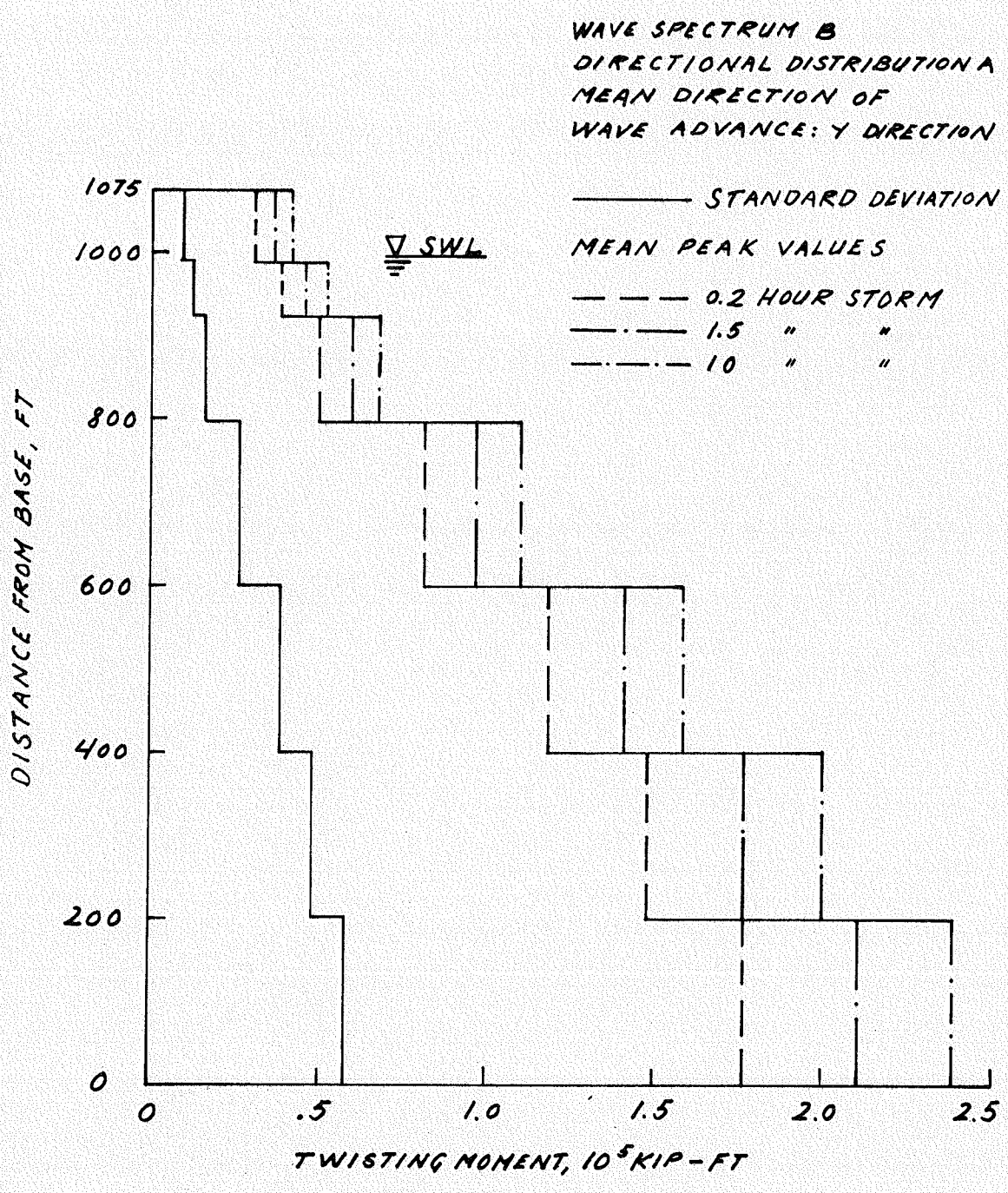

FIG. 6.24 TWISTING MOMENT DISTRIBUTION FOR TOWER 4

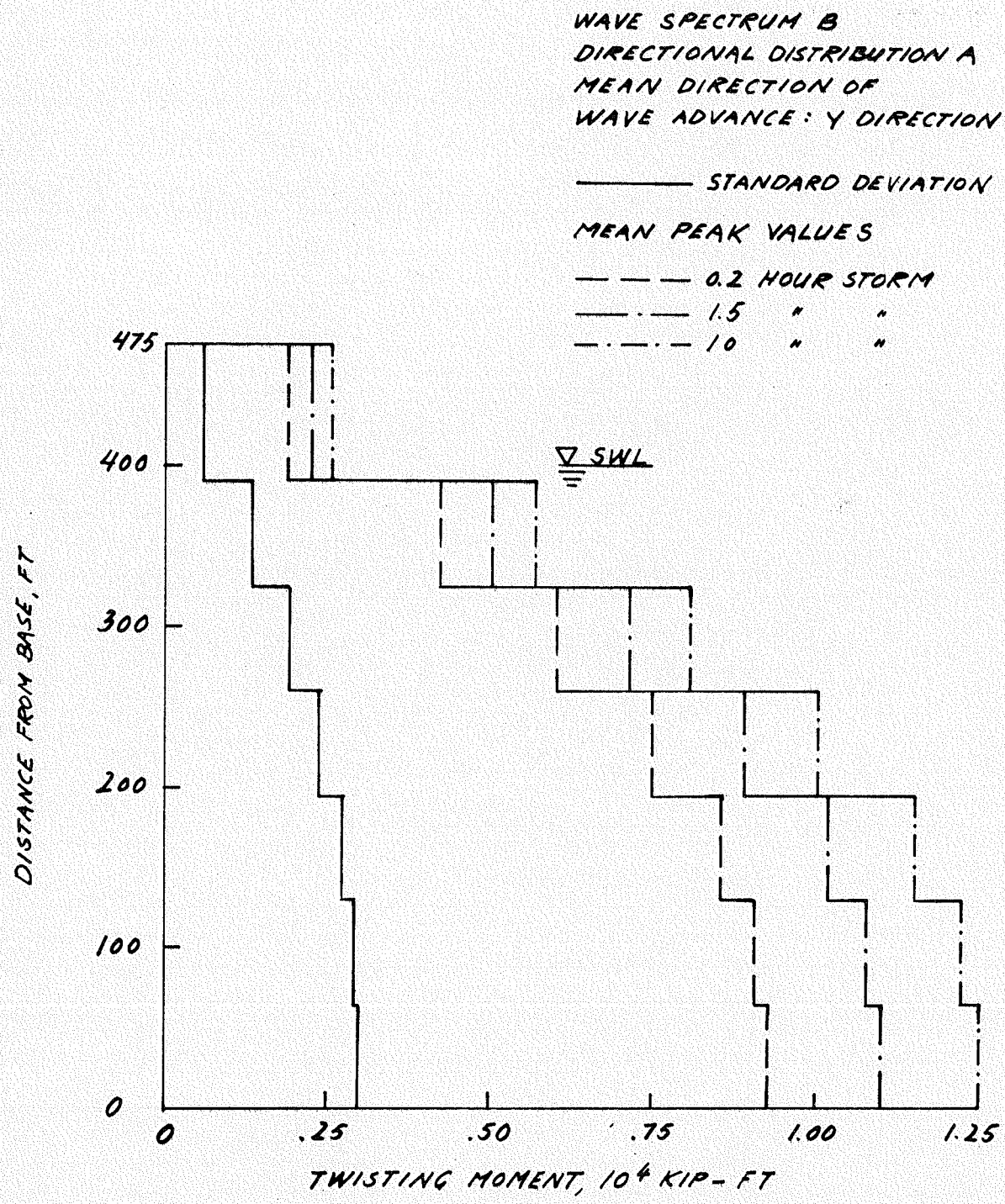

FIG. 6.25 TWISTING MOMENT DISTRIBUTION FOR TOWER 7

Shear force and bending moment distributions in y-direction for Towers 1 through 4 are shown in Figs. 6.26 through 6.33. These figures include standard deviations and mean peak values for 0.2, 1.5 and 10 hour storms. Wave spectrum B and directional distribution A with mean direction of wave advance in the y-direction are used for these results. The concentration of loading towards the top of the towers, especially the deeper ones, can be noticed from the curves for the shear distribution, Figs. 6.26, 6.28, 6.30 and 6.32. The quantities that have most interest are the shear forces and bending moments at the base. The mean peak values for these quantities in the y-direction are plotted versus storm duration for Tower 1 in Fig. 6.34 and 6.35. Figure 6.34 shows these quantities for storms specified by one-dimensional wave spectrum B and direction distribution A and C with mean direction of wave advance having 0, 45 and 90 degree angle with the x-axis (plane of symmetry). Figure 6.35 shows mean peak values for base shear forces and bending moments for 3 different storm intensities specified by directional spectra described by directional distribution A and by one-dimensional wave spectra A, B and C, corresponding to wind speeds of 50, 75 and 100ft/sec, respectively. Mean direction of wave advance is perpendicular to the plane of symmetry. Combining the translations and rotations of the structure the shear forces and bending moments in the frames through the tower legs are found. These are important quantities, especially for towers with little torsional rigidity, because for such towers the rotational responses may have a significant effect on the horizontal leg displacements.

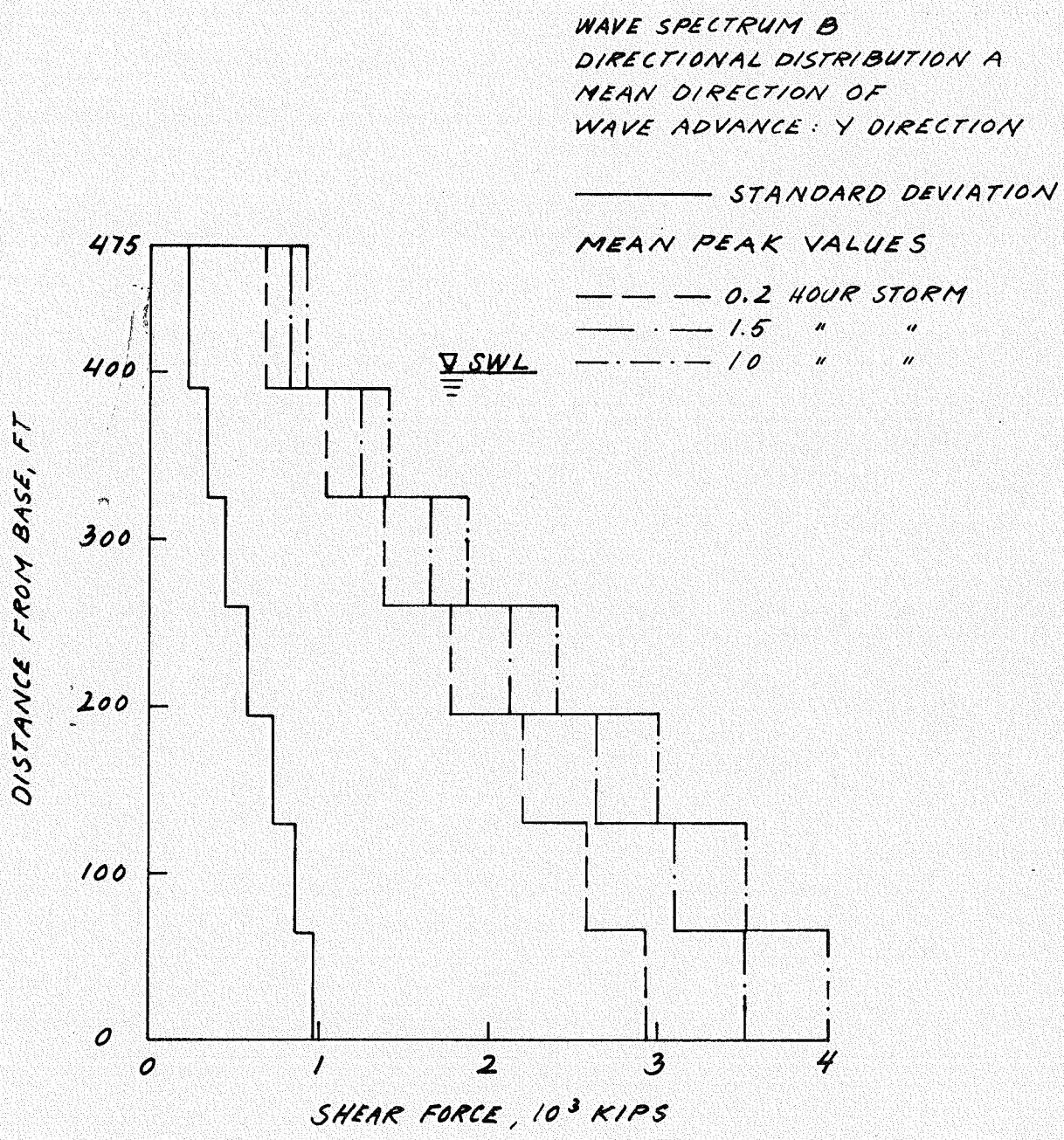

FIG. 6.26 SHEAR FORCE DISTRIBUTION IN Y-DIRECTION FOR TOWER I

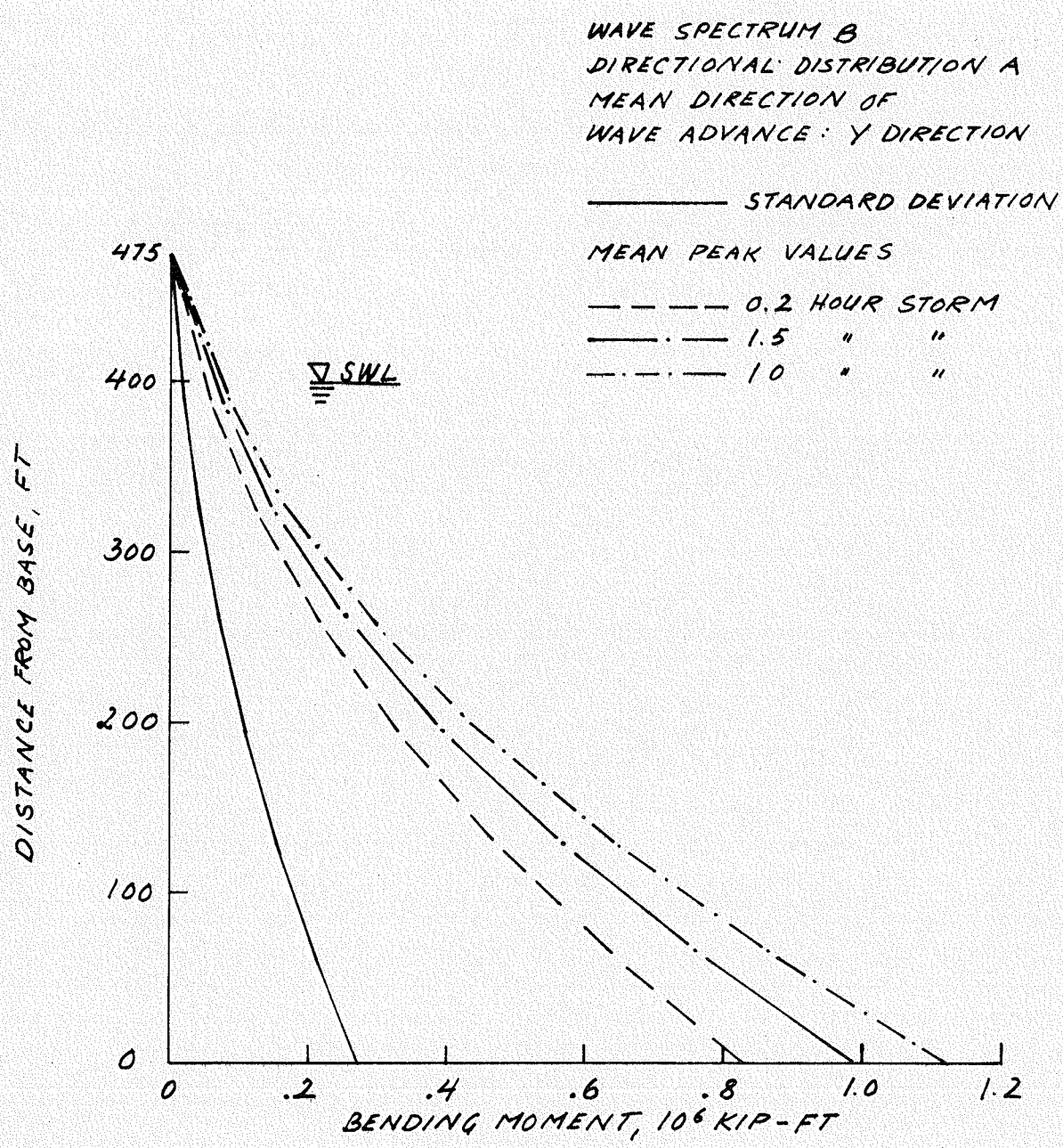

FIG. 6.27 BENDING MOMENT DISTRIBUTION IN Y-DIRECTION FOR TOWER 1

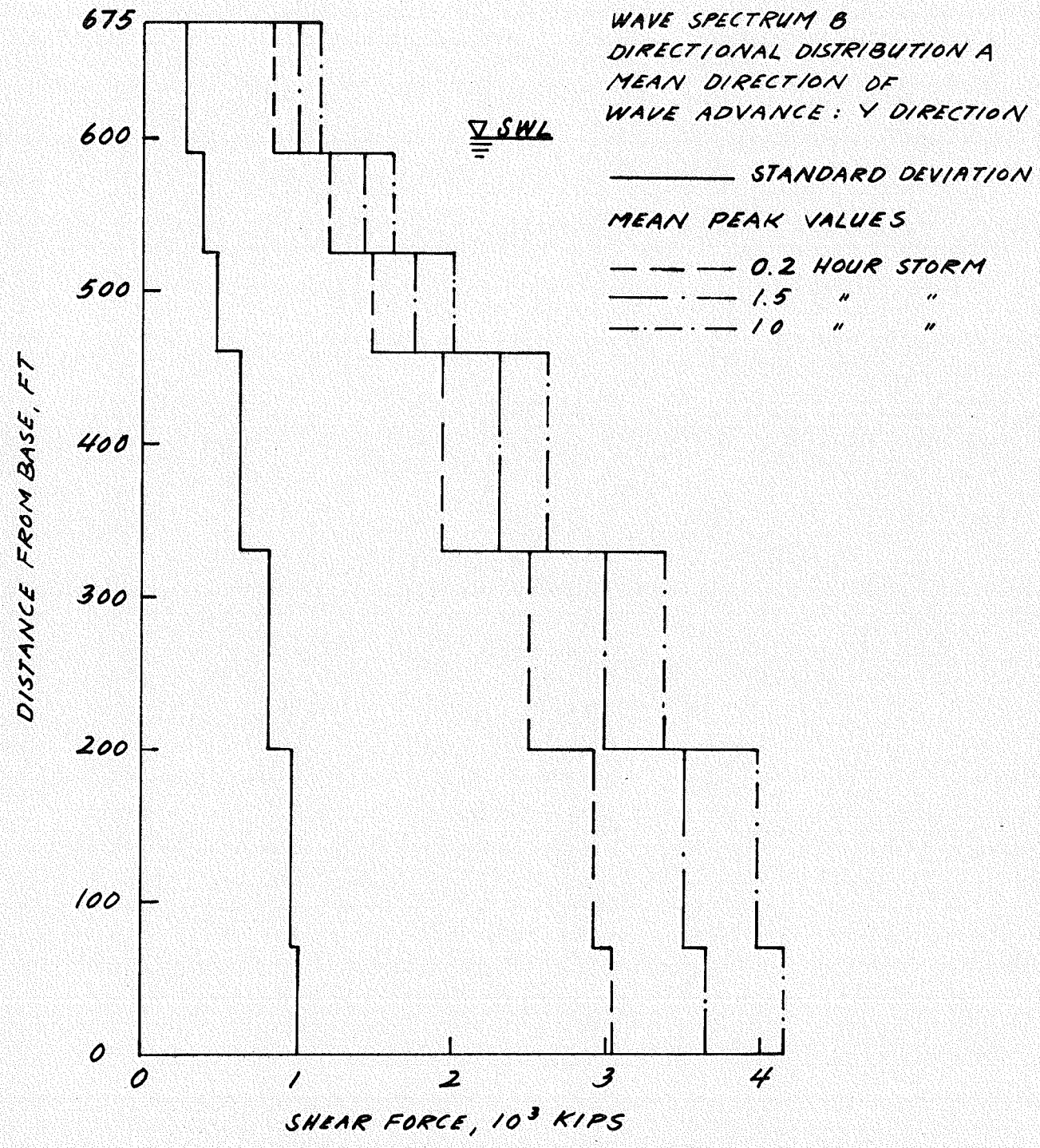

FIG. 6.28 SHEAR FORCE DISTRIBUTION IN Y-DIRECTION FOR TOWER 2

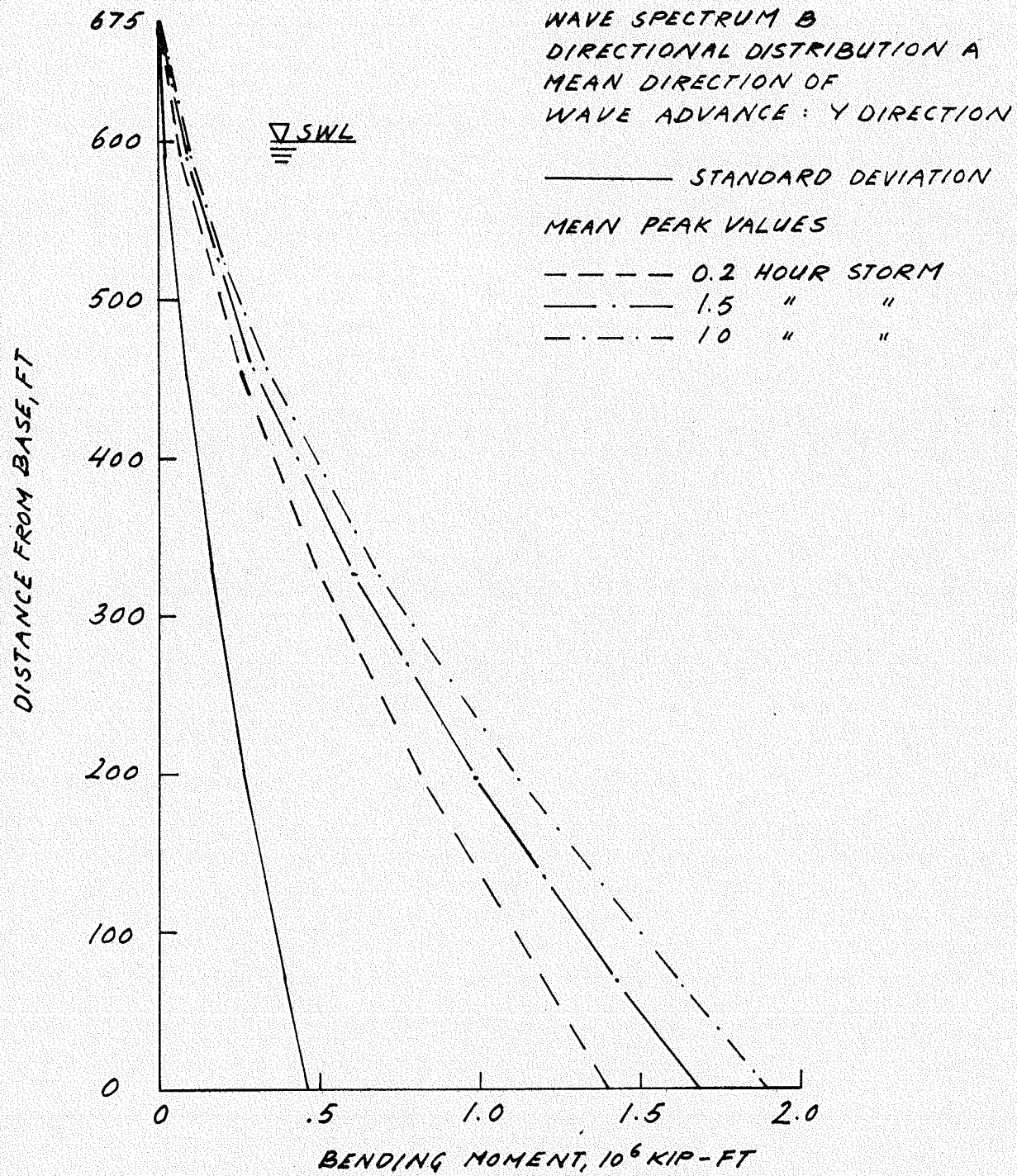

FIG. 6.29 BENDING MOMENT DISTRIBUTION IN Y-DIRECTION FOR TOWER 2

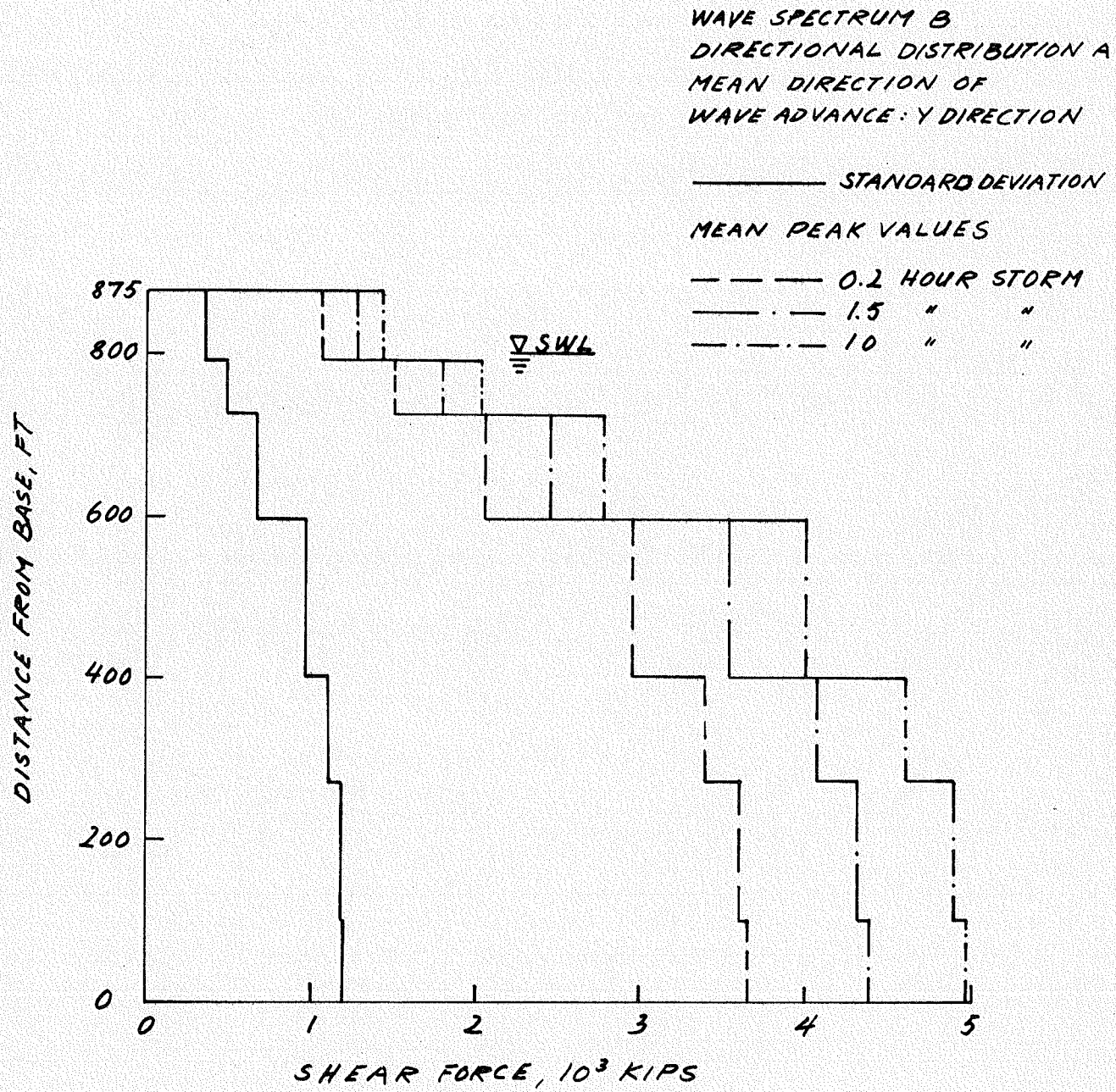

FIG. 6.30 SHEAR FORCE DISTRIBUTION IN Y-DIRECTION FOR TOWER 3

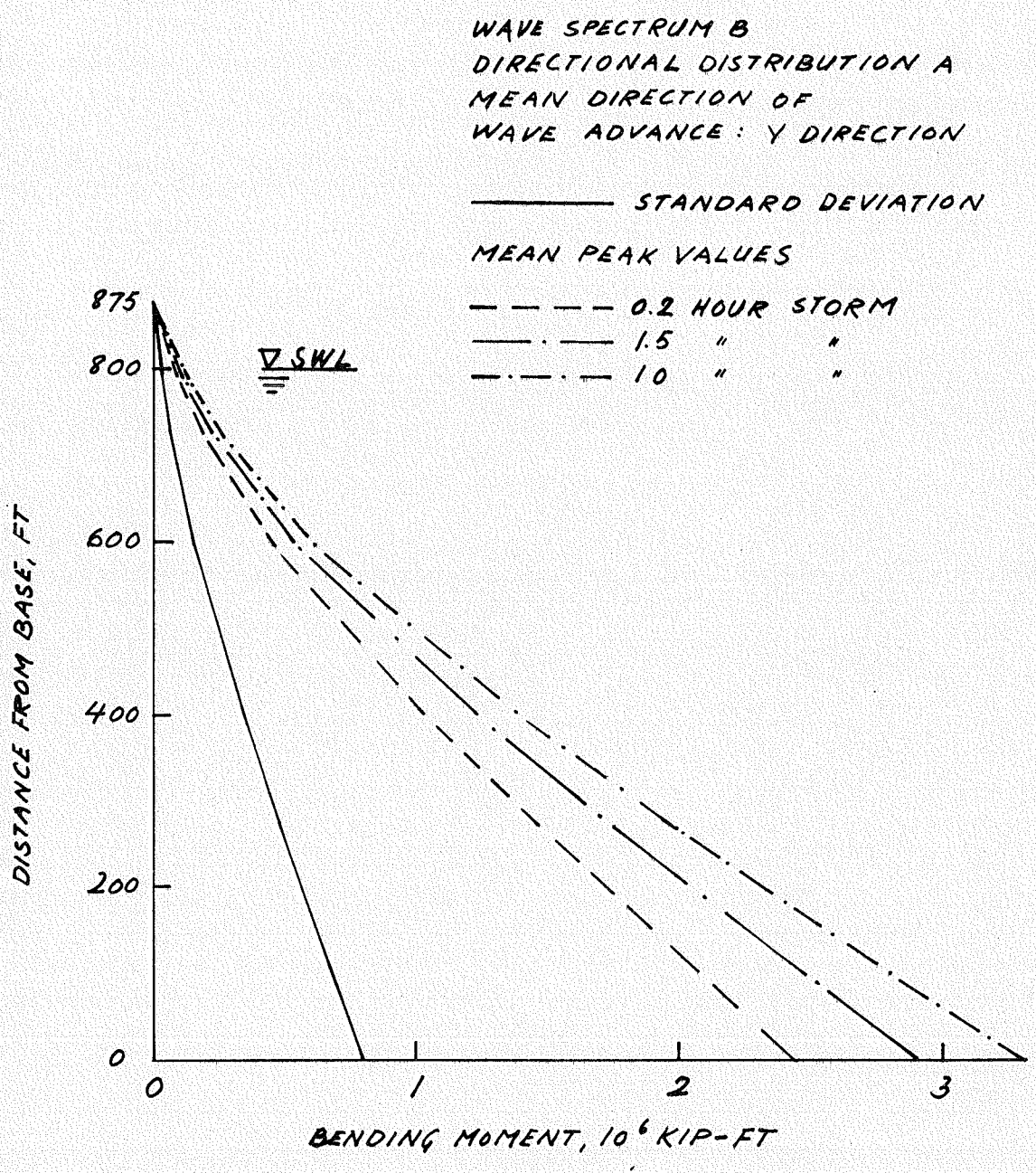

FIG. 6.31 BENDING MOMENT DISTRIBUTION IN Y-DIRECTION FOR TOWER 3

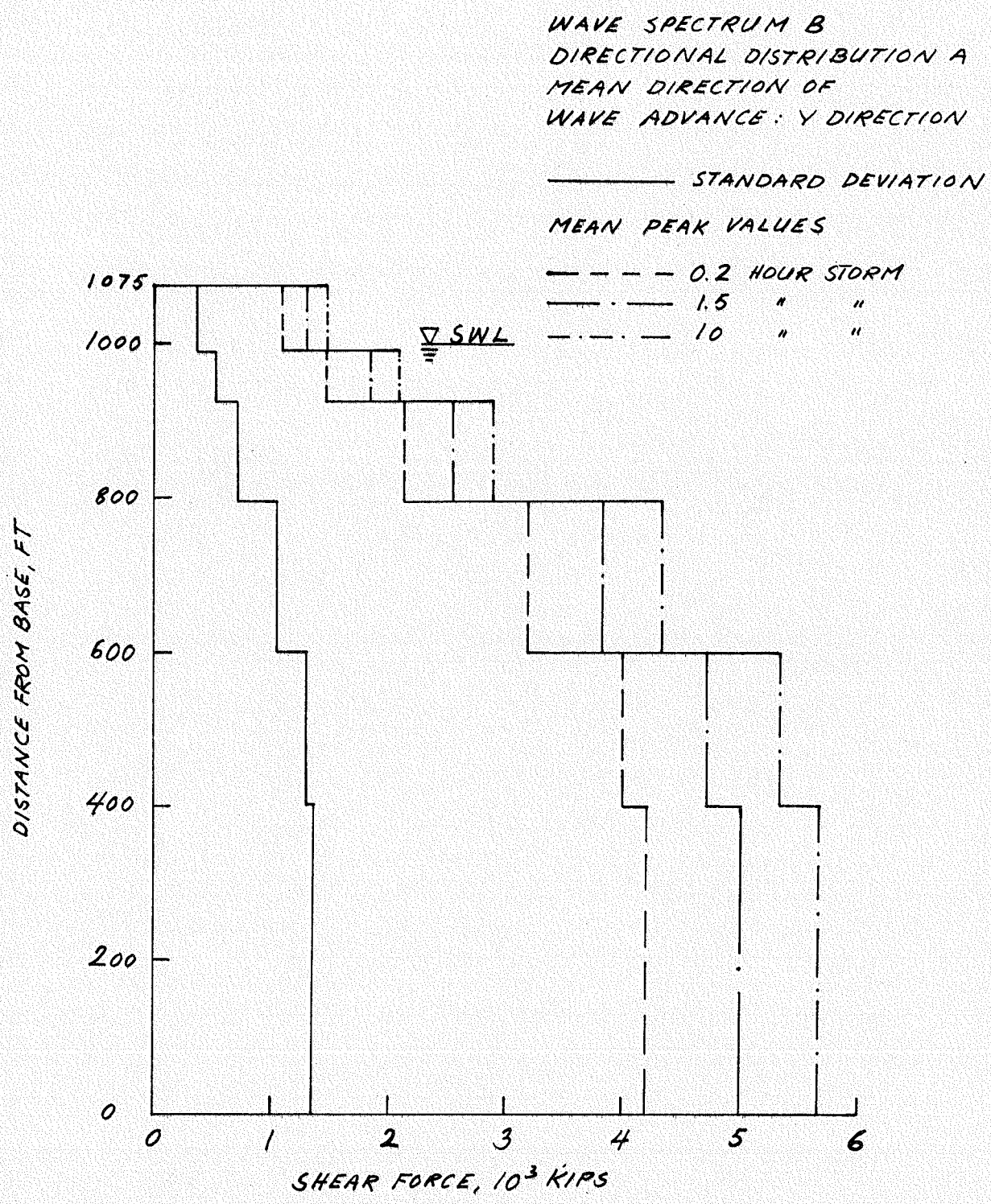

FIG. 6.32 SHEAR FORCE DISTRIBUTION
IN Y-DIRECTION FOR TOWER 4

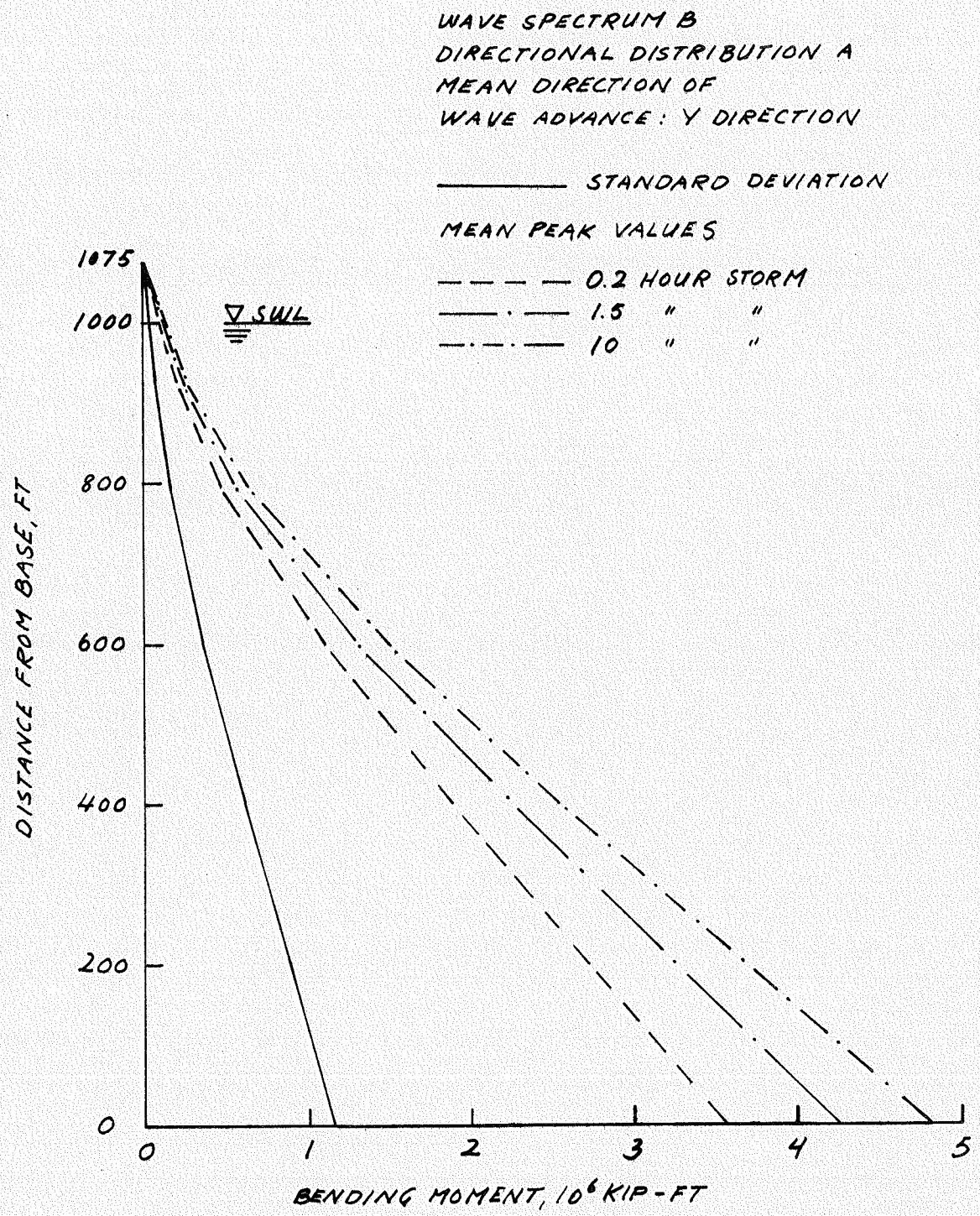

FIG. 6.33 BENDING MOMENT DISTRIBUTION IN Y-DIRECTION FOR TOWER 4

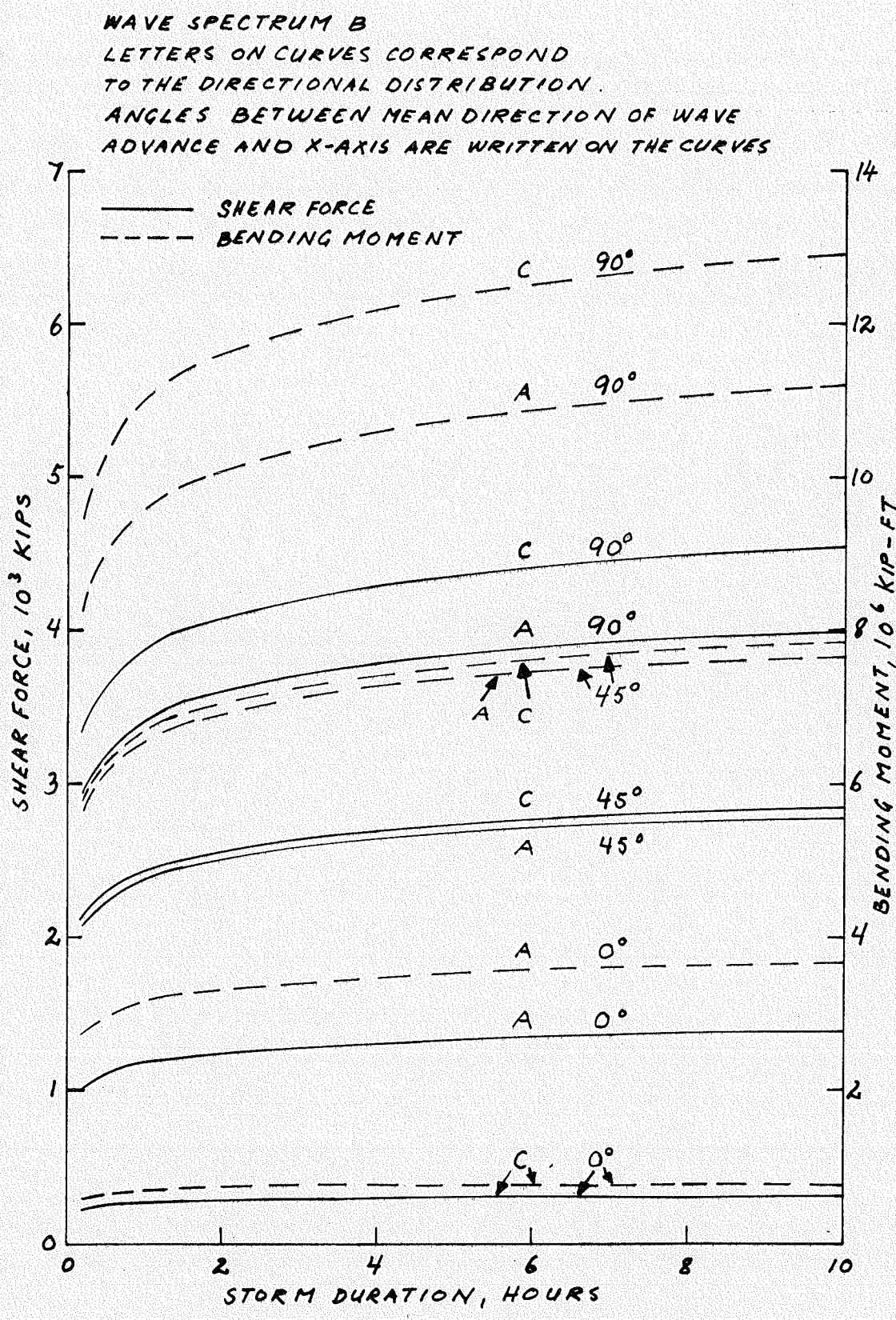

FIG. 6.34 MEAN PEAK SHEAR FORCES AND BENDING MOMENTS IN Y-DIRECTION AT BASE VS. STORM DURATION. TOWER 1

DIRECTIONAL DISTRIBUTION A
MEAN DIRECTION OF WAVE ADVANCE: Y-DIRECTION

LETTER	WAVE SPECTRUM	WIND SPEED
A	A	50 FT/SEC
B	B	75 "
C	C	100 "

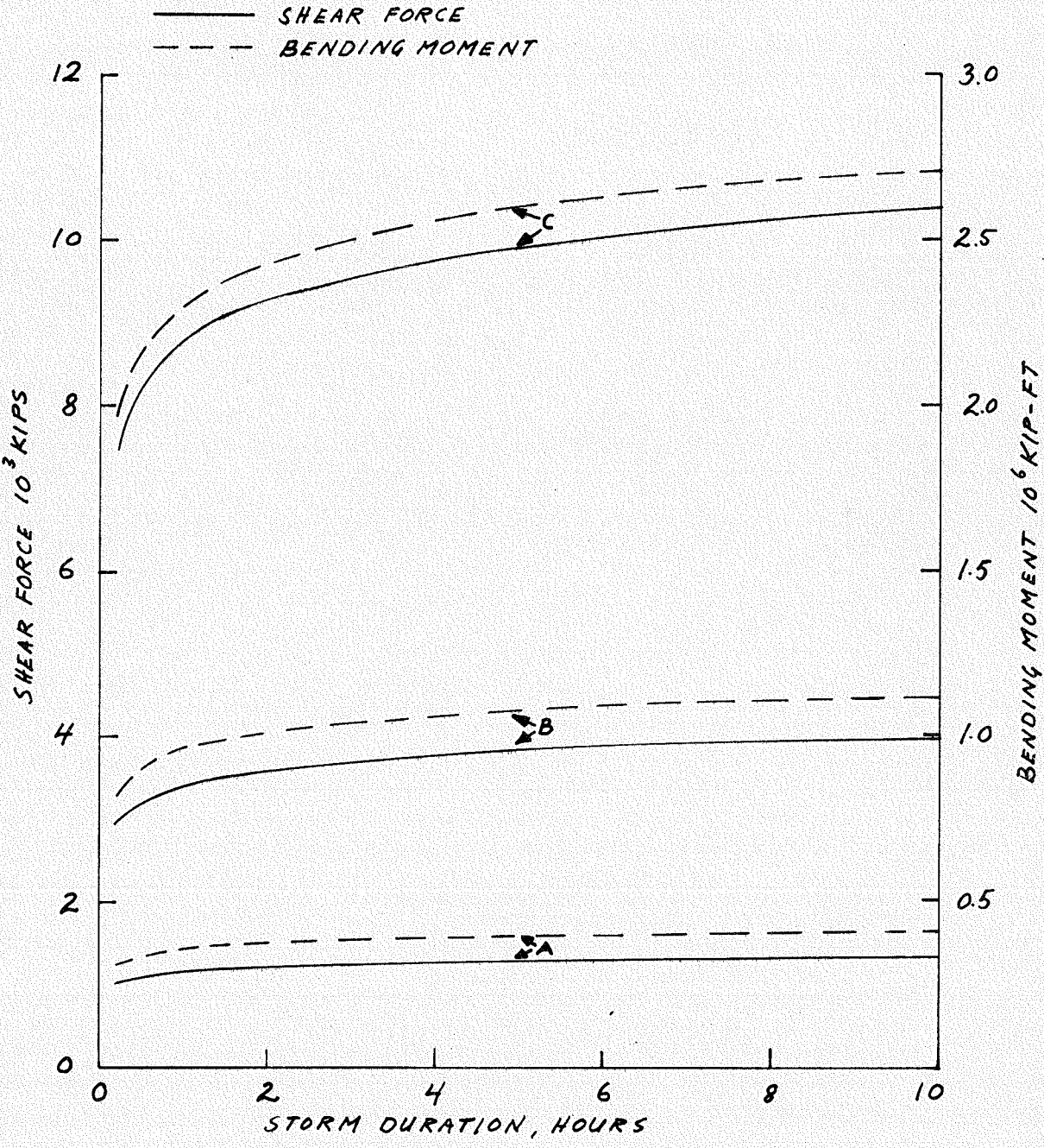

FIG. 6.35 MEAN PEAK VALUES OF SHEAR FORCES AND BENDING MOMENTS VS. STORM DURATION. TOWER 1

Throughout this investigation structural modal damping ratios of 5% of critical have been used for the submerged towers. To check the effect of structural damping, 4 examples using 2% damping have been calculated, namely 3 examples for Tower 1 and 1 example for Tower 4. These changes in damping ratios from 5 to 2% caused insignificant changes in response. In these examples, however, the effect of damping is very little because the directional spectra used do not contain the high frequency waves, since most of the energy in the wave spectrum is concentrated at frequencies significantly lower than the first natural frequencies of the towers. Since torsion of the structures have very little effect on overall response, the effect of damping on response may be studied in one horizontal direction using the one-dimensional wave height spectrum. Computationally this is a significantly simpler problem and therefore the higher frequency waves can more easily be included.

Key factors in this type of investigation are the coefficients of inertia C_M and the coefficients of drag C_D. These have been assigned values of 2.0 and 1.4, respectively. Decreasing the coefficient of drag C_D to 1.0 caused reduction in the structural response as shown in Fig. 6.36. It is interesting to notice how the importance of the drag coefficient increases with the severity of the storm (wind speed). This is due to the fact that drag forces depend on relative velocities squared between water particles and structure. The increase in drag force with storm intensity can also be deduced from Fig. 6.37, which shows how the optimized modal hydrodynamic damping ratio for the first coupled translational-rotational mode depends on storm intensity (wind

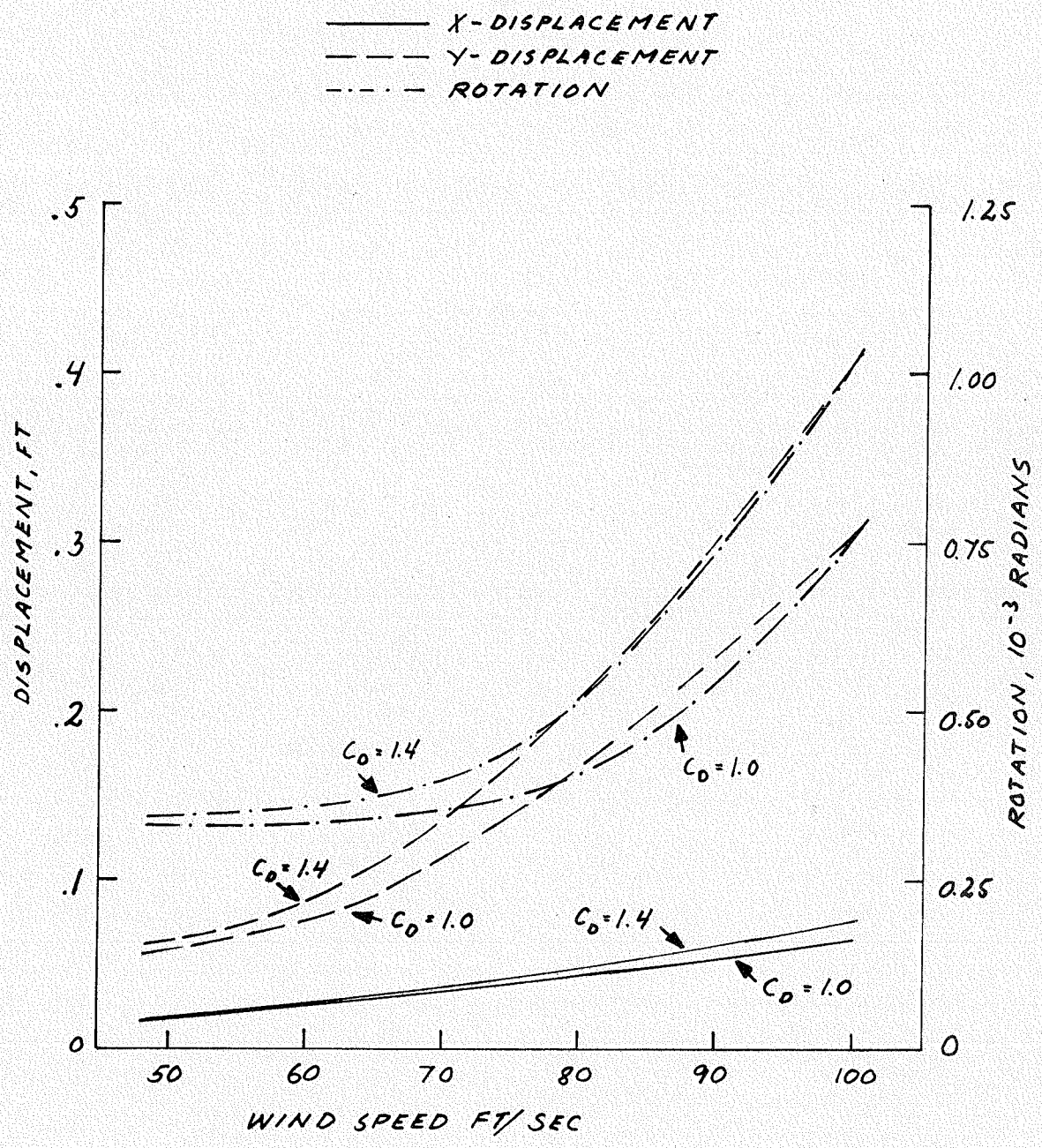

FIG. 6.36 STANDARD DEVIATIONS OF DISPLACEMENTS AND ROTATION VS. WIND SPEED FOR C_D = 1.0 AND C_D = 1.4 . TOWER 1

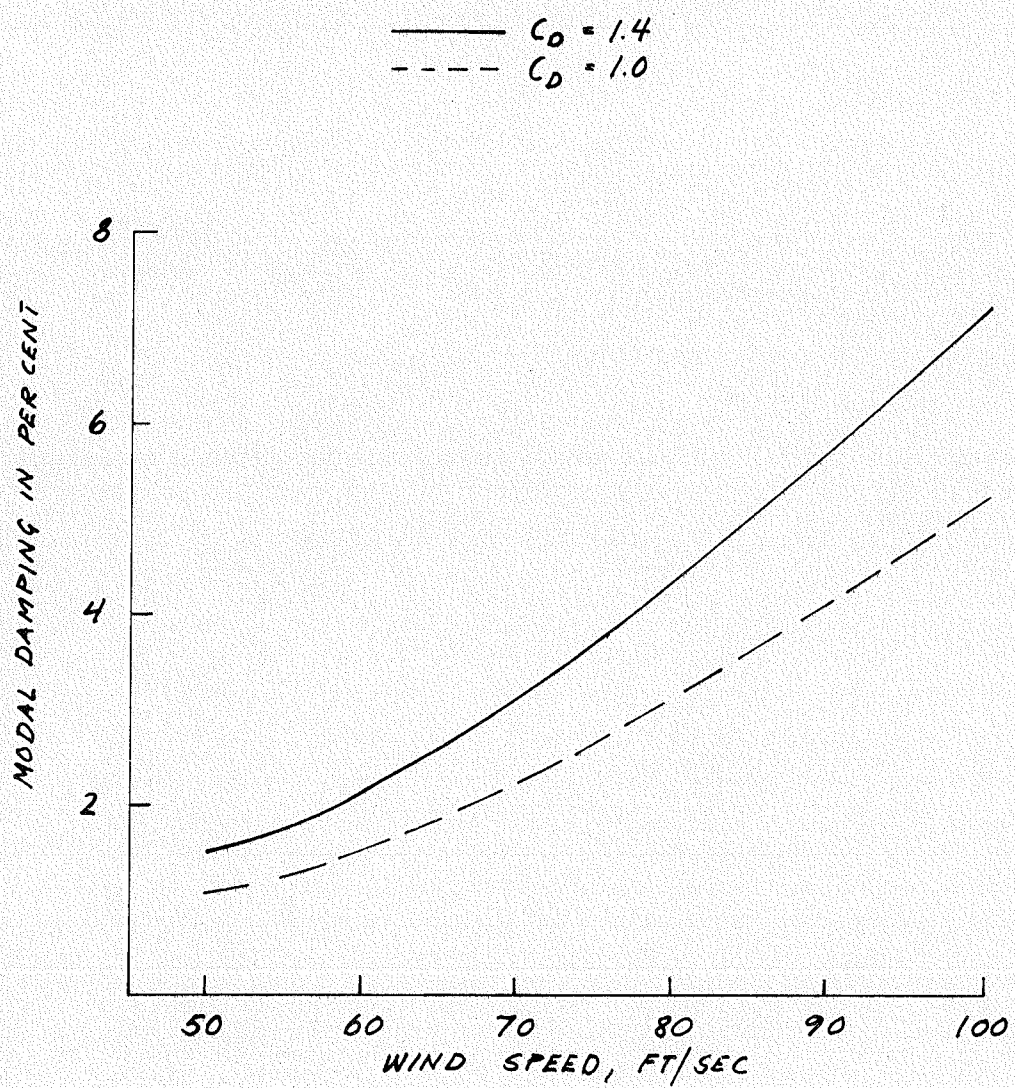

FIG. 6.37 OPTIMIZED HYDRODYNAMIC DAMPING FOR 1. COUPLED TRANSLATIONAL ROTATIONAL MODE VS. WIND SPEED. TOWER 1

speed) for $C_D = 1.0$ and for $C_D = 1.4$.

As mentioned previously in this chapter, pg. 82, only the lowest normal modes are included in the analysis. Figure 6.38 and 6.39 show the response when 1,2,3 or 4 modes are included for coupled translational-rotational vibration (Note that in the calculation of these quantities 4 modes were included.) It is seen that the two first modes are most important, but also that modes 3 and 4 should not be ignored. Since modes 1 and 2 and modes 3 and 4 can be looked upon as pairs, i.e. the shape of their translational and rotational components are similar, 4 coupled modes should be included in the dynamic analysis. For uncoupled vibrations in the x-direction, at least 2 modes should be included in the dynamic analysis. Inclusion of higher modes will increase the cost of computer solution, while it will have little effect on the computed results.

WAVE SPECTRUM B
DIRECTIONAL DISTRIBUTION A
MEAN DIRECTION OF WAVE ADVANCE:
Y-DIRECTION

NUMBER OF MODES INCLUDED:
— — — LOWEST MODE ONLY
— · — · — 2 LOWEST MODES
——— 3 AND 4 LOWEST MODES

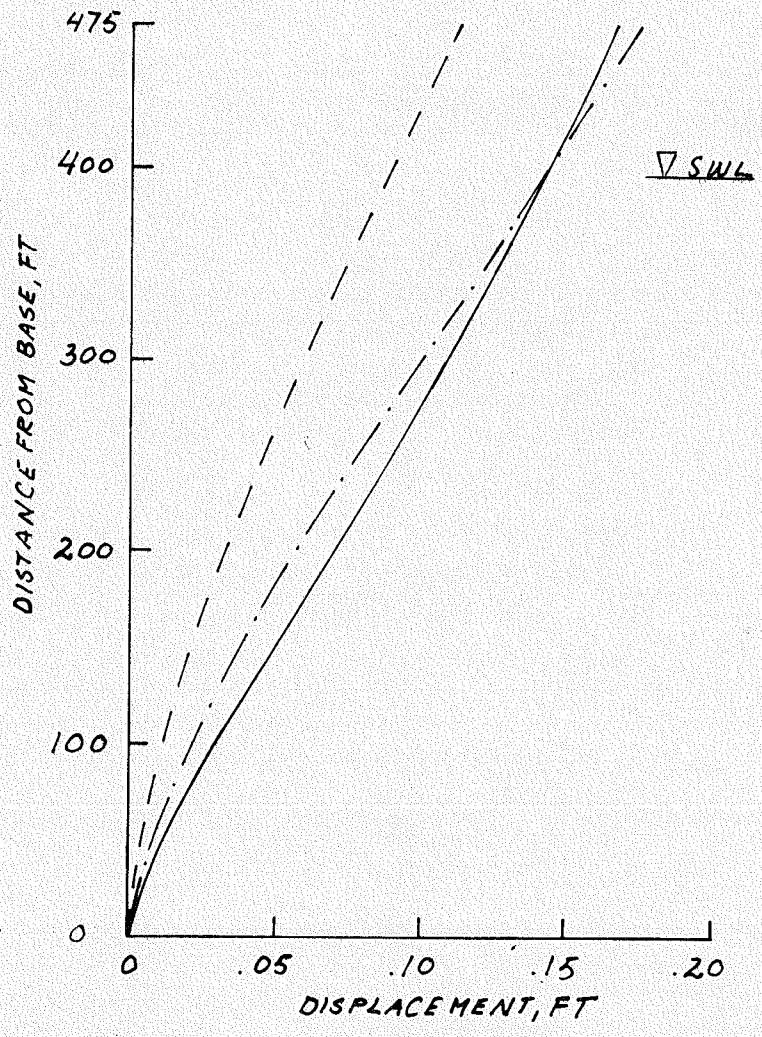

FIG. 6.38 STANDARD DEVIATIONS OF DISPLACEMENTS IN Y-DIRECTION WHEN 1, 2, 3 OR 4 LOWEST MODES ARE INCLUDED. TOWER 1

WAVE SPECTRUM B
DIRECTIONAL DISTRIBUTION A
MEAN DIRECTION OF WAVE ADVANCE:
Y-DIRECTION

NUMBER OF MODES INCLUDED:
— — — LOWEST MODE ONLY
— · — · — 2 LOWEST MODES
——— 3 AND 4 LOWEST MODES

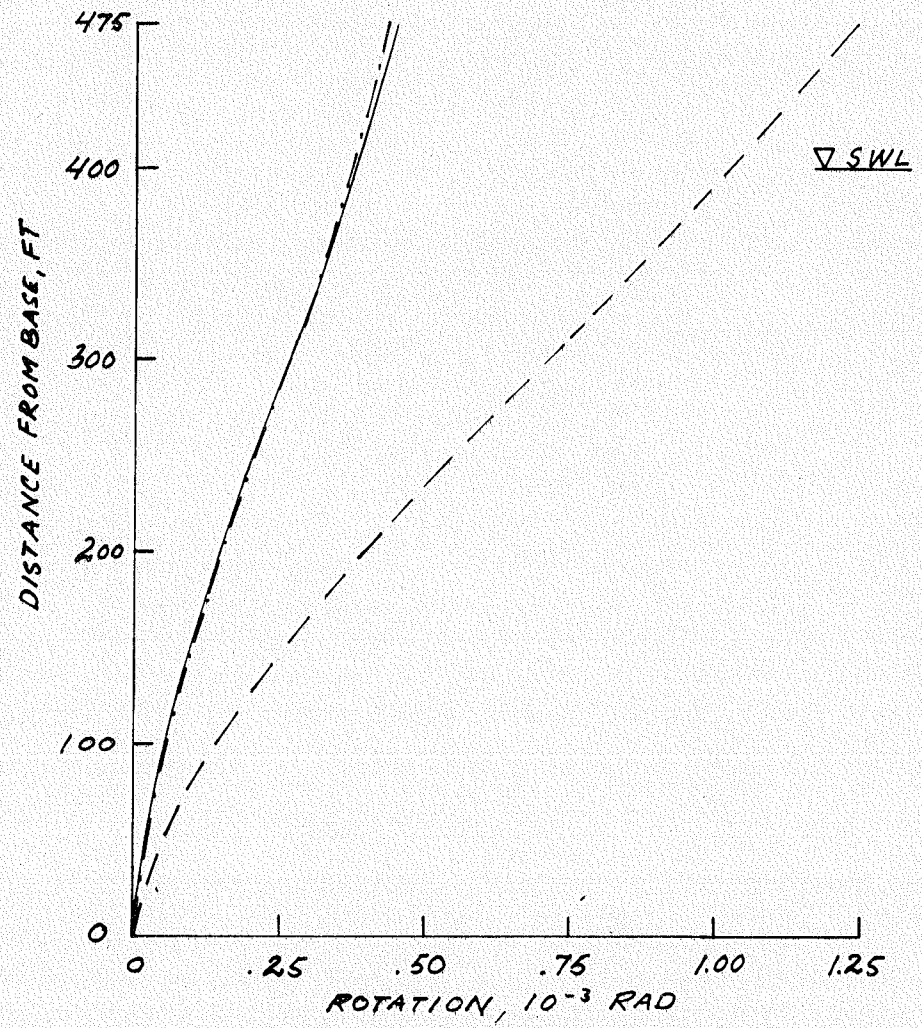

FIG. 6.39 STANDARD DEVIATIONS OF ROTATIONS WHEN 1, 2, 3 OR 4 LOWEST MODES ARE INCLUDED. TOWER 1

CHAPTER VII

SUMMARY AND CONCLUSIONS

A theory and two computer programs have been developed to determine statistics of the dynamic response of offshore towers subjected to random wave forces. Translational vibrations in the orthogonal horizontal directions and rotational vibrations about a vertical axis were considered. The waves were assumed to be zero mean Gaussian processes described by directional spectra. Linear wave theory and the Morrison wave force equation were then used to calculate statistics of the forces on the structure. Masses were lumped at horizontal levels. Drag forces were linearized. Normal mode superposition was used to solve the equations of motions through the frequency domain. Damping in the various modes were uncoupled by an optimization technique. Statistics of displacements in the horizontal directions, rotations about a vertical axis, shear forces and twisting and bending moments were obtained for 7 deep water towers. The rotations of the towers about their vertical axes have been of special interest. Calculation of the response of a 7 level structure (21 degrees of freedom), symmetric about a vertical plane, required approximately 1 minute central processor time on a CDC 6400 computer when 11 frequencies were used in the numerical integration of the spectral density functions.

Based upon this investigation, the following conclusions and recommendations can be deduced:

(1) A stochastic analysis should be carried out to determine the overall dynamic response of offshore towers to be built in locations where hostile sea conditions occur, when the wave spectra (linear waves) seems to be a reasonably good approximation to reality.

(2) Both inertia and drag forces should be included in the dynamic analysis.

(3) Full water-structure interaction should be included in the dynamic analysis. This interaction does not include the phenomenon of eddy shedding and the associated lateral force as it is not clear yet how to handle this problem in the wave spectra approach.

(4) Rotational response normally has small effect on the total response; thus, for many structures a two-dimensional analysis using the one-dimensional wave height spectrum gives sufficient accuracy.

(5) The directional spread of the waves has greatest effect on rotational response when the mean direction of wave advance is parallel to the plane of symmetry.

(6) The directional spread of the waves has little effect on rotational response of towers symmetric about one vertical plane when the mean direction of wave advance is perpendicular to the plane of symmetry.

(7) In a three-dimensional dynamic analysis, at least 6 normal modes of vibration should be included; thus for structures symmetric about a vertical plane the analysis requires 2 modes in the horizontal direction parallel to the plane of symmetry and 4 modes for coupled vibration in the direction orthogonal to the plane of symmetry and rotation.

(8) Two storms, coming from different directions, have less effect on rotation of the structure than do the same two storms

coming from the single direction giving largest rotational response.

(9) It is computationally significantly simpler to study resonance and the effect of damping of the structure in a two-dimensional analysis.

(10) The expected or mean extreme value of response may be used as an approximation of the most extreme value, since the extreme value distribution is narrow; however, the distribution should be considered when selecting design forces.

(11) Extreme values of response increase slowly with storm duration; approximately 10% as to the duration increases from 2 to 10 hours.

REFERENCES

1. Stokes, G.G., "On the Theory of Oscillatory Waves", Mathematical and Physical Papers, I, Cambridge: Cambridge University Press, 1880.

2. Lamb, Sir Horace, "Hydrodynamics", 6th ed. New York: Dover Publications, Inc., 1945.

3. Morison, J.R., M.P. O'Brien, J.W. Johnson and S.A. Schaaf, "The Force Exerted by Surface Waves on Piles", Petroleum Trans., 189, TP 2846 (1950), pp 149-154.

4. Foster, E.T., "Statistical Prediction of Wave Induced Response in Deep Ocean Tower Structures", Technical Report HEL-9-14, Hydraulic Engineering Laboratory, University of California, Berkeley, October 1967.

5. Foster, E.T., "Model for Nonlinear Dynamics of Offshore Towers", Journal of Engineering Mechanics Division, ASCE, Vol. 96, No. EM1, February 1970, pp 41-67.

6. Malhotra, A.K. and J. Penzien, "Stochastic Analysis of Offshore Tower Structures", Earthquake Engineering Research Center, Report No. EERC 69-6, University of California, Berkeley, June 1969.

7. Malhotra, A.K. and J. Penzien, "Nondeterministic Analysis of Offshore Tower Structures", Journal of Engineering Mechanics Division, Proc. ASCE, Vol. 96, No. EM6, December 1970, pp 985-1003. Discussion by S.K. Chakrabarti, in Vol. 97, EM3, June 1971, pp 1028-1029.

8. Malhotra, A.K. and J. Penzien, "Response of Offshore Structures to Random Wave Forces", Journal of Structural Division, Proc. ASCE, Vol. 96, No. ST10, October 1970, pp 2155-2173.

9. Penzien, J., M.K. Kaul and B. Berge, "Stochastic Response of Offshore Towers to Random Sea Waves and Strong Motion Earthquakes", Computers and Structures, Vol. 2, December 1972, pp 733-755.

10. Burke, B.G. and J. Tighe, "A Time Series Model for Dynamic Behavior of Offshore Structures", Journal Society of Petroleum Engineers, Vol. 12, No. 2, April 1972, pp 156-170.

11. Shubinski, R.P., E.L. Wilson and L.G. Selna, "Dynamic Response of Deep Water Structures", Conference on Civil Engineering in the Oceans, Proc. ASCE, San Francisco, 1967, pp 123-146.

12. Selna, L., and D. Cho, "Resonant Response of Offshore Structures", Journal of Waterways, Harbors and Coastal Engineering Division, Proc. ASCE, Vol. 98, No. WW1, February 1972, pp 15-24.

13. Nath, J.H., and D.R.F. Harleman, "Dynamics of Fixed Towers in Deep-Water Random Waves", Journal of Waterways and Harbors Division, Proc. ASCE, Vol. 95, No. WW9, November 1969, pp 539-556.

14. Nath, J.H., and D.R.F. Harleman, "Response of Vertical Cylinder to Random Waves", Journal of Waterways and Harbors Division, Proc. ASCE, Vol. 96, No. WW2, May 1970, pp 373-386.

15. Agershou, H.A., and J.J. Edens, "Fifth and First Order Wave-Force Coefficients for Cylindrical Piles", Coastal Engineering: Santa Barbara Specialty Conference, October 1965, ASCE 1966, pp 219-248.

16. Laird, A.D.K. "Water Forces on Flexible Oscillating Cylinders", Journal of Waterways and Harbors Division, Proc. ASCE Vol. 88, WW3, 1962, pp 125-137.

17. Petrauskas, C. "Hydrodynamic Damping and "Added Mass" for Flexible Offshore Platforms", Hydraulic Engineering Laboratory, Report HEL 9-23, University of California, Berkeley, May 1973.

18. Bendat, J.S., "Principles and Applications of Random Noise Theory", Wiley, N.Y., 1958.

19. Clarke and Disney, "Probability and Random Processes for Engineers and Science", Wiley, N. Y., 1970.

20. Cox, D.R. and H.D. Miller,"The Theory of Stochastic Processes", Wiley, N.Y., 1965.

21. Crandall, S.H., editor, "Random Vibration", Technology Press, Cambridge, Massachusetts, 1958.

22. Crandall, S.H. and W.D. Mark, "Random Vibration in Mechanical Systems", Academic Press, New York, 1963.

23. Davenport, W.B., Jr., and Root, W.L., "An Introduction to the Theory of Random Signals and Noise", McGraw-Hill, N.Y. 1958.

24. Lanning, J.H. Jr., and R.H. Battin, Random Processes in Automatic Control", McGraw-Hill, N.Y. 1956.

25. Lin, Y.K., "Probabilistic Theory of Structural Dynamics", McGraw Hill, N.Y., 1967.

26. Parzen, E., "Stochastic Processes",Holden-Day, San Francisco, 1962.

27. Robson, J.D., "An Introduction to Random Vibration", Edinburgh University Press, England, 1963.

28. Gumbel, E.J., "Statistics of Extremes", Columbia University Press, New York, 1958.

29. Rice, S.O. "Mathematical Analysis of Random Noise", Bell System Technical Journal, 23, July 1944, pp 282-332; and 24, January 1945, pp 46-156. Also in "Selected Papers on Noise and Stochastic Processes", N. Wax, editor, Dover Publ. New York, 1954, pp 133-294.

30. Cartwright, D.E. and M.S. Longuet-Higgins, "Statistical Distribution on the Maxima of a Random Function", Proceeding Royal Society of London, Series A, Vol. 237, 1956, pp 212-232.

31. Davenport, A.G., "Note on the Distribution of the Largest Value of a Random Function with Application to Gust Loading", Proc. Inst. Civil Engrg., Paper No. 6739, 1964.

32. Kryloff, N. and N. Bogoliuboff, "Introduction to Nonlinear Mechanics: Approximate Asymptotic Methods", Princeton University Press, 11, 1943.

33. Borgman, L.E., A Spectral Analysis of Ocean Wave Forces on Piling", Journal of Waterways and Harbors Division, Proc. ASCE, Vol. 93, No. WW2, pp 129-156.

34. Kinsman, B., "Wind Waves",Prentice Hall Inc., Englewood Cliffs, New Jersey, 1965.

35. Borgman, L.E., "Directional Spectra Models for Design Use for Surface Waves", Hydraulic Engineering Laboratory, Technical Report HEL 1-12, University of California, Berkeley, June 1969.

36. Panicker, N.N., "Determination of Directional Spectra of Ocean Waves from Gage Arrays", Hydraulic Engineering Laboratory, Technical Report HEL 1-18, University of California, Berkeley, August 1971.

37. Lonquet-Higgins, M.S., D.E. Cartwright, and N.D. Smith, "Observations of the Directional Spectrum of Sea Waves Using the Motions of a Floating Buoy", Ocean Wave Spectra, Prentice-Hall Inc., Englewood Cliffs, New Jersey, 1963, pp 111-132.

38. Gumbel, E.J., J.A. Greenwood and D. Durand, "The Circular Normal Distribution Theory and Tables", American Statistical Association Journal, March, 1953, pp 131-152.

39. Report from Committee 1: "Environmental Conditions. Chapter 5 Directional Spectra", pp 36-39 Proceedings of the Fourth International Ship Structures Congress", Tokyo, Sept. 1970, The Society of Naval Architects of Japan, Feb. 1971.

40. Wiegel, R.L., "Oceanographical Engineering", Prentice-Hall, Englewood Cliffs, N.J., 1964.

41. Campbell, G.C. and R.M. Foster, "Fourier Integrals for Practical Applications", Van Nostrand, N.Y., 1942.

42. Blackman, R.B. and J.W. Tukey, "The Measurement of Power Spectra from the Point of Communications Engineering", Bell System Technical Journal, January and March 1958 (also in Dover Publ. New York, 1959).

43. Olver, F.W.J., "Bessel Functions of Integer Order", Handbook of Mathematical Functions, by M. Abramowits and I.A. Stegun (editors), National Bureau of Standards Applied Mathematics Series, No. 55.

44. Bathe, K.J. and E.L. Wilson,"Solution Methods for Eigenvalue Problems in Structural Mechanics", International Journal for Numerical Methods in Engineering, Vol. 6, 1973, pp 213-226.

45. Pierson, W.J., Jr., and L. Moskowitz, "A Proposed Spectral Form For Fully Developed Wind Seas Based on the Similarity Theory of S.A. Kitaigorodskii", Journal of Geophysical Research, Vol. 69, No. 24, Dec. 15, 1964, pp 5181-5190.

APPENDIX A

STRUCTURAL DATA

In the following pages data for the 7 deep water towers used in the case studies are given. Units are feet, kips, seconds and radians.

OFFSHORE TOWER NO. 1. HEIGHT OF TOWER 475. FT. DEPTH OF WATER 400. FT. 7 LEVELS.

NODAL COORDINATES IN FT. VERTICAL COORDINATE Z IS ZERO AT SURFACE AND POSITIVE DOWNWARDS
HORIZONTAL COORDINATE Y IS NEGATIVE FOR NODE 1 AND 2 AND POSITIVE FOR NODE 3 AND 4

LEVEL	VERTICAL COORD. Z	HORIZONTAL COORD. NODE 1 AND 3 X	Y	HORIZONTAL COORD. NODE 2 AND 4 X	Y
1	-.7500E+02	-0.	.4000E+02	.8000E+02	.2400E+02
2	.1000E+02	-0.	.4500E+02	.8900E+02	.2675E+02
3	.7500E+02	-0.	.5000E+02	.9800E+02	.2950E+02
4	.1400E+03	-0.	.5500E+02	.1070E+03	.3225E+02
5	.2050E+03	-0.	.6000E+02	.1160E+03	.3500E+02
6	.2700E+03	-0.	.6500E+02	.1250E+03	.3775E+02
7	.3350E+03	-0.	.7000E+02	.1340E+03	.4050E+02

SUBMERGED VOLUME IN CU.FT. AND PROJECTED AREAS IN SQ.FT. AT EACH NODE
X-AREA AND Y-AREA MEAN PROJECTED AREA PERPENDICULAR TO THE X AND Y DIRECTION

LEVEL	NODE 1 AND 3 VOLUME	X-AREA	Y-AREA	NODE 2 AND 4 VOLUME	X-AREA	Y-AREA
2	.9700E+04	.4450E+04	.4650E+04	.5200E+04	.1450E+04	.1550E+04
3	.9200E+04	.3820E+04	.3960E+04	.5100E+04	.1220E+04	.1320E+04
4	.1040E+05	.3960E+04	.4160E+04	.6200E+04	.1400E+04	.1460E+04
5	.1300E+05	.4110E+04	.4320E+04	.9000E+04	.1530E+04	.1600E+04
6	.1560E+05	.4270E+04	.4500E+04	.1140E+05	.1910E+04	.1980E+04
7	.3030E+05	.8300E+04	.8700E+04	.2860E+05	.3300E+04	.3500E+04

STRUCTURAL MASS MATRIX. DIAGONAL OF SUBMATRICES

UNITS. TRANSLATION KIP SEC SQUARED PER FT. TRANSLATIONROTATION KIP SEC SQUARED
ROTATION KIP FT SEC SQUARED

LEVEL	TRANSLATION	TRANSLATION IN Y-DIR.-ROTATION	ROTATION
1	.3300E+03	.1050E+05	.5300E+06
2	.1010E+03	.3250E+04	.3600E+06
3	.8120E+02	.3220E+04	.3920E+06
4	.1250E+03	.4160E+04	.5640E+06
5	.1260E+03	.6200E+04	.8600E+06
6	.1510E+03	.7890E+04	.1170E+07
7	.2580E+03	.1580E+05	.2480E+07

STIFFNESS MATRICES

TRANSLATION IN X-DIRECTION UNITS KIP PER FT

	1	2	3	4	5	6	7
1	.1370E+05	-.1940E+05	.1130E+04	-.5890E+02	.1770E+04	.2910E+03	.1120E+04
2	-.1940E+05	.4590E+05	-.2510E+05	.2460E+03	-.2240E+04	.1600E+04	-.6520E+03
3	.1130E+04	-.2510E+05	.4960E+05	-.2520E+05	.9300E+03	-.1500E+04	.5860E+03
4	-.5890E+02	.2460E+03	-.2520E+05	.5320E+05	-.2810E+05	.1570E+04	-.1570E+04
5	.1770E+04	-.2240E+04	.9300E+03	-.2810E+05	.6020E+05	-.3360E+05	.3850E+04
6	.2910E+03	.1600E+04	-.1500E+04	.1570E+04	-.3360E+05	.6890E+05	-.4070E+05
7	.1120E+04	-.6520E+03	.5860E+03	-.1570E+04	.3850E+04	-.4070E+05	.9210E+05

COUPLED TRANSLATION IN Y-DIRECTION AND ROTATION
UNITS. FIRST 7 ROWS KIP PER FT. LAST 7 ROWS KIP

	1	2	3	4	5	6	7
1	.1350E+05	-.1620E+05	.1080E+04	.1160E+03	.1170E+04	.5780E+03	.6300E+03
2	-.1420E+05	.3750E+05	-.2030E+05	-.8890E+02	-.1350E+04	.5540E+03	.3000E+02
3	.1080E+04	-.2030E+05	.3980E+05	-.2030E+05	.6820E+03	-.8430E+03	.1510E+03
4	.1160E+03	-.8890E+02	-.2030E+05	.4300E+05	-.2270E+05	.1300E+04	-.1260E+04
5	.1170E+04	-.1350E+04	.6820E+03	-.2270E+05	.4830E+05	-.2710E+05	.3290E+04
6	.5780E+03	.5540E+03	-.8430E+03	.1300E+04	-.2710E+05	.5540E+05	-.3280E+05
7	.6300E+03	.3000E+02	.1510E+03	-.1260E+04	.3290E+04	-.3280E+05	.7360E+05
8	.3600E+06	-.4320E+06	.2880E+05	.3100E+04	.3120E+05	.1520E+05	.1680E+05
9	-.4810E+06	.1110E+07	-.6010E+06	-.2630E+04	-.4000E+05	.1640E+05	.8900E+03
10	.3530E+05	-.6620E+06	.1300E+07	-.6630E+06	.2230E+05	-.2750E+05	.4950E+04
11	.4140E+04	-.3170E+04	-.7220E+06	.1520E+07	-.8100E+06	.4640E+05	-.4500E+05
12	.4640E+05	-.5220E+05	.2640E+05	-.8780E+06	.1870E+07	-.1050E+07	.1270E+06
13	.2410E+05	.2310E+05	-.3510E+05	.5410E+05	-.1130E+07	.2310E+07	-.1370E+07
14	.2810E+05	.1340E+04	.6750E+04	-.5620E+05	.1470E+06	-.1470E+07	.3290E+07

UNITS. FIRST 7 ROWS KIP. LAST 7 ROWS KIP FT.

	8	9	10	11	12	13	14
1	.3600E+06	-.4810E+06	.3530E+05	.4140E+04	.4640E+05	.2410E+05	.2810E+05
2	-.4320E+06	.1110E+07	-.6620E+06	-.3170E+04	-.5220E+05	.2310E+05	.1340E+04
3	.2880E+05	-.6010E+06	.1300E+07	-.7220E+06	.2640E+05	-.3510E+05	.6750E+04
4	.3100E+04	-.2630E+04	-.6630E+06	.1520E+07	-.8780E+06	.5410E+05	-.5620E+05
5	.3120E+05	-.4000E+05	.2230E+05	-.8100E+06	.1870E+07	-.1130E+07	.1470E+06
6	.1520E+05	.1640E+05	-.2750E+05	.4640E+05	-.1050E+07	.2310E+07	-.1470E+07
7	.1680E+05	.8900E+03	.4950E+04	-.4500E+05	.1270E+06	-.1370E+07	.3290E+07
8	.4590E+08	-.6120E+08	.4260E+07	.2490E+06	.6420E+07	.2360E+07	.4230E+07
9	-.6120E+08	.1580E+09	-.9480E+08	.1030E+06	-.8460E+07	.5000E+07	-.1170E+07
10	.4260E+07	-.9480E+08	.2060E+09	-.1190E+09	.4340E+06	-.6470E+07	.1950E+07
11	.2490E+06	.1030E+06	-.1190E+09	.2660E+09	-.1520E+09	.9320E+07	-.9630E+07
12	.6420E+07	-.8460E+07	.4340E+06	-.1520E+09	.3530E+09	-.2130E+09	.2710E+08
13	.2360E+07	.5000E+07	-.6470E+07	.9320E+07	-.2130E+09	.4700E+09	-.2990E+09
14	.4230E+07	-.1170E+07	.1950E+07	-.9630E+07	.2710E+08	-.2990E+09	.7210E+09

OFFSHORE TOWER NO. 2. HEIGHT OF TOWER 679. FT. DEPTH OF WATER 0. FT. 7 LEVELS.

NODAL COORDINATES IN FT. VERTICAL COORDINATE Z IS ZERO AT SURFACE AND POSITIVE DOWNWARDS
HORIZONTAL COORDINATE Y IS NEGATIVE FOR NODE 1 AND 2 AND POSITIVE FOR NODE 3 AND 4

LEVEL	VERTICAL COORD. Z	HORIZONTAL COORD. NODE 1 AND 3 X	Y	HORIZONTAL COORD. NODE 2 AND 4 X	Y
1	-.7500E+02	-0.	.4000E+02	.8000E+02	.2400E+02
2	.1000E+02	-0.	.4500E+02	.8900E+02	.2675E+02
3	.7500E+02	-0.	.5000E+02	.9800E+02	.2950E+02
4	.1400E+03	-0.	.5500E+02	.1070E+03	.3225E+02
5	.2700E+03	-0.	.6500E+02	.1250E+03	.3775E+02
6	.4000E+03	-0.	.7500E+02	.1430E+03	.4325E+02
7	.5300E+03	-0.	.8500E+02	.1610E+03	.4875E+02

SUBMERGED VOLUME IN CU.FT. AND PROJECTED AREAS IN SQ.FT. AT EACH NODE
X-AREA AND Y-AREA MEAN PROJECTED AREA PERPENDICULAR TO THE X AND Y DIRECTION

LEVEL	NODE 1 AND 3 VOLUME	X-AREA	Y-AREA	NODE 2 AND 4 VOLUME	X-AREA	Y-AREA
2	.9850E+04	.4450E+04	.4490E+04	.5100E+04	.1480E+04	.1555E+04
3	.9200E+04	.3810E+04	.4000E+04	.5100E+04	.1215E+04	.1275E+04
4	.1790E+05	.6070E+04	.6370E+04	.1180E+05	.2200E+04	.2310E+04
5	.3020E+05	.8600E+04	.9040E+04	.2140E+05	.3400E+04	.3570E+04
6	.3790E+05	.9100E+04	.9570E+04	.2980E+05	.3900E+04	.4100E+04
7	.4590E+05	.1052E+05	.1105E+05	.3650E+05	.5100E+04	.5360E+04

STRUCTURAL MASS MATRIX. DIAGONAL OF SUBMATRICES

UNITS. TRANSLATION KIP SEC SQUARED PER FT. TRANSLATION-ROTATION KIP SEC SQUARED
ROTATION KIP FT SEC SQUARED

LEVEL	TRANSLATION	TRANSLATION IN Y-DIR.-ROTATION	ROTATION
1	.4000E+03	.1050E+05	.5300E+06
2	.1010E+03	.3250E+04	.3600E+06
3	.2120E+02	.3220E+04	.3920E+06
4	.1650E+03	.7100E+04	.9150E+06
5	.3220E+03	.1500E+05	.2270E+07
6	.4100E+03	.2270E+05	.3880E+07
7	.4170E+03	.2930E+05	.5580E+07

STRUCTURAL MASS MATRIX

SUBMATRICES OF X-/ROTATION UNITS KIP PER FT

	1	2	3	4	5	6	7
1	.1195E+05	-.1838E+05	.9641E+02	.8438E+03	.1383E+04	.5195E+03	.2708E+03
2	-.1[illegible]E+05	.4116E+05	-.2363E+05	-.1145E+04	.4351E+02	.2369E+03	.1027E+03
3	.3[illegible]E+02	-.2363E+05	.4920E+05	-.2497E+05	-.8477E+03	.2271E+03	.1268E+03
4	.[illegible]E+03	-.1148E+06	-.2497E+05	.4007E+05	-.1419E+05	-.5001E+03	.2103E+03
5	.[illegible]E+06	-.3611E+02	-.3477E+03	-.1419E+05	.3047E+05	-.1623E+05	-.1953E+03
6	.[illegible]E+04	.2961E+03	.2271E+03	-.5001E+03	-.1623E+05	.3466E+05	-.1934E+05
7	.[illegible]E+03	.1267E+03	.1268E+03	.2103E+03	-.1953E+03	-.1934E+05	.7844E+05

SUBMATRICES OF TRANSLATION IN Y-DIRECTION AND ROTATION
UNITS. FIRST 7 ROWS KIP PER FT. LAST 7 ROWS KIP

	1	2	3	4	5	6	7
1	.1114E+05	-.1326E+05	.7712E+02	.6781E+03	.1106E+04	.4156E+03	.2166E+03
2	-.1[illegible]E+05	.3293E+05	-.1890E+05	-.9163E+03	.3489E+02	.1895E+03	.8215E+02
3	.7[illegible]E+02	-.1890E+05	.3936E+05	-.1998E+05	-.6782E+03	.1817E+03	.1015E+03
4	.5[illegible]E+03	-.9183E+03	-.1998E+05	.3206E+05	-.1135E+05	-.4001E+03	.1683E+03
5	.1[illegible]E+04	.3480E+02	-.3782E+03	-.1135E+05	.2437E+05	-.1299E+05	-.1562E+03
6	.2[illegible]E+03	.1856E+03	.1817E+03	-.4001E+03	-.1299E+05	.2773E+05	-.1547E+05
7	.1[illegible]E+03	.1013E+03	.1015E+03	.1683E+03	-.1562E+03	-.1547E+05	.6275E+05
1	.2[illegible]E+04	-.1063E+05	.2050E+04	.1800E+05	.2940E+05	.1110E+05	.5780E+04
2	-.2[illegible]E+05	.2770E+05	-.5610E+05	-.2720E+05	.1030E+04	.562E+04	.2440E+04
3	.1[illegible]E+04	-.5170E+06	.1290E+07	-.6520E+06	-.2220E+05	.5940E+04	.3320E+04
4	.5[illegible]E+05	-.3270E+05	-.7120E+06	.1150E+07	-.4050E+06	-.1430E+05	.6000E+04
5	.4[illegible]E+05	.1450E+04	-.2820E+05	-.4730E+06	.1010E+07	-.5410E+06	-.5510E+04
6	.1[illegible]E+05	.9040E+04	.8660E+04	-.1910E+05	-.6190E+06	.1320E+07	-.7370E+06
7	.1[illegible]E+05	.4410E+04	.5440E+04	.9040E+04	-.8390E+04	-.8300E+06	.3360E+07

UNITS. FIRST 7 ROWS KIP. LAST 7 ROWS KIP FT.

	8	9	10	11	12	13	14
1	.2[illegible]E+06	-.3930E+05	.2520E+04	.2410E+05	.4600E+05	.1980E+05	.1160E+05
2	-.3[illegible]E+06	.9770E+05	-.6170E+06	-.3270E+05	.1450E+04	.9040E+04	.4410E+04
3	.2[illegible]E+04	-.5610E+05	.1290E+07	-.7120E+06	-.2820E+05	.8660E+04	.5440E+04
4	.1[illegible]E+05	-.2720E+05	-.6520E+06	.1150E+07	-.4730E+06	-.1910E+05	.9040E+04
5	.2[illegible]E+05	.1030E+04	-.2220E+05	-.4050E+06	.1010E+07	-.6190E+06	-.8380E+04
6	.1110E+05	.5620E+04	.5940E+04	-.1430E+05	-.5410E+06	.1320E+07	-.8300E+06
7	.5780E+04	.2440E+04	.3320E+04	.6000E+04	-.6510E+04	-.7370E+06	.3360E+07
8	.3[illegible]E+08	-.5050E+09	.3230E+06	.3110E+07	.5960E+07	.2570E+07	.1590E+07
9	-.5[illegible]E+08	.140E+09	-.8870E+08	-.4700E+07	.2100E+06	.1310E+07	.6380E+06
10	.2[illegible]E+06	-.8870E+08	.2040E+09	-.1130E+09	-.4500E+07	.1380E+07	.8750E+06
11	.3[illegible]E+07	-.4700E+07	-.1130E+09	.1990E+09	-.8240E+08	-.3330E+07	.1580E+07
12	.2[illegible]E+07	.2100E+06	-.4500E+07	-.8240E+08	.2070E+09	-.1270E+09	-.1720E+07
13	.2570E+07	.1310E+07	.1380E+07	-.3330E+07	-.1270E+09	.3100E+09	-.1950E+09
14	.1590E+07	.6380E+06	.8750E+06	.1580E+07	-.1720E+07	-.1950E+09	.8920E+09

OFFSHORE TOWER NO. 3. HEIGHT OF TOWER 875. FT. DEPTH OF WATER 600. FT. 7 LEVELS.

NODAL COORDINATES IN FT. VERTICAL COORDINATE Z IS ZERO AT SURFACE AND POSITIVE DOWNWARDS
HORIZONTAL COORDINATE Y IS NEGATIVE FOR NODE 1 AND 3 AND POSITIVE FOR NODE 2 AND 4

LEVEL	VERTICAL COORD. Z	HORIZONTAL COORD. NODE 1 AND 3 X	Y	HORIZONTAL COORD. NODE 2 AND 4 X	Y
1	-.7500E+02	-0.	.4000E+02	.8000E+02	.2400E+02
2	.1000E+02	-0.	.4500E+02	.8900E+02	.2675E+02
3	.7500E+02	-0.	.5000E+02	.9800E+02	.2950E+02
4	.2050E+03	-0.	.6000E+02	.1160E+03	.3500E+02
5	.4000E+03	-0.	.7500E+02	.1430E+03	.4325E+02
6	.5300E+03	-0.	.8500E+02	.1610E+03	.4875E+02
7	.7000E+03	-0.	.9810E+02	.1845E+03	.5595E+02

SUBMERGED VOLUME IN CU.FT. AND PROJECTED AREAS IN SQ.FT. AT EACH NODE
X-AREA AND Y-AREA MEAN PROJECTED AREA PERPENDICULAR TO THE X AND Y DIRECTION

LEVEL	NODE 1 AND 3 VOLUME	X-AREA	Y-AREA	NODE 2 AND 4 VOLUME	X-AREA	Y-AREA
2	.1000E+05	.6210E+04	.6520E+04	.4400E+04	.1100E+04	.1150E+04
3	.1630E+05	.8170E+04	.8580E+04	.8050E+04	.1540E+04	.1620E+04
4	.3950E+05	.1440E+05	.1510E+05	.2330E+05	.3310E+04	.3480E+04
5	.4830E+05	.1460E+05	.1530E+05	.3320E+05	.3490E+04	.3660E+04
6	.4440E+05	.1450E+05	.1520E+05	.3710E+05	.4250E+04	.4460E+04
7	.6700E+05	.1810E+05	.1900E+05	.5660E+05	.7900E+04	.8300E+04

STRUCTURAL MASS MATRIX. DIAGONAL OF SUBMATRICES

UNITS. TRANSLATION KIP SEC SQUARED PER FT, TRANSLATION-ROTATION KIP SEC SQUARED
ROTATION KIP FT SEC SQUARED

LEVEL	TRANSLATION	TRANSLATION IN Y-DIR.-ROTATION	ROTATION
1	.2300E+03	.1050E+05	.5300E+06
2	.1610E+03	.3250E+04	.3600E+06
3	.1460E+03	.5130E+04	.6300E+06
4	.2490E+03	.1770E+05	.2520E+07
5	.4510E+03	.2690E+05	.5030E+07
6	.4560E+03	.3130E+05	.6070E+07
7	.6500E+03	.5340E+05	.1220E+08

STIFFNESS MATRICES

TRANSLATION IN X-DIRECTION UNITS KIP PER FT

	1	2	3	4	5	6	7
1	.1331E+05	-.1575E+05	.4132E+03	.1410E+04	.9038E+03	.3993E+03	.1335E+03
2	-.1475E+05	.4102E+05	-.2377E+05	-.6800E+03	.1158E+03	.9172E+02	.1177E+03
3	.4132E+03	-.2377E+05	.3698E+05	-.1369E+05	-.3698E+02	.1302E+03	.3307E+03
4	.1410E+04	-.6800E+03	-.1369E+05	.2409E+05	-.1117E+05	.3760E+03	-.2358E+03
5	.3038E+03	.1158E+03	-.3698E+02	-.1117E+05	.2857E+05	-.1828E+05	.6792E+03
6	.3993E+03	.9172E+02	.1302E+03	.3750E+03	-.1328E+05	.3242E+05	-.1546E+05
7	.1335E+03	.1177E+03	.3307E+03	-.2358E+03	.6792E+03	-.1546E+05	.5243E+05

COUPLED TRANSLATION IN Y-DIRECTION AND ROTATION
UNITS. FIRST 7 ROWS KIP PER FT. LAST 7 ROWS KIP

	1	2	3	4	5	6	7
1	.1113E+05	-.1340E+05	.3305E+03	.1123E+04	.6430E+03	.3195E+03	.1068E+03
2	-.1254E+05	.4381E+05	-.1901E+05	-.5440E+03	.9267E+02	.7337E+02	.9416E+02
3	.3305E+03	-.1901E+05	.2959E+05	-.1095E+05	-.2958E+02	.1042E+03	.3046E+03
4	.1123E+04	-.5440E+03	-.1095E+05	.1927E+05	-.8934E+04	.3000E+03	-.1886E+03
5	.6430E+03	.9267E+02	-.2958E+02	-.8934E+04	.2285E+05	-.1462E+05	.5434E+03
6	.3195E+03	.7337E+02	.1042E+03	.3000E+03	-.1462E+05	.2593E+05	-.1237E+05
7	.1068E+03	.9416E+02	.3046E+03	-.1886E+03	.5434E+03	-.1237E+05	.4195E+05
8	.2940E+06	-.3570E+05	.9820E+04	.3010E+05	.1710E+05	.8510E+04	.2850E+04
9	-.3570E+05	.5740E+05	-.5640E+06	-.1610E+05	.2750E+04	.2160E+04	.2790E+04
10	.9820E+04	-.5640E+05	.9660E+06	-.3580E+06	-.9660E+03	.3400E+04	.3950E+04
11	.3010E+05	-.1610E+05	-.3580E+06	.7450E+06	-.3460E+06	.1160E+05	-.7290E+04
12	.1710E+05	.2750E+04	-.1090E+07	-.3460E+06	.1090E+07	-.6970E+06	.2590E+05
13	.8510E+04	.2160E+04	.1390E+07	.1160E+05	-.6970E+06	.1390E+07	-.6640E+06
14	.2850E+04	.2790E+04	.3950E+04	-.7290E+04	.2590E+05	-.6640E+06	.2580E+07

UNITS. FIRST 7 ROWS KIP. LAST 7 ROWS KIP FT.

	8	9	10	11	12	13	14
1	.2940E+06	-.3570E+05	.9820E+04	.3010E+05	.1710E+05	.8510E+04	.2850E+04
2	-.3570E+05	.5740E+05	-.5640E+06	-.1610E+05	.2750E+04	.2160E+04	.2790E+04
3	.9820E+04	-.5640E+06	.9660E+06	-.4230E+06	-.1410E+04	.5580E+04	.1870E+05
4	.3010E+05	-.1610E+05	-.3580E+06	.7450E+06	-.4260E+06	.1610E+05	-.1160E+05
5	.1710E+05	.2750E+04	-.9660E+03	-.3460E+06	.1090E+07	-.7850E+06	.3340E+05
6	.8510E+04	.2160E+04	.3400E+04	.1160E+05	-.6970E+06	.1390E+07	-.7610E+06
7	.2850E+04	.2790E+04	.3950E+04	-.7290E+04	.2590E+05	-.6640E+06	.2580E+07
8	.3800E+08	-.5100E+08	.1390E+07	.5630E+07	.3800E+07	.2220E+07	.8650E+06
9	-.5100E+08	.1400E+09	-.8900E+08	-.3050E+07	.6390E+06	.5700E+06	.8410E+06
10	.1390E+07	-.8900E+08	.1530E+09	-.6730E+08	-.2250E+06	.8930E+06	.3000E+07
11	.5630E+07	-.3050E+07	-.6730E+08	.1410E+09	-.8080E+08	.3060E+07	-.2210E+07
12	.3800E+07	.6390E+06	-.2250E+06	-.8080E+08	.2560E+09	-.1840E+09	.7870E+07
13	.2220E+07	.5700E+06	.8930E+06	.3060E+07	-.1840E+09	.3690E+09	-.2020E+09
14	.8650E+06	.8410E+06	.3000E+07	-.2210E+07	.7870E+07	-.2020E+09	.7870E+09

OFFSHORE TOWER NO. 4. HEIGHT OF TOWER 1075. FT. DEPTH OF WATER 1000. FT. 7 LEVELS.

NODAL COORDINATES IN FT. VERTICAL COORDINATE Z IS ZERO AT SURFACE AND POSITIVE DOWNWARDS
HORIZONTAL COORDINATE Y IS NEGATIVE FOR NODE 1 AND 3 AND POSITIVE FOR NODE 3 AND 4

LEVEL	VERTICAL COORD. Z	HORIZONTAL COORD. NODE 1 AND 3 X	Y	HORIZONTAL COORD. NODE 2 AND 4 X	Y
1	-.7500E+02	-0.	.4000E+02	.8000E+02	.2400E+02
2	.1000E+02	-0.	.4500E+02	.8900E+02	.2675E+02
3	.7500E+02	-0.	.5000E+02	.9800E+02	.2950E+02
4	.2050E+03	-0.	.6000E+02	.1160E+03	.3500E+02
5	.4000E+03	-0.	.7500E+02	.1430E+03	.4325E+02
6	.6000E+03	-0.	.9039E+02	.1707E+03	.5171E+02
7	.8000E+03	-0.	.1058E+03	.1984E+03	.6027E+02

SUBMERGED VOLUME IN CU.FT. AND PROJECTED AREAS IN SQ.FT. AT EACH NODE
X-AREA AND Y-AREA MEAN PROJECTED AREA PERPENDICULAR TO THE X AND Y DIRECTION

	NODE 1 AND 3			NODE 2 AND 4		
LEVEL	VOLUME	X-AREA	Y-AREA	VOLUME	X-AREA	Y-AREA
2	.1000E+05	.6210E+04	.6520E+04	.4400E+04	.1100E+04	.1150E+04
3	.1530E+05	.8170E+04	.8580E+04	.8050E+04	.1540E+04	.1620E+04
4	.3660E+05	.1340E+05	.1410E+05	.2330E+05	.3320E+04	.3480E+04
5	.5470E+05	.1830E+05	.1920E+05	.4030E+05	.4820E+04	.5060E+04
6	.5880E+05	.1940E+05	.2030E+05	.5390E+05	.5640E+04	.5920E+04
7	.1200E+06	.3280E+05	.2390E+05	.1050E+06	.8750E+04	.9180E+04

STRUCTURAL MASS MATRIX. DIAGONAL OF SUBMATRICES

UNITS. TRANSLATION KIP SEC SQUARED PER FT. TRANSLATION-ROTATION KIP SEC SQUARED
ROTATION KIP FT SEC SQUARED

LEVEL	TRANSLATION	TRANSLATION IN Y-DIR.-ROTATION	ROTATION
1	.1300E+03	.1050E+05	.5300E+06
2	.1010E+03	.3250E+04	.3600E+06
3	.1450E+03	.5130E+04	.6300E+06
4	.3660E+03	.1770E+05	.3520E+07
5	.5370E+03	.3210E+05	.5550E+07
6	.5650E+03	.4870E+05	.1000E+08
7	.1191E+04	.1063E+06	.2520E+08

STIFFNESS MATRICES

COUPLED TRANSLATION IN X-DIRECTION UNITS KIP PER FT

	1	2	3	4	5	6	7
1	.1400E+05	-.1688E+05	.2563E+03	.1530E+04	.8359E+03	.3352E+03	.1549E+03
2	-.1688E+05	.4197E+05	-.2414E+05	-.8506E+03	.1670E+03	.1797E+03	.8486E+02
3	.2563E+03	-.2414E+05	.3761E+05	-.1377E+05	-.5937E+02	.1439E+03	.7271E+02
4	.1530E+04	-.8506E+03	-.1377E+05	.2408E+05	-.1126E+05	.3615E+03	.2243E+03
5	.8359E+03	.1670E+03	-.5937E+02	-.1126E+05	.2221E+05	-.1189E+05	.3754E+03
6	.3352E+03	.1797E+03	.1439E+03	.3615E+03	-.1189E+05	.2348E+05	-.1245E+05
7	.1549E+03	.8486E+02	.7271E+02	.2243E+03	.3754E+03	-.1245E+05	.2765E+05

COUPLED TRANSLATION IN Y-DIRECTION AND ROTATION
UNITS. FIRST 7 ROWS KIP PER FT. LAST 7 ROWS KIP

	1	2	3	4	5	6	7
1	.1120E+05	-.1352E+05	.2050E+03	.1224E+04	.6538E+03	.2682E+03	.1239E+03
2	-.1352E+05	.3358E+05	-.1932E+05	-.6805E+03	.1336E+03	.1405E+03	.6788E+02
3	.2050E+03	-.1932E+05	.3009E+05	-.1102E+05	-.4794E+02	.1151E+03	.5816E+02
4	.1224E+04	-.6805E+03	-.1102E+05	.1927E+05	-.9011E+04	.2892E+03	.1794E+03
5	.6538E+03	.1336E+03	-.4794E+02	-.9011E+04	.1777E+05	-.9510E+04	.3004E+03
6	.2682E+03	.1405E+03	.1151E+03	.2892E+03	-.9510E+04	.1878E+05	-.9962E+04
7	.1239E+03	.6788E+02	.5816E+02	.1794E+03	.3004E+03	-.9962E+04	.2212E+05
8	.2682E+06	-.3600E+06	.5460E+04	.3260E+05	.1780E+05	.7150E+04	.3300E+04
9	-.4010E+06	.9870E+06	-.5730E+06	-.2020E+05	.3960E+04	.4170E+04	.2010E+04
10	.6690E+04	-.6310E+06	.9840E+06	-.3600E+06	-.1570E+04	.3760E+04	.1900E+04
11	.4740E+05	-.2630E+05	-.4260E+06	.7460E+06	-.3480E+06	.1120E+05	.6950E+04
12	.3180E+05	.6360E+04	-.2290E+04	-.4300E+06	.8480E+06	-.4530E+06	.1430E+05
13	.1280E+05	.8000E+04	.6650E+04	.1650E+05	-.5410E+06	.1070E+07	-.5670E+06
14	.8240E+04	.4480E+04	.3840E+04	.1190E+05	.1990E+05	-.6590E+06	.1460E+07

UNITS. FIRST 7 ROWS KIP. LAST 7 ROWS KIP FT.

	8	9	10	11	12	13	14
1	.2680E+06	-.4010E+06	.6690E+04	.4740E+05	.3180E+05	.1280E+05	.8240E+04
2	-.3600E+06	.9870E+06	-.6310E+06	-.2630E+05	.6360E+04	.8000E+04	.4480E+04
3	.5460E+04	-.5730E+06	.9840E+06	-.4260E+06	-.2290E+04	.6650E+04	.3840E+04
4	.3260E+05	-.2020E+05	-.3600E+06	.7460E+06	-.4300E+06	.1650E+05	.1190E+05
5	.1780E+05	.3960E+04	-.1570E+04	-.3480E+06	.8480E+06	-.5410E+06	.1990E+05
6	.7150E+04	.4170E+04	.3760E+04	.1120E+05	-.4530E+06	.1070E+07	-.6590E+06
7	.3300E+04	.2010E+04	.1900E+04	.6950E+04	.1430E+05	-.5670E+06	.1460E+07
8	.3825E+08	-.5150E+08	.8610E+06	.6120E+07	.4130E+07	.1790E+07	.1070E+07
9	-.5150E+08	.1420E+09	-.9060E+08	-.3790E+07	.9190E+06	.1230E+07	.6600E+06
10	.8610E+06	-.9060E+08	.1560E+09	-.6780E+08	-.3650E+06	.1060E+07	.6170E+06
11	.6120E+07	-.3790E+07	-.6780E+08	.1410E+09	-.8140E+08	.3130E+07	.2270E+07
12	.4130E+07	.9190E+06	-.3650E+06	-.8140E+08	.1990E+09	-.1270E+09	.4680E+07
13	.1790E+07	.1230E+07	.1060E+07	.3130E+07	-.1270E+09	.3010E+09	-.1860E+09
14	.1070E+07	.6600E+06	.6170E+06	.2270E+07	.4680E+07	-.1860E+09	.4820E+09

OFFSHORE TOWER NO. 5. HEIGHT OF TOWER 475. FT. DEPTH OF WATER 400. FT. 7 LEVELS

NODAL COORDINATES IN FT. VERTICAL COORDINATE Z IS ZERO AT SURFACE AND POSITIVE DOWNWARDS
HORIZONTAL COORDINATE Y IS NEGATIVE FOR NODE 1 AND 2 AND POSITIVE FOR NODE 3 AND 4

LEVEL	VERTICAL COORD. Z	HORIZONTAL COORD. NODE 1 AND 3 X	HORIZONTAL COORD. NODE 1 AND 3 Y	HORIZONTAL COORD. NODE 2 AND 4 X	HORIZONTAL COORD. NODE 2 AND 4 Y
1	-.7500E+02	-0.	.4000E+02	.8000E+02	.2400E+02
2	.1000E+02	-0.	.4500E+02	.8900E+02	.2675E+02
3	.7500E+02	-0.	.5000E+02	.9800E+02	.2950E+02
4	.1400E+03	-0.	.5500E+02	.1070E+03	.3225E+02
5	.2050E+03	-0.	.6000E+02	.1160E+03	.3500E+02
6	.2700E+03	-0.	.6500E+02	.1250E+03	.3775E+02
7	.3350E+03	-0.	.7000E+02	.1340E+03	.4050E+02

SUBMERGED VOLUME IN CU.FT. AND PROJECTED AREAS IN SQ.FT. AT EACH NODE
X-AREA AND Y-AREA MEAN PROJECTED AREA PERPENDICULAR TO THE X AND Y DIRECTION

LEVEL	NODE 1 AND 3 VOLUME	NODE 1 AND 3 X-AREA	NODE 1 AND 3 Y-AREA	NODE 2 AND 4 VOLUME	NODE 2 AND 4 X-AREA	NODE 2 AND 4 Y-AREA
2	.9730E+04	.4450E+04	.4650E+04	.5200E+04	.1450E+04	.1550E+04
3	.9200E+04	.3820E+04	.3960E+04	.5100E+04	.1220E+04	.1320E+04
4	.1040E+05	.3940E+04	.4160E+04	.6200E+04	.1400E+04	.1460E+04
5	.1300E+05	.4110E+04	.4320E+04	.9000E+04	.1530E+04	.1600E+04
6	.1560E+05	.4270E+04	.4500E+04	.1140E+05	.1910E+04	.1980E+04
7	.3050E+05	.8300E+04	.8700E+04	.2860E+05	.3300E+04	.3500E+04

STRUCTURAL MASS MATRIX. DIAGONAL OF SUBMATRICES

UNITS. TRANSLATION KIP SEC SQUARED PER FT. TRANSLATION-ROTATION KIP SEC SQUARED
ROTATION KIP FT SEC SQUARED

LEVEL	TRANSLATION	TRANSLATION IN Y-DIR.-ROTATION	ROTATION
1	.3300E+03	.1050E+05	.5300E+06
2	.1010E+03	.3250E+04	.3600E+06
3	.8920E+02	.3220E+04	.3920E+06
4	.1050E+03	.4160E+04	.5640E+06
5	.1260E+03	.6200E+04	.9600E+06
6	.1510E+03	.7890E+04	.1170E+07
7	.2950E+03	.1580E+05	.2480E+07

STIFFNESS MATRICES

TRANSLATION IN X-DIRECTION UNITS KIP PER FT

	1	2	3	4	5	6	7
1	.1470E+05	-.1440E+05	.1130E+04	-.5890E+02	.1770E+04	.2910E+03	.1120E+04
2	-.1440E+05	.4530E+05	-.2810E+05	.2460E+03	-.2240E+04	.1600E+04	-.6520E+03
3	.1130E+04	-.2810E+05	.4960E+05	-.2520E+05	.9300E+03	-.1500E+04	.5850E+03
4	-.5890E+02	.2460E+03	-.2520E+05	.5320E+05	-.2810E+05	.1570E+04	-.1570E+04
5	.1770E+04	-.2240E+04	.9300E+03	-.2810E+05	.6020E+05	-.3360E+05	.3850E+04
6	.2910E+03	.1600E+04	-.1500E+04	.1570E+04	-.3360E+05	.5890E+05	-.4070E+05
7	.1120E+04	-.6520E+03	.5850E+03	-.1570E+04	.3850E+04	-.4070E+05	.9210E+05

SYMMETRY TRANSLATION IN Y-DIRECTION AND ROTATION
UNITS. FIRST 7 ROWS KIP PER FT. LAST 7 ROWS KIP

	1	2	3	4	5	6	7
1	.1550E+05	-.1520E+05	.1080E+04	.1160E+03	.1170E+04	.5780E+03	.6300E+03
2	-.1520E+05	.4760E+05	-.2030E+05	-.8890E+02	-.1350E+04	.5540E+03	.3000E+02
3	.1080E+04	-.2030E+05	.3980E+05	-.2030E+05	.6820E+03	-.8430E+03	.1510E+03
4	.1160E+03	-.8890E+02	-.2030E+05	.4300E+05	-.2270E+05	.1300E+04	-.1260E+04
5	.1170E+04	-.1350E+04	.6820E+03	-.2270E+05	.4930E+05	-.2710E+05	.3290E+04
6	.5780E+03	.5540E+03	-.8430E+03	.1300E+04	-.2710E+05	.5540E+05	-.3280E+05
7	.6300E+03	.3000E+02	.1510E+03	-.1260E+04	.3290E+04	-.3280E+05	.7360E+05
8	.3110E+06	-.3744E+05	.2494E+05	.2685E+04	.2702E+05	.1316E+05	.1455E+05
9	-.4156E+06	.9613E+06	-.5205E+06	-.2274E+04	-.3+64E+05	.1420E+05	.7703E+03
10	.3057E+05	-.5733E+06	.1126E+07	-.5742E+06	.1931E+05	-.2382E+05	.4287E+04
11	.3585E+04	-.2745E+04	-.6253E+06	.1316E+07	-.7015E+06	.4018E+05	-.3897E+05
12	.4018E+05	-.4521E+05	.2286E+05	-.7604E+06	.1619E+07	-.9093E+06	.1100E+06
13	.2067E+05	.2001E+05	-.3040E+05	.4685E+05	-.9786E+06	.2001E+07	-.1186E+07
14	.2434E+05	.1160E+04	.5846E+04	-.4867E+05	.1273E+06	-.1273E+07	.2849E+07

UNITS. FIRST 7 ROWS KIP. LAST 7 ROWS KIP FT.

	8	9	10	11	12	13	14
1	.3114E+06	-.4166E+06	.3057E+05	.3585E+04	.4018E+05	.2067E+05	.2434E+05
2	-.3741E+06	.9613E+06	-.5733E+06	-.2745E+04	-.4521E+05	.2001E+05	.1160E+04
3	.2494E+05	-.5205E+06	.1126E+07	-.6253E+06	.2286E+05	-.3040E+05	.5846E+04
4	.2685E+04	-.2274E+04	-.5742E+06	.1316E+07	-.7604E+06	.4685E+05	-.4867E+05
5	.2702E+05	-.3464E+05	.1931E+05	-.7015E+06	.1619E+07	-.9786E+06	.1273E+06
6	.1316E+05	.1420E+05	-.2382E+05	.4018E+05	-.9093E+06	.2001E+07	-.1273E+07
7	.1455E+05	.7708E+03	.4287E+04	-.3897E+05	.1100E+06	-.1186E+07	.2849E+07
8	.3442E+08	-.4590E+08	.3195E+07	.1867E+06	.4815E+07	.1770E+07	.3172E+07
9	-.4590E+08	.1185E+09	-.7110E+08	.7725E+05	-.6345E+07	.3750E+07	-.8775E+06
10	.3195E+07	-.7110E+08	.1545E+09	-.8925E+08	.3255E+06	-.4852E+07	.1462E+07
11	.1867E+06	.7725E+05	-.8925E+08	.1995E+09	-.1140E+09	.6990E+07	-.7222E+07
12	.4815E+07	-.6345E+07	.3255E+06	-.1140E+09	.2647E+09	-.1597E+09	.2032E+08
13	.1770E+07	.3750E+07	-.4852E+07	.6990E+07	-.1597E+09	.3525E+09	-.2242E+09
14	.3172E+07	-.8775E+06	.1462E+07	-.7222E+07	.2032E+08	-.2242E+09	.5407E+09

OFFSHORE TOWER NO. 6. HEIGHT OF TOWER 475. FT. DEPTH OF WATER 400. FT. 7 LEVELS.

NODAL COORDINATES IN FT. VERTICAL COORDINATE Z IS ZERO AT SURFACE AND POSITIVE DOWNWARDS
HORIZONTAL COORDINATE Y IS NEGATIVE FOR NODE 1 AND 2 AND POSITIVE FOR NODE 3 AND 4

LEVEL	VERTICAL COORD. Z	HORIZONTAL COORD. NODE 1 AND 3 X	Y	HORIZONTAL COORD. NODE 2 AND 4 X	Y
1	-.7500E+02	-0.	.8000E+02	.1600E+03	.4800E+02
2	.1000E+02	-0.	.9000E+02	.1780E+03	.5350E+02
3	.7500E+02	-0.	.1000E+03	.1960E+03	.5900E+02
4	.1400E+03	-0.	.1100E+03	.2140E+03	.6450E+02
5	.2050E+03	-0.	.1200E+03	.2320E+03	.7000E+02
6	.2700E+03	-0.	.1300E+03	.2500E+03	.7550E+02
7	.3350E+03	-0.	.1400E+03	.2680E+03	.8100E+02

SUBMERGED VOLUME IN CU.FT. AND PROJECTED AREAS IN SQ.FT. AT EACH NODE
X-AREA AND Y-AREA MEAN PROJECTED AREA PERPENDICULAR TO THE X AND Y DIRECTION

LEVEL	NODE 1 AND 3 VOLUME	X-AREA	Y-AREA	NODE 2 AND 4 VOLUME	X-AREA	Y-AREA
2	.9730E+04	.4450E+04	.4650E+04	.5200E+04	.1450E+04	.1550E+04
3	.9200E+04	.3820E+04	.3960E+04	.5100E+04	.1220E+04	.1320E+04
4	.1040E+05	.3960E+04	.4160E+04	.6200E+04	.1400E+04	.1460E+04
5	.1300E+05	.4110E+04	.4320E+04	.9000E+04	.1530E+04	.1630E+04
6	.1560E+05	.4270E+04	.4500E+04	.1140E+05	.1910E+04	.1980E+04
7	.4030E+05	.8300E+04	.8700E+04	.2960E+05	.3300E+04	.3500E+04

STRUCTURAL MASS MATRIX. DIAGONAL OF SUBMATRICES

UNITS. TRANSLATION KIP SEC SQUARED PER FT. TRANSLATION-ROTATION KIP SEC SQUARED
ROTATION KIP FT SEC SQUARED

LEVEL	TRANSLATION	TRANSLATION IN Y-DIR.	ROTATION-ROTATION
1	.3300E+03	.2100E+05	.2120E+07
2	.1010E+03	.6500E+04	.1440E+07
3	.3920E+02	.6440E+04	.1570E+07
4	.1050E+03	.8320E+04	.2260E+07
5	.1240E+03	.1240E+05	.3440E+07
6	.1510E+03	.1580E+05	.4670E+07
7	.2660E+03	.3160E+05	.9920E+07

STIFFNESS MATRICES

TRANSLATION IN X-DIRECTION UNITS KIP PER FT

	1	2	3	4	5	6	7
1	.1670E+05	-.1080E+05	.1130E+04	-.5890E+02	.1770E+04	.2510E+03	.1120E+04
2	-.1080E+05	.4590E+05	-.2510E+05	.2460E+03	-.2240E+04	.1800E+04	-.4620E+03
3	.1130E+04	-.2510E+05	.4960E+05	-.2520E+05	.9300E+03	-.1900E+04	.5850E+03
4	-.5890E+02	.2460E+03	-.2520E+05	.5320E+05	-.2810E+05	.1570E+04	-.1570E+04
5	.1770E+04	-.2240E+04	.9300E+03	-.2810E+05	.6020E+05	-.3360E+05	.3850E+04
6	.2510E+03	.1800E+04	-.1900E+04	.1570E+04	-.3360E+05	.6290E+05	-.4670E+05
7	.1120E+04	-.4620E+03	.5850E+03	-.1570E+04	.3850E+04	-.4670E+05	.9210E+05

COUPLED TRANSLATION IN Y-DIRECTION AND ROTATION
UNITS. FIRST 7 ROWS KIP PER FT. LAST 7 ROWS KIP

	1	2	3	4	5	6	7
1	.1260E+05	-.1620E+05	.1080E+04	.1160E+03	.1170E+04	.5780E+03	.6300E+03
2	-.1620E+05	.3750E+05	-.2030E+05	-.8890E+02	-.1350E+04	.6540E+03	.3000E+02
3	.1080E+04	-.2030E+05	.3980E+05	-.2030E+05	.6820E+03	-.3430E+03	.1510E+03
4	.1160E+03	-.8890E+02	-.2030E+05	.4300E+05	-.2270E+05	.1300E+04	-.1260E+04
5	.1170E+04	-.1350E+04	.6820E+03	-.2270E+05	.4830E+05	-.2710E+05	.3290E+04
6	.5780E+03	.6540E+03	-.8430E+03	.1300E+04	-.2710E+05	.5540E+05	-.4280E+05
7	.6300E+03	.3000E+02	.1510E+03	-.1260E+04	.3290E+04	-.4280E+05	.7360E+05
8	.7200E+04	-.8640E+04	.5760E+05	.6200E+04	.6240E+05	.3040E+05	.3260E+05
9	-.9620E+06	.2220E+07	-.1202E+07	-.5260E+04	-.8000E+05	.3280E+05	.1780E+04
10	.7060E+05	-.1324E+07	.2600E+07	-.1326E+07	.4460E+05	-.5500E+05	.9900E+04
11	.8280E+04	-.6340E+04	-.1444E+07	.3040E+07	-.1620E+07	.9280E+05	-.9000E+05
12	.9280E+05	-.1044E+06	.5280E+05	-.1756E+07	.3740E+07	-.2100E+07	.2540E+06
13	.4820E+05	.4620E+05	-.7020E+05	.1082E+06	-.2260E+07	.4620E+07	-.2740E+07
14	.5620E+05	.2680E+04	.1350E+05	-.1124E+06	.2940E+06	-.2940E+07	.6580E+07

UNITS. FIRST 7 ROWS KIP. LAST 7 ROWS KIP FT.

	8	9	10	11	12	13	14
1	.7200E+04	-.9620E+06	.7060E+05	.8280E+04	.9280E+05	.4820E+05	.5620E+05
2	-.8640E+04	.2220E+07	-.1324E+07	-.6340E+04	-.1044E+06	.4620E+05	.2680E+04
3	.5760E+05	-.1202E+07	.2600E+07	-.1444E+07	.5280E+05	-.7020E+05	.1350E+05
4	.6200E+04	-.5260E+04	-.1326E+07	.3040E+07	-.1756E+07	.1082E+06	-.1124E+06
5	.6240E+05	-.8000E+05	.4460E+05	-.1620E+07	.3740E+07	-.2260E+07	.2940E+06
6	.3040E+05	.3280E+05	-.5500E+05	.9280E+05	-.2100E+07	.4620E+07	-.2940E+07
7	.3360E+05	.1780E+04	.9900E+04	-.9000E+05	.2540E+06	-.2740E+07	.6580E+07
8	.1836E+09	-.2448E+09	.1704E+08	.9960E+06	.2568E+08	.9440E+07	.1692E+08
9	-.2448E+09	.6320E+09	-.3792E+09	.4120E+06	-.3384E+08	.2000E+08	-.4680E+07
10	.1704E+08	-.3792E+09	.8240E+09	-.4760E+09	.1736E+07	-.2588E+08	.7800E+07
11	.9960E+06	.4120E+06	-.4760E+09	.1064E+10	-.6080E+09	.3728E+08	-.3852E+08
12	.2568E+08	-.3384E+08	.1736E+07	-.6080E+09	.1412E+10	-.8520E+09	.1084E+09
13	.9440E+07	.2000E+08	-.2588E+08	.3728E+08	-.8520E+09	.1880E+10	-.1196E+10
14	.1692E+08	-.4680E+07	.7800E+07	-.3852E+08	.1084E+09	-.1196E+10	.2884E+10

OFFSHORE TOWER NO. 7. HEIGHT OF TOWER 475. FT. DEPTH OF WATER [illegible] FT. 7 LEVELS.

NODAL COORDINATES IN FT. VERTICAL COORDINATE Z IS ZERO AT SURFACE AND POSITIVE DOWNWARDS
HORIZONTAL COORDINATE Y IS NEGATIVE FOR NODE 1 AND 2 AND POSITIVE FOR NODE 3 AND 4

LEVEL	VERTICAL COORD. Z	HORIZONTAL COORD. NODE 1 AND 3 X	Y	HORIZONTAL COORD. NODE 2 AND 4 X	Y
1	-.7500E+02	-.4000E+02	.3200E+02	.4000E+02	.3200E+02
2	-.1000E+02	-.4450E+02	.3560E+02	.4450E+02	.3560E+02
3	.7500E+02	-.4900E+02	.3920E+02	.4900E+02	.3920E+02
4	.1400E+03	-.5350E+02	.4280E+02	.5350E+02	.4280E+02
5	.2050E+03	-.5800E+02	.4640E+02	.5800E+02	.4640E+02
6	.2700E+03	-.6250E+02	.5000E+02	.6250E+02	.5000E+02
7	.3350E+03	-.6700E+02	.5360E+02	.6700E+02	.5360E+02

SUBMERGED VOLUME IN CU.FT. AND PROJECTED AREAS IN SQ.FT. AT EACH NODE
X-AREA AND Y-AREA MEAN PROJECTED AREA PERPENDICULAR TO THE X AND Y DIRECTION

LEVEL	NODE 1 AND 3 VOLUME	X-AREA	Y-AREA	NODE 2 AND 4 VOLUME	X-AREA	Y-AREA
2	.7450E+04	.2950E+04	.3100E+04	.7450E+04	.2950E+04	.3100E+04
3	.7150E+04	.2520E+04	.2640E+04	.7150E+04	.2520E+04	.2640E+04
4	.8300E+04	.2680E+04	.2810E+04	.8300E+04	.2680E+04	.2810E+04
5	.1100E+05	.2820E+04	.2960E+04	.1100E+05	.2820E+04	.2960E+04
6	.1350E+05	.3090E+04	.3240E+04	.1350E+05	.3090E+04	.3240E+04
7	.2970E+05	.5800E+04	.6100E+04	.2970E+05	.5800E+04	.6100E+04

[illegible] MASS MATRIX, DIAGONAL OF SUBMATRICES

UNITS, TRANSLATION KIP SEC SQUARED PER FT. ROTATION KIP FT SEC SQUARED

LEVEL	TRANSLATION	ROTATION
1	[illegible]	.1350E+06
2	.1150E+04	.1280E+06
3	.1020E+04	.1370E+06
4	.1090E+04	.1920E+06
5	.1360E+04	.2710E+06
6	.1630E+04	.3770E+06
7	.3700E+04	.7300E+06

[illegible] MATRICES

[illegible] IN X-DIRECTION UNITS FT PER KIP

	1	2	3	4	5	6	7
1	[illegible]	.2070E-03	.1490E-03	.1010E-03	.6080E-04	.2940E-04	.9400E-05
2	[illegible]	.1790E-03	.1400E-03	.9750E-04	.6150E-04	.3230E-04	.1130E-04
3	.1[illegible]	.1490E-03	.1360E-03	.9600E-04	.6200E-04	.3470E-04	.1270E-04
4	.1[illegible]	.1050E-03	.9600E-04	.9700E-04	.6400E-04	.3680E-04	.1410E-04
5	.6[illegible]	.6150E-04	.6200E-04	.6400E-04	.6750E-04	.4030E-04	.1540E-04
6	.2[illegible]	.3230E-04	.3470E-04	.3680E-04	.4030E-04	.4390E-04	.1900E-04
7	.9[illegible]	.1130E-04	.1270E-04	.1410E-04	.1540E-04	.1800E-04	.1930E-04

[illegible] IN Y-DIRECTION UNITS FT PER KIP

	1	2	3	4	5	6	7
1	.1[illegible]	.2590E-03	.1860E-03	.1260E-03	.7600E-04	.3720E-04	.1180E-04
2	.2[illegible]	.2300E-03	.1750E-03	.1220E-03	.7690E-04	.4070E-04	.1410E-04
3	.1[illegible]	.1750E-03	.1700E-03	.1200E-03	.7750E-04	.4340E-04	.1590E-04
4	.1[illegible]	.1220E-03	.1200E-03	.1210E-03	.8000E-04	.4600E-04	.1760E-04
5	.7[illegible]	.7690E-04	.7750E-04	.8000E-04	.8440E-04	.5040E-04	.1920E-04
6	.3[illegible]	.4070E-04	.4340E-04	.4600E-04	.5040E-04	.5490E-04	.2250E-04
7	.1[illegible]	.1410E-04	.1590E-04	.1760E-04	.1920E-04	.2250E-04	.2290E-04

[illegible] UNITS RAD PER KIP FT

	1	2	3	4	5	6	7
1	.[illegible]	.8100E-07	.5280E-07	.3270E-07	.1900E-07	.8300E-08	.2430E-08
2	.[illegible]	.4650E-07	.4460E-07	.2850E-07	.1660E-07	.8100E-08	.2630E-08
3	.5[illegible]	.4440E-07	.3930E-07	.2540E-07	.1520E-07	.7900E-08	.2680E-08
4	.3[illegible]	.2850E-07	.2540E-07	.2350E-07	.1430E-07	.7670E-08	.2730E-08
5	.1[illegible]	.1660E-07	.1520E-07	.1430E-07	.1400E-07	.7750E-08	.2750E-08
6	.8[illegible]	.8100E-08	.7900E-08	.7670E-08	.7750E-08	.7830E-08	.2980E-08
7	.2[illegible]	.2630E-08	.2680E-08	.2730E-08	.2750E-08	.2980E-08	.2830E-08